Assessment of the Effects of Road Geometry on Irish Accident Rates and Driving Behaviour

By

David Kaneswaran B.Sc.

October 2014

A dissertation submitted in fulfilment of the

requirement for the degree of

MSc. (Research)

Department of Computer Science

Faculty of Science and Engineering

National University of Ireland, Maynooth

Head of Department: Dr. Adam Winstanley

Supervisors: Dr.Charles Markham & Dr.Sean Commins

Declaration

This thesis has not been submitted in whole or in part to this or any other University for any other Degree and is, except where otherwise stated, the original work of the author.

Signed _____

David Kaneswaran

Abstract

The following thesis documents the work carried out throughout two main experiments. The first experiment analyses driver crash data and extracts from it accidents that may have occurred as a result of road segments with bad geometry. A visualisation and analysis of this crash data is presented to better determine the relationship 'if any' between road geometry and accident points. The second experiment then examines driver behaviour on road segments that also contain bad bends using a purpose built driving simulator. This experiment is 'driver centric' as it measures behaviour such as eye movement. Both experiments examine contrasting Irish roadways with an aim to better understand the driver when negotiating various geometries. Findings from the crash data analysis initially show the majority of accidents occurring on straight segments of the road types examined. However, when these accident frequencies are normalised against the percentage of road that consist of straights and bends, interesting signals appear on road types that combine sharp bends with higher road speed limits. Results from driver eye behaviour analysis show drivers fixating on regions of the road based on visible geometry or available sight distance. For example, drivers fixate on areas at the road bend while negotiating sharp bends and fixate further on or above the road surface when traversing straight segments.

Acknowledgements

I would like to thank my supervisors Dr.Charles Markham and Dr.Sean Commins for their constant encouragement, patience and invaluable advice throughout this research.

The research in this thesis was funded by an IRCSET EMBARK grant by the Irish Research Council. Their support is gratefully acknowledged. At this point I would like to acknowledge statisticians at the RSA of Ireland for their help in providing a comprehensive accident data set for research purposes.

I would also like to thank my research collaborators and co-authors Michael Brogan and Dr.Catherine Deegan at Blanchardstown Institute of Technology. At Maynooth University, I would like to thank all of the staff at the Computer Science department for their support and wisdom.

Finally and most importantly, I would like to thank my partner Faela and my beautiful daughter Ruby for their unconditional love and support throughout this journey.

Acronyms

NUIM	National University of Ireland, Maynooth
RSA of Ireland	Road Safety Authority of Ireland
DoT	Department of Transportation
NRA of Ireland	National Roads Authority of Ireland
NHTSA	National Highway Traffic Safety Administration
RoC	Radius of Curvature
GIS	Geographical Information System
SRA	The Swedish Road Administration
CCR	Curvature Change Rate
CCD	Charge Coupled Device
NIR- LEDs	Near Infra-Red Light Emitting Diodes
XML	Extensible Mark-up Language
ARC rate	Accident to Radius of Curvature rate

Table of Contents

List of Tables

Chapter 2 Backgrounds and Methods

Chapter 3 Analysis of Accident Data with Geometric Characteristics

Chapter 4 Examining Interactivity Between Driver Behaviour and Road Geometry

List of Figures

Chapter 1 Introduction

Chapter 2 Backgrounds and Methods

Chapter 3 Analysis of Accident Data with Geometric Characteristics

Chapter 4 Examining Interactivity Between Driver Behaviour and Road Geometry

Chapter 5 Conclusions and Future Work

Chapter 1

Introduction

The following study uses accident data analysis and driving behaviour analysis to answer two research questions. The first research question investigates if a relationship between road geometry and Irish accident rates exists and the second question asks if road geometry can affect certain driver behaviours. To examine these topics, two experiments were developed. The following chapter describes the motivation for this study and gives a brief description of the two experiments and methods used. The chapter concludes with an overview and thesis outline.

1.1 Motivation

In Ireland, road fatalities have been decreasing consistently since 2006 through the actions of bodies such as the Road Safety Authority (RSA) of Ireland, An Garda Síochána (Irish Police Force) and the National Roads Authority (NRA) of Ireland [1][2]. This has been achieved through many initiatives to change driver behaviour and modify the road infrastructure. One of the primary initiatives focusing on changing driver behaviour in Ireland is public awareness campaigning. These campaigns produced by the RSA of Ireland are focused on factors such as impaired driving through alcohol or drug use, excess driving speed, seat belt use, mobile phone use and other

accident contributors. However, very few public awareness campaigns promote the awareness of road curvature and its dangers with the exception of general 'excess driving speed' campaigns. This is despite the fact that out of 729 road deaths that have occurred between 2009 and 2012, 178 of these fatalities were reported to have happened on bends. The main sources of information for Irish road safety campaigns evolve from statistical reports amassed by the RSA of Ireland [1]. The presence of a relationship between accident frequency and road bends identified in this RSA study may suggest to future policy's makers the importance of including road geometry in such campaigns.

In addition to the 178 fatalities counted during a straightforward analysis of the RSA data acquired, a further 3000 non-fatal collisions (from a total of 23,235 collisions) where reported to have occurred on road bends [2]. Furthermore, 3400 collision locations remain unclassified as to what type of road character the collision occurred on (i.e. a straight, a bend, a hillcrest etc.). This study aims to contribute to this unclassified data by developing a technique to classify the road curvature at accident locations using analytical methods rather than the subjective assessment made currently. Three main parameters influence road safety; the vehicle, driver behaviour and route environment or road infrastructure [3]. A number of important initiatives have improved vehicle safety like the Irish National Car Testing (NCT) service and the European New Car Assessment [4][5]. However, road safety reports have shown that although vehicle safety improvements have contributed to the reduction in crash severity and thus reduced fatalities, the numbers of accidents remain consistent [6]. These trends from past reports are shown in Figure 1.1 with accidents remaining consistent above 40,000 while fatalities decrease over a 12 year period.

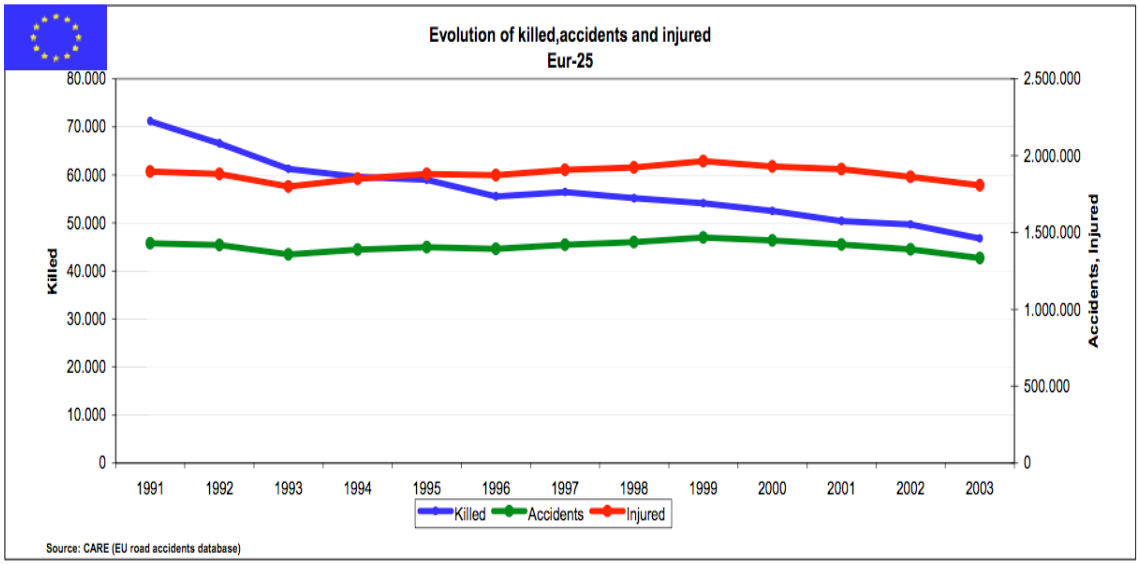

Figure 1.1 CARE EU statistics showing decrease in fatalities with accidents remaining constant [6].

In support, recent Irish collision reports also show decreases in fatalities with non-fatal accident counts remaining consistent above 5,500 from 2009-2012 with highest counts occurring in 2009 and 2012 [2][7]. This study aims to examine elements of these two remaining factors ; road environment and driver behaviour and their relationship to each other.

In recent years, engineering bodies have issued road design standards to coincide with information drawn from road safety reports. While impact assessments and road safety reports measure reported accident data trends, road design standards have been adopted to modify the road environment. These reports focussing on road design, consider the areas with high accident concentration in order to anticipate and identify strategies to prevent accidents. This includes improving the road geometry and road environment [8]. This study also aims to examine the road environment by analysing accident concentration and road geometric characteristics at each of these accident sites in order to determine the role *road geometry* plays on accident rates.

In addition to route environment, driver behaviour was examined in this study. The motivation behind driver behaviour studies was to analyse behaviours such as eye gaze to better understand where in the road environment the driver was looking and to determine areas of the road drivers are accessing. Unlike the accident concentration data obtained by a statistical analysis of crash data, this information was observed in real time and was measured using a driving simulator which allowed customised scenarios to be created. These scenarios measured perceptual information to help gain an understanding of how drivers interacted with the road as a result of changes in visible *road geometry* on contrasting Irish road types.

1.2 Experiment Method Overview

Many traffic accidents are the product of several factors such as human error, weather conditions, surrounding vehicle and road conditions, some of which will be discussed throughout this thesis [2]. However, this study focuses mainly on accident rates occurring at geometric features of the road. The following is a brief description of the methods used to determine the effects of road geometry on accident rates and driving behaviour. The first experiment was developed to bind road geometric characteristics to accident data in order to determine a correlation between road curvature and accident frequency. As well as road geometry, external factors to the roads environment such as driver behaviours were then explored in experiment two. This experiment developed a system to monitor eye behaviour at geometric road features such as bends and straights in order to obtain visual exploration data for further analysis.

This study began by examining a data set of over 23,000 accident points [2]. Collision information was extracted from this data set and mapped as accident occurrences over the Irish road network using a purpose built C# program. The RSA provides an online web GUI that also models collision statistics over the Irish road network, however, the site provides limited interaction with the data and it does not allow the user to extract data for individual roads. The C# program designed for this experiment allows for the individual selection of roads and for the binding of accidents to these individual roads using a distance threshold calculation. The system then calculates the radius of curvature (RoC) value for the road points local to the accident. The accident is then assigned this local RoC value and is further categorised into bend types of various radius lengths for analysis. Further parameters on weather and road surface conditions were also examined on bend categories that showed spikes in accident frequency. This was done in order to examine additional environmental factors that may have contributed to the collision. An output of this experiment is an accident rate based on the type of road geometry local to the accident. This system is repeated for three Irish road types; motorways (M), national (N) and regional roads (R) in order to compare these bend categories and their given accident rates amongst different road types. A fourth category known as local road (L) was not studied.

The second aim of this study was to design and test a reality-based practical, low-cost driving simulator and integrate additional features to the simulator that allow for the physiological and cognitive assessment of the driver in response to geometric road features. Physiological assessment involved the integration of eye-tracking for monitoring eye gaze. Further driving behaviour under varying driving situations were measured. These included reaction times that were measured when acceleration

increases/decreases occurred specifically in response to curvature. To develop this simulator, video data of road segments were recorded of the R406 regional road and the M3 motorway. The video data was then played back as a video sequence in the driving simulator. The rural road scenario contained hazardous bends and dangerous obstructions while the motorway segment contained low levels of stimulation, slow developing bends and no obstructions. One hypothesis of this experiment was that driver's gaze fixation may be 'near of field' on the rural routes due to higher expectations of danger/obstructions and 'far of field' on the motorway road segment. Thirty-five participants were asked to drive both route scenarios using the driving simulator. The output of this experimental tool was a data set for each participant that included parameters such as eye fixation co-ordinates and acceleration pedal data. The data set for each participant was integrated into a GUI to display a visualisation of where each driver looked. Further quantitative information was then extracted from these visualisations and translated using projective transformation to obtain look-ahead distances. By examining contrasting road features on different road types, information was gained as to whether road geometry affords a change in the observed driving behaviour.

1.3 Thesis Outline

This dissertation consists of 5 chapters. This introduction has discussed the motivations behind this study and an overview of the methods used in the two experiments that follow. Chapter two examines related work and fundamental knowledge needed for both the experiments. Chapter three discusses the analysis of a large data set acquired from

the Irish Road Safety Authority. Methods for binding accident geo-data to road geo-data are also described and methods for classifying road curvatures and their geometric characteristics are then presented. Chapter four documents the driving simulator built for the second experiment. Preparatory measures were taken to verify the simulators purpose of use. These measures are presented in order to validate the use of video data as an accurate road model. The simulator was used for behavioural assessment and the output data from participants was then analysed and will be discussed to examine driver interaction on road bends.

Results and conclusions of each of the experiments are collected and presented at the end of each chapter. Chapter 5 discusses results drawn from the entire study with an aim to guide the reader to future work that will draw conclusions from these two experiments.

Chapter 2

Background and Methods

The following chapter contains two sections. The first section discusses accident data and some of the disadvantages of its use in accident data analysis. The effects of road geometry on accident rates are then discussed to justify the need for investigating road bends. Elements of road geometry are then described, with an emphasis on horizontal alignment. The technique used for measuring horizontal curvature is then presented. Factors such as weather and road surface conditions are briefly examined as they are considered possible environmental contributors to accident rates examined in Chapter 3. The second section of the chapter briefly describes the history of driving simulators and validates the driving simulator used in this study as an accurate measurement tool for assessing driving behaviour. Research perspectives relating to eye-fixation are then explored in order to better determine where drivers fixate when negotiating bends. The chapter concludes with a description of the integrated tool used to measure eye behaviour data and the technique used to translate this data to look-ahead distance values for analysis.

2.1 Accident Data

The main source of data for Chapter 3 is accident data. Traditionally road safety measures rely heavily on crash data to tell a story of what has been 'recorded' on roads [1][2][9][10][11][12]. Emphasis is placed on the fact that the accident events used in this study are reported data, not observed data.

In Ireland, An Garda Síochána (the Irish policing authority) records crash data at or after the crash site has been visited. This data can provide useful information on the collision type, the number of people involved, the characteristics of the road and environmental factors such as weather and surface conditions. A disadvantage to this data is that it is estimated based on second hand information obtained by either the people involved in the collision or by the An Garda Síochána on or after visiting the crash site [13]. For example, post-crash reports may result in bias opinions from the driver influencing speed and time of collision in order to avoid penalties/prosecution. In addition, the location of the accident may also be estimated by the An Garda Síochána due to cars being projected further from the point of collision [12]. Table 2.1 shows road characteristics generated from the RSA data collected from years 2009-2012. Classifiers labelled "Other" or "Not specified " amount to 3477 accidents with unspecified road characteristics. Thus amounting to almost 15 % of the entire dataset.

Table 2.1 Collisions classified by road geometry over a four-year period (2009 – 2012)

ROAD CHARACTER	FATAL	SERIOUS INJURY	MINOR INJURY	TOTAL	%
Straight	434	962	13659	15055	64.8
Bend	178	325	3232	**3735**	**16.1**
Hillcrest	18	39	351	408	1.8
Some Gradient	37	40	483	560	2.4
Other	17	41	693	751	3.2
Not specified	45	146	2535	2726	11.7
TOTAL	729	1553	20953	**23235**	100.0

Reports from Irish Traffic Corps have also indicated that during data acquisition the reporting officer makes a binary decision as to whether the accident is on a bend or on a straight segment [14]. No geographic information systems (GIS) are used afterwards to determine if the initial geo-location was accurately placed on or close to a bend. This study develops a system using accident geo-data to determine if accidents have occurred on bends and also presents a technique to classify the accident into a road bend type.

In addition to crash data being incomplete there exists miscalculations of the severity of the accident due to injuries establishing over longer periods of time [15]. The Swedish Road Administration (SRA) have tried to combat this problem by implementing crash acquisition databases which combine both police and hospital data to minimise loss of data [16].

Other ways of collecting data include direct observational methods from the roadside. This collision or vehicle information can be collected via the use of video. For example,

studies by Brownfield at al (2003) used video data to monitor accident rates and congestion at over 100 sites [17]. However, observed video data was limited in that it could at best describe the vehicle and its behaviour. Descriptions of the driver like gender, age and factors such as 'alcohol use' could not be obtained unless using the previous method of reporting accident data [13].

These concerns surrounding reporting accurate crash data have also been accompanied with concerns of accurately obtaining 'unreported' crash data. As this study was primarily investigating geometric features as a possible cause of accidents, the main category of drivers being investigated were single vehicles collisions or run-off-road collisions near a bend. A possible disadvantage for single off-road collisions with no other vehicles involved is that crash data for these incidents may remain unreported. Studies have shown that one of the most unreported of all incidents is the 'near miss' or 'near crash' whereby cars may have come close to conflict or where a car has been 'run-off-road' without enough damage done to warrant reporting [13][18][19].

Methods of gathering 'near miss' data were combated by the *100-Car Naturalistic Driving Study* sponsored by the U.S. National Highway Traffic Safety Administration (NHTSA)[19]. The study tracked the behaviour of 100 drivers for more than one year using vehicles instrumented with video and sensor devices. Using this controlled observational method to collect crash data, it was possible to show that the frequency of near misses had a strong linear relationship to the frequency of real crashes. This implied that a near miss could also be used as a quality predictor for the frequency of actual crashes [19]. Table 2.2 is sourced from the NHTSA study and shows the ratio for crash to near-crash events for road alignment types. *Curve and Straight Grades* are road alignments on vertical elevations and *Curve and Straight Level* are road alignments on

level road segments. The numbers shown in Table 2.2 indicate the frequency of accidents measured in the given alignment. As the ratio for the *Curve Grade* and *Curve level* are the highest, the results indicate driving errors being most likely to result in crashes on curved alignments.

Table 2.2 Table Crash and near crash by road alignment [19]

Alignment	Crash	Near-Crash	Ratio
Curve Grade	3	7	.43
Curve Level	13	99	.13
Straight Grade	1	15	.07
Straight Level	52	638	.08

This study implies that a crash unreported on a bend may hold greater weight as a crash predictor to that unreported on a straight. Thus increasing the possible dangers of bend related collisions.

2.2 Irish Crash Data Analysis.

Over 23,200 accidents were recorded in Ireland between 2009 and 2012. This accident data was provided by the RSA of Ireland in the form of four comma-separated files for each year mentioned, the analysis of which is discussed further in Chapter 3. In order to obtain a data set relevant to the current study, these accidents had to be re-classified and sorted. Initially all accidents were classified according to road geometry. Table 2.3 shows geometric data processed from the entire accident data set. Of the 3,735 accident events reported on bends, 2,194 of these involved single vehicles as shown in Table 2.3. Table 2.3 also shows 102 fatal single vehicle accidents occurring on bends. However, as many single vehicle accidents that have occurred at bends may have been due to other environmental factors such as weather and surface conditions, these 2,194 are further classified in Table 2.4 and Table 2.5.

Table 2.3 Fatal collisions related to single vehicles on bends (2009 – 2012)

Description of Factors	**Accident Count**	**Percentage of Total Accidents on Bends**
Accidents on bends	3735	100%
Accidents involving 2 or more vehicles on bends	1526	41%
Accidents with *single vehicle* on bends	**2194**	59%
		Percentage of Total Fatalities on Bends
Fatal accidents from total of 23235 collisions	729	100%
Fatal accidents on bends	178	24%
Fatal *single vehicle* accidents on bends	**102**	14%
Fatal *single vehicle* accidents on straights	265	36%

Table 2.4 shows almost 70% of these single accidents occurring on dry weather conditions and about 25% occurring in wet weather conditions.

Table 2.4 Single vehicle collisions classified by Weather Condition (2009 – 2012)

Weather Condition	Accident Frequency	%
Dry	1508	**68.7**
Wet	538	24.5
Frost/ Ice	59	2.68
Snow	7	0.31
Fog/ Mist	23	1.04
High Winds	3	0.13
Other	3	0.13
Unknown	53	2.41
TOTAL	2194	100

Given that accident frequency is higher in dry weather conditions it was expected that road surface conditions would hold similar distribution. However, this was not the case as Table 2.5 shows slightly larger amounts of collisions occurring in wet road surface conditions. This may be the case in instances were weather conditions have changed dramatically but road surface conditions have not, thus road conditions are possibly underestimated by the driver. In addition, time taken by authorities to reach the accident scene may also have an influence as to how accurate surface conditions are reported.

Table 2.5 Single vehicle collisions classified by Road Surface Condition (2009 – 2012)

Road Surface	Fatal	Serious Injury	Minor Injury	Total	%
Dry	49	108	780	937	42.7
Wet	46	73	891	1010	**46.0**
Frost / Ice	4	7	184	195	8.9
Snow	1	0	19	20	0.9
Other	2	1	20	23	1.0
Unknown /Not Specified	0	0	9	9	0.4
TOTAL	102	189	1903	2194	100

Due to the dynamics of weather and the nature of crash data acquisition, these measurements can only be approximated. However, the exploration of such factors was necessary in order to highlight other environmental factors in areas with bad road geometry. In addition, these environmental factors are examined in the results formed at

the end of Chapter 3 in order to eliminate these conditions as contributing factors to irregular accident occurrences.

2.3 Effects of Road Geometry on Accident Rates

The effects of road geometry on accident rates are an ongoing argument amongst academic researchers and transportation bodies. Various road safety reports suggest that while 'driver error' is usually the primary reason for an accident, the geometric characteristics of the road's infrastructure also plays a significant role in the events leading up to the accident. For example, French DoTs have shown that consistent road geometry and appropriate signalling ease the task of the driver therefore dramatically reducing the risk of driver error [20]. As a result, road authorities have recommended the removal of unnecessary bends and the lengthening of curves, thus easing the demands of the driver. An example of this is shown in Figure 2.1 from the Irish NRA road link design manual [8].

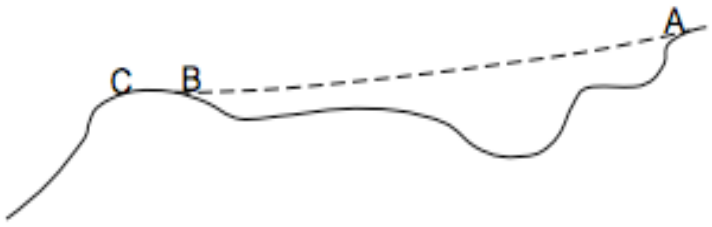

Figure 2.1 Link design showing curve C being lengthened to remove further bends

However, British transportation design reports do not agree with the suggestion of road geometry being a major issue involved in accidents rates. A number of studies carried out by British transportation bodies on rural roads aiming to correlate personal injury

accident rates with horizontal curvature suggest that accident rates are unlikely to be affected by moderate changes in road design parameters [21]. These studies estimate road layout as a contributing factor in only a small number of accidents. Furthermore, the effects of layout parameters such as gradients, sight distance in combination with horizontal curvature were necessary in order to show slight increases in accident rates. Thus reflecting the influence of factors other than road layout.

Although the French and British transportation bodies have opposing views as to whether or not road geometry is a significant cause of road accidents [20][21], it is widely accepted in literature that elements of road geometry such as horizontal curvature are a significant contributing factor to accident rates. This is illustrated in early work by researchers Cairney et al. (2000), Persaud et al. (2000) and Torbic et al. (2004) who all report increases in crash rates as a result of road curvature [22][23][24]. In a report by Cairney et al (2000) on the relationship between crash risk and rural highways in Australia, the authors conclude that single vehicle crashes increase as curvature increases particularly at curvatures below radius lengths of 200m [22]. Furthermore, Persaud et al (2000) reported a similar trend in crash rate increases on curved roadways in America. These studies also argue that crashes on bends tended to be more severe than that of straight roadways, with results of up to three times the amount of fatalities occurring on road bends [23]. In addition, road reports by Torbic et al (2004) present similar approximations of accident rates in their *Guide for Reducing Collisions on Horizontal Curves* [24]. The authors reported a crash rate for horizontal curvature three times than that of straight/tangent sections of roadway and approximate that 76% of fatal crashes are single-vehicle run-off-road collisions related to road curves.

Due to the relatively small sample size, conclusions drawn from the accident data can be inconclusive due to statistical noise. However, examining the aforementioned reports from larger populations and transportation bodies helped reduce the rarity of such data and provided a better understanding of crash rates with respect to curvature. For example, findings by Torbic et al (2004) were the result of analysing up to 43,000 fatalities in 2002 alone, a number that would take a country the size of Ireland over 200 years to amass (based on a current average of 189 fatalities per year).

This study aimed to analyse the effects of road geometry on accident rates. The above literature has suggested horizontal curvature as a significant causal factor in this relationship. However, there are a number of other design elements that should be considered. A breakdown of some of the other design elements adapted by Lyinam, Lyinam and Ergun (2003) are shown in Table 2.6 [25]. Early studies suggest that in order to further analyse the relationship between road geometry and accident rates, it is necessary to further classify road geometry into various road 'design elements' as some elements alone may be higher causal factors [26][27].

Table 2.7 Design elements classified by contributing factors to road safety[25]

Design element	Contributing factor to Accidents
Roadway	*Number of Lanes (Lane)* *Lane Width (Foot/m)* *Surface Condition (Good/Bad)*
Vertical Alignment	*Grade on Tangent (%)* *Grade on Curve (%)* *Sight Distance (Feet/m)*
Horizontal Alignment	*Degree on Curve (Degree)*
Shoulder	*Width (Foot/m)* *Surface Condition (Good/Bad)*
Traffic Control	*Delineator (Yes or No)* *Guide Sign (Yes or No)* *Lighting (Yes or No)* *Marking (Yes or No) -*
Median	*Median Width (Foot/m)*

By examining the 'relationship' between the elements shown in Table 2.7 further findings can be derived. Variations can be seen in accident rates when road elements like shoulder width and lane numbers are changed supporting further the argument that road geometry characteristics do affect accident rates. For example, studies by Othman et al (2009) suggest that curves with high accident rates can be improved by restricting lane changing manouevers [16]. Ahmed 2011 supports this argument by stating that sites with higher degrees of curvature, wider medians (*narrow barrier used to separate*

opposing traffic flows) and increases in lane numbers are factors for lowering crash rates [28]. However, the same study by Ahmed also suggests that the degree of curvature is negatively correlated with crash risk, supporting previous research by Stewart and Chudworth (1990). These studies suggest that the sense of danger along sharp curves may increase the drivers alertness, thus decreasing accident rates by causing the drivers to be more cautious with their speed [28][29].

These findings motivated the current study to focus on 'horizontal curvature' design elements on Irish road types to better determine if Irish accident rates are high as a result of road bends. As well as being highlighted by the literature, the "horizontal curvature" design element was also investigated as this information could be estimated from map data that could then be correlated with RSA data in the form of GPS information detailing the accident location (discussed in Chapter 3). This would have been more difficult with many of the other elements shown in Table 2.6.

2.4 Theoretical Foundations for the Analysis of the Effects of Road Geometric on Accident Rates.

The following section examines horizontal curvature and methods used to measure this type of alignment. Factors influencing horizontal curvature such as curve types are also introduced in order to highlight curvatures prevalent to accident frequency.

2.4.1 Horizontal Alignment

Horizontal and vertical curves are the two most important factors in geometric design for roadways [30]. A horizontal curve provides a transition between two tangent (straight) sections of roadway (see Figure 2.2 *Simple Curve*) allowing a vehicle to safely negotiate a bend. Vertical curves are the second of the two transitional curves. These curves transition between two sloped roadways and are important in allowing the driver to negotiate the roads elevation rate (grade). Figure 2.2 shows four of the most common types of horizontal curves where ***r*** is radius length.

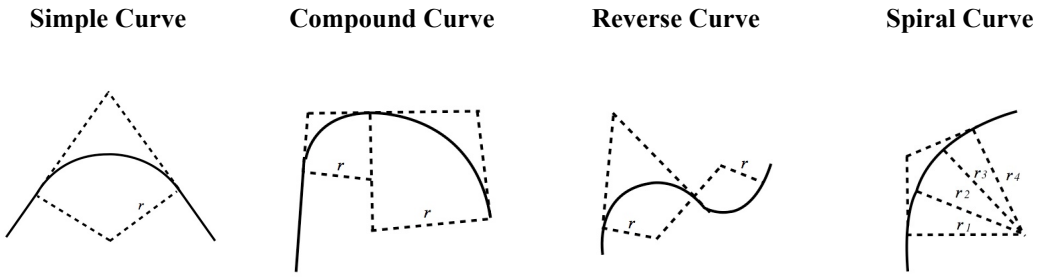

Figure 2.2 Horizonatal Curves [30]

A *simple curve* shown in Figure 2.2 is an arc of a circle. The length of the radius of the circle determines whether the curve is sharp or flat. Short radius lengths mean sharp curves and vice versa. *Compound curves* consist of two *simple curves* joined and curving in the same direction. Although these curves are commonly needed, safety reports have highlighted the need for eliminating these curves [24]. This is due to the abrupt changes in curvature requiring considerable steering effort by drivers to negotiate the successive curves. Similarly, investigations by Lippold et al. (1997) of consecutive curves showed accident rate increases on stretches of road where the alignment changed from large into small curves [31]. *Reverse curves* have similar defects. This curve consists of two simple curves joined but curving in opposite direction. Road engineering guides have recommended that a reverse curve should not be used where possible [30]. In addition, investigation of the curvature change rate (CCR) has shown that consecutive elements of alignment can in fact higher accident risk [32]. Curves of this type require balanced alignment where the rate of change of consecutive elements are within a defined range [32]. In doing so, the driver's speed is not changed abruptly.

This study examines accident frequencies on three Irish road types; motorways, national and regional roadways. The benefit of examining contrasting road types is that they each contain geometric attributes that afford different driving speeds. For example, while motorways normally contain gradual transition curves that allow for higher speed limits of up to 120km/h, regional roads warrant lower speed limits ranging from 40km/h to 80km/h based on a higher concentration of road bends. However, Irish national roads are assigned speed limits of up to 100km/h and quite often contain multiple bends

similar to that of regional roads. It is the transitions between consecutive curves on this road type that may support findings from Lippold (1997) and Gatti (2005) the most.

In contrast to extreme changes in consecutive curves, studies have also shown that where alignment changes are minute like those of gradual transition curves, accident rates can also increase. Studies by Lippold (1997) and Stewart and Chudworth (1990) suggest that these accident increases can be high due to drivers maintaining high speeds unaware of a severe change in alignment approaching [31][29]. This suggests that the use of transition curves in certain alignments can be as dangerous as sharp curve changes. Nevertheless, transitional curves remain commonly used in road design as they are necessary to reduce radial forces when a vehicle travels along a curve. The smoother the transition from tangent to curve, the more gradual the increases in radial force. Similarly smoother transitions exiting from curves to tangents result in gradual decreases in radial force. A curve that holds these properties is the *spiral curve* (see Figure 2.2) made up of continuously changing radius lengths. This curve commonly used in roadway design as it is used to transition between simple and compound curves [30]. Studies have shown that spiral curves increase safety on curves by allowing the driver the means of tracking a curve that fits the design of the alignment [33]. Figure 2.3 models the varying radius lengths of a spiral curve used in the current study (where green line ***r*** equals radius length). It shows radius lengths continuously changing gradually throughout the curve.

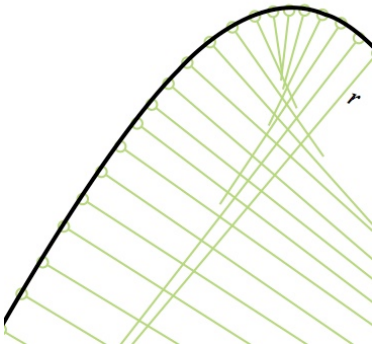

Figure 2.3 Model of varying radius lengths being measured on curve

2.4.2 Road Curvature Design Factors

Although authorities like the RSA of Ireland and many international road safety administrations use accident concentration statistics to design and promote safety initiatives, it is transportation engineering bodies that are most interested in roadway design factors such as traffic volume and road geometry to approximate accident frequency [34]. Increasingly, preventative measures are being implemented early in the road design stage to overcome the need and costs of removing road segments after they have been built (see road link design shown in Figure 2.1). European standards and practice such as the TEM (Trans European North South Motorway project), US Bodies (FHWA Federal Highway Admistration) and countless international DoTs have produced country/state specific road design manuals and studies in a bid to improve safe traffic operation [8][21][36][37][38].

The concept of self-explaining roads is discussed in these design manuals and is based on the idea that roads should be built in such a way as to induce driving behaviour ‘simply by its design’. For example, studies have suggested that physical measures of

design elements should have the ability to persuade the road user to reduce speed voluntarily [38]. The idea is that well designed roads should prompt appropriate speed and steering manoeuvres on curves to allow roads to be safely driven regardless of curve types. Thus, 'design speeds' are topical in these road design manuals on account of driver speed being considered an integral factor in safe traffic operation.

Road design speeds are defined as the maximum safe speed for which the road is designed [35]. For example, Irish motorways hold a maximum permissible speed limit of 120km/h. Table 2.7 shows the value of 650m for a transitional curve being approached at 120 km/h and 1000m for a speed of 140km/h. This figure of 650m will be considered when classifying bend types in Chapter 3.

Table 2.7 Minimum Radii for Horizontal Alignment [35]

Design Speed (km/h):	140	120	100	80
Minimum Horizontal Radii (m):	1000	650	450	240

As discussed, when traversing horizontal alignment, the curve should be such that the driver notices no abrupt breaks in continuity in order to reduce radial forces. Radial forces, for example centripetal force act on a vehicle as it traverses a road bend. In addition, there is a minimum radii for the road curve for different types of design speed (as shown in Table 2.7)[35]. To estimate these design speeds it is first appropriate to calculate using the geometry of the road and Newtonian mechanics, the highest velocity achievable on a bend without slipping. The following equation 2.1 shows safe speed estimation for the max velocity on an arc.

$$V_{\max} = \sqrt{g\mu_s r}$$

(2.1)

Where **g** is acceleration due to gravity, μ_s the coefficient of static friction, and **r** the radius of curvature. It is from this value that safe speeds are proportionally estimated and thus assigned to design speeds or V_d [39]. Furthermore, the roads operating speed or the V_{85} is obtained by monitoring the 85th percentile of vehicle speed while traffic is free flowing and unrestricted by speed limits [40]. Consistent design occurs when the difference between the both the V_d and V_{85} is less than or equal to 10km/h, any speed difference between these two speeds above 20km/h is not permissible [41].

Another possible factor considered for safe traffic operation (and shown as an element in equation (2.1)) is the value of the road's friction or road surface condition. In Ireland, regional and national roadway segments can often contain bad road surface conditions due to weather conditions and 'wear and tear'. Although design improvements are available for modern road types like motorways, rural roads in Ireland fall below current design standards [42]. Factors such as excess rain can cause the road to break and sag leading to the breakdown of road surface and therefore an increase in accident rate [43]. Studies by Cairney et al (2008) report increases in accident rates when decreases are shown in the texture or surface of the road. These studies conclude that the resealing of roadways lead to proportionate decreases in accident rates.

Advanced engineering models for road structures consider factors such as crossfall and superelevation when discussing curve design speeds as they play a role in the minimum horizontal radii for curves. Crossfall is the angle at which the road slopes away from the road centre to facilitate the disposal of rainwater shown in Figure 2.4 (a).

Superelevation is the angle at which the road banks on a horizontal curve as shown in Figure 2.4 (b).

(a)

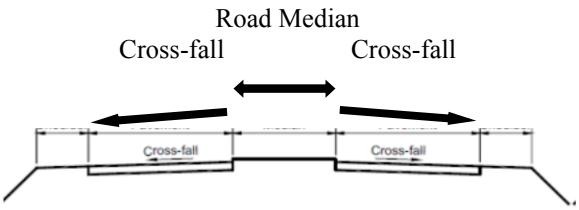

Figure 2.4 (a) Crossfall showing camber in road[30]

(b)

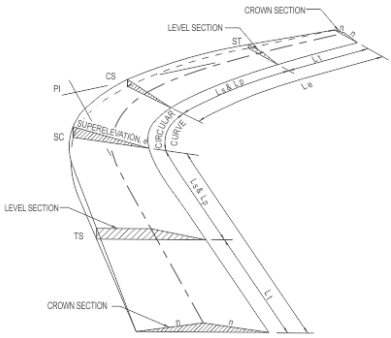

Figure 2.4 (b) Superelevation on a curve [30]

Commonly seen at racetracks, this banking or camber of the roadway reduces the radial forces being demanded of the car when traversing a bend. For the current study superelevation was not included in the road curvature model as the geo-data analysed did not contain altitude information. Furthermore, the main segments of roads containing bends examined in the current study are that of national and regional category normally driven at lower speeds than that of motorways (where superelevation is most commonly used).

2.4.3 Road Curvature Analysis for Horizontal Alignment.

A number of methods were explored in the current study to analyse the road curvature at horizontal alignment. Problems existed at the beginning of curvature analysis where road geometry data was incomplete. In the absence of detailed road geometry data, a measure of the roads sinuosity or sinuosity index (SI) was explored. In addition fractal geometry, commonly used to measure perimeters was also used as a measurement option in order to gain an overall curvature of a road. However, the method chosen for this study was that which measures the radius of an arc created by fitting a circle to a curved road segment,

The SI was examined in the current study to measure curvature by dividing *the distance measured between two points along a road* by the *straight line distance between the start and end point* [44]. This method has been used in previous Irish studies to measure horizontal alignment at lower resolution (1km) where detailed road geometry was also unavailable [45]. However, as the data quality of acquired roads increased in the current study, the use of the sinuosity index became redundant and proved more useful for measuring entire routes as opposed to smaller road segments.

In addition, fractal geometry was also considered as it can be used to measure the complexity of a regions perimeter. Fractal dimension analysis has been used to assist in the measurement of borders and coastlines [46]. The process of measuring fractal dimension works by measuring the total perimeter length as a function of different lengths of ruler. By decreasing the ruler size ($\boldsymbol{\lambda}$), the length of the curved road $\mathbf{L(\lambda)}$ increases. This effect can be summarised by the following equation

So that

$$L(\lambda)= n\lambda^{1-D} \tag{2.2}$$

Where $\boldsymbol{\lambda}$ is length of the ruler,

$\boldsymbol{L(\lambda)}$ is the length of perimeter based on unit measurement length λ,

$\boldsymbol{n}$ is the number of steps of length λ and

$\boldsymbol{D}$ is the fractal dimension of the rough line.

Taking the log of both sides, equation (2.2) can be rewritten as

$$\log L(\lambda) = (1-D)\log\lambda + \log n \tag{2.3}$$

which is the equation of a line (a log-log plot of the perimeter length vs the ruler length). The slope of this line m is equal to 1-D which gives a measurement of the fractal dimension in equation (2.4)[46][47].

$$D = 1 - m \tag{2.4}$$

$\boldsymbol{D}$ is the fractal dimension, measures the rate at which the distance changes as a function of the ruler length. Typical $\boldsymbol{D}$ values are between 1 (straight) and 2.5 (high complexity). The higher the dimension the more the line curves. These measurements were used on the three road types used in the current study. However, results suggested very low fractal dimensions for all road types suggesting very straight or smooth roadways. It is estimated that this similarity was due to the high percentage of straight sections weighting heavier in these calculations. Fractal dimension is a measure of complexity

along a route for this study a direct measure of curvature at each point along the route was more useful.

It was concluded that both methods examined were found to be more useful in measuring entire routes at a macro level and that in order to examine road segments at a smaller scale, data for the road geometry would need to be improved. Methods for improving road data quality are discussed in Chapter 3. Upon improving road data points, the ability to analyse the road at a micro level was possible and a method to determine the radius of curvature (RoC) for each road point was used. This method was also used as it is the most commonly used measurement for simple and spiral curves and has been widely used in transportation literature as a standard criterion for measuring curvature [16][30].

2.4.4 Radius of Curvature

Intuitively the curvature of a circle is directly defined by the length of the circles radius ***R***. The shorter ***R*** is, the greater the curvature of the circles arc thus the greater the radial force acting on the vehicle if bound to a circle. “The radius of curvature of the curve at a particular point is defined as the radius of the approximating circle” [48]. Therefore a simple circle can be loosely drawn given a local section of a curve as shown in Figure 2.5.

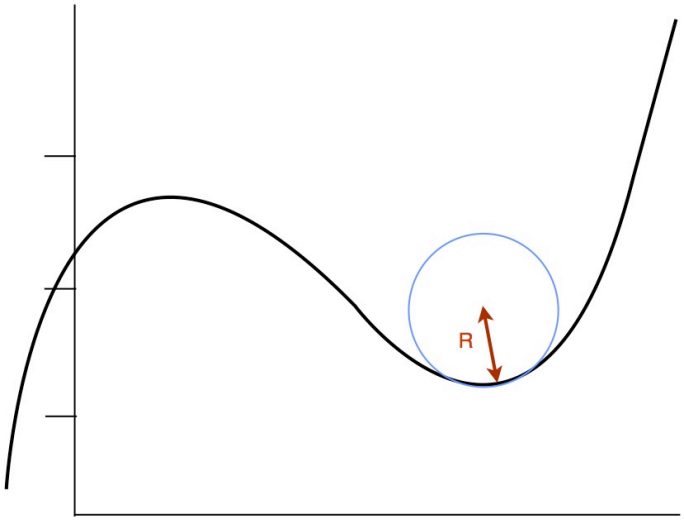

Figure 2.5 Circle Osculating a Curved Section

Given that we have access to three points (road data points) local to the curve, the method using the equation of the circle was chosen and is illustrated in Figure 2.6.

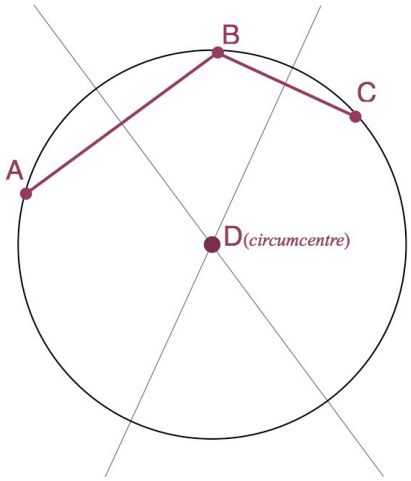

Fig 2.6. Simple Circle Centre using Circumcentre of Perpendicular Bisectors

Figure 2.6 shows a circle passing through the three local points ***A,B*** and ***C***. The ***x*** value for the centre of the circle was determined by finding the intersection points of the two perpendicular slopes m_1 and m_2 of adjoining lines $A(x_1,y_1)$ $B(x_2,y_2)$ and $B(x_2,y_2)C(x_3,y_3)$ as shown in equation (2.3).

$$X_{centre} = \frac{m_1 m_2 (y_1 - y_3) + m_2 (x_1 + x_2) - m_1 (x_2 + x_3) 2 (m_2 + m_1)}{2 (m_2 - m_1)} \tag{2.4}$$

the known values and **x** are then substituted into equation (2.4) to find the y value centre

$$Y_{centre} = -\frac{1}{2}\left(x - \frac{x_1 + x_2}{2}\right) + \frac{y_1 + y_2}{2} \tag{2.5}$$

and finally the radius was found by using the Euclidean distance formula from **A**,**B** or **C** to the centre point **X**centre,**Y**centre (equation 2.6).

$$R_{radius} = \sqrt{(x_A - x_{centre})^2 + (y_A - y_{centre})^2} \tag{2.6}$$

The application of this formula is discussed in Chapter 3 whereby three road points local to the accident are assigned radius of curvature values. This method was used to give each accident a local road curvature value.

2.5 Linking the Effects of Road Geometry on Accident Rates with the Effects of Road Geometry on Driver Behaviour

While the previous sections concentrated on road geometry and its effect on accident rates, it is clear from the analysis of accident statistics and data from the RSA of Ireland, (see Table 2.4 and 2.5) that many other factors can contribute towards accidents on bends. Such factors include weather and weather-related road surface conditions (e.g. dry, wet, ice, snow). In addition, this study has also highlighted physical design factors such as road width, road banking, successive curve types, road texture condition and design speeds as contributors to bend-related accident rates. While weather conditions cannot be avoided, research has shown that it is possible to reduce 'driver error' by implementing road design standards that afford safer traffic operation, thus decreasing collisions as a result of changes in road geometry [20].

However, while improvements in road geometry elicit safer traffic operation, studies have also suggested that elements of road geometry can affect driving behaviour. Driving behaviours such as eye fixation or 'where we look' have been reported as behaviour parameters that influence accident rates on road bends [49][50][51][52]. For example, studies on driving behaviours at contrasting bend types reported driver's sight distance as a factor in the reduction of driver error based on the measure of visible geometry available [49][53][54]. These studies suggest that in addition to road geometry having an effect on accident rates based on a safe traffic environment, road geometry can also affect accident rates based on driving behaviour parameters.

There have been many ways of analysing driver behaviour including naturalistic driving and real-time video observation as discussed in the methods of collecting accident data

Section 2.1. However, these methods commonly rely on observing drivers in their natural daily driving routine (e.g. commutes), and as such is an uncontrolled environment [55]. One popular method to assess driver behaviour is through the use of driving simulators. The advantage of using driving simulators is that driver behaviours can be observed while deliberately placed in controlled dangerous scenarios. In addition as simulators are based in a laboratory environment, more profile information can be obtained on the driver (e.g. age, gender) unlike real-time video observations. The following section discusses the background literature and methods used to analyse driving behaviour such as eye movement on contrasting road types. A method to transform eye gaze into look-ahead distances in order to determine how far drivers are looking ahead at varying geometry is then described. As the development and use of a driving simulator is employed in this study to collect eye gaze data, literature relating to simulators integrated with eye tracking devices is explored. In addition, topics relating to the effects of road geometry on eye-gaze are also discussed.

2.6 Brief History of Driving Simulators

The first vehicle-based simulation can be traced back as early as 1929 when Edwin A Link introduced his “Pilot Maker” a blue box modelling an airplane cabin on a moving platform [56]. Aircraft simulators were used for training in the Second World War for over 500,000 pilots and continued to be used for different scientific and training purposes [56]. Thirty years later in 1960, the first interactive driving simulator was introduced at the University of California consisting of a projected picture on a wall, a moveable seat in a drivers cab and simulated force feedback [57]. Modest advancements in the simuators visual technology have included changes from a wall to a projector screen [58]. Further progress in video projection technologies allowed the still projected image to be extended to an “on-the-rails” video sequence whereby the driver could observe road scenes but had no lateral control of the vehicle. With the advent of digital computer-generated imagery, virtual worlds and scenarios could be constructed to allow the user to change their point of view in the visual stream unlike video. Currently researchers are incorporating steering dynamics into video sequences to allow more freedom of control in a driving scenario [59]. The experimental method in Chapter four uses a video-based simulator as this type of simulator still holds an advantage over even the most modern graphical simulators in that of the *fidelity* of the visual cue system.

2.7 Driving Simulator Fidelity and Purpose Validation

Meister (1995) defines simulator 'fidelity' as "*the degree to which a simulator matches aspects of driving on the road*" [60]. Kappler (2005) uses a similar term 'transfer' to deal with actions for simulator tasks that require similar activities to the original situation [56]. There are a number of different types of research-based simulators with a wide range of capabilities and fidelities. Examples of a high-fidelity simulators are the VTI's simulator (Sweden, Europe) and the NADS simulator (Iowa, USA)[61][62].These high fidelity simulators consist of a partial/full car mock-up, hydraulic movement and upto 360° of moving screen [63]. High-fidelity simulators like ones used by Toyota and Daimler Benz require specialist dedicated hardware and are high cost[63][64]. Medium fidelity simulators like the driving system found at the TRL (Berkshire, England) also use a car mock-up, however, visual streams are restricted to 180° field of view with basic hydraulic hardware systems[65]. This study uses a purpose built low-fidelity simulator. Low-fidelity simulators are more common in academic research due to their low-cost PC-based setup. A basic version consists of a single or multi-screen set-up that allows the user to interact with a road-based model to simulate the driving experience typically using a low-cost gaming steering wheel and pedals as input controls.

During the development of this simulator, preliminary testing was carried out to ensure that the simulator was designed effectively to measure eye behaviour and reaction speeds [66]. Research has suggested that sign legability can be poor in low fidelity simulators [67]. Factors like these were considered in the development of the simulator to ensure the visual stream contained enough detail to afford eye movement and driver

reaction. Details of the preliminary testing procedures carried out using a dual-fidelity simulator were documented in Kaneswaran et al (2013)[66]. The paper outlines an experiment that consisted of two simulator fidelities (video and graphical model) being compared to ground-truth information of the same real world route. The results from these tests showed that when compared, average simulator driving speeds at given bends correlated with that of driver's actual ground-truth speeds. The variations in speed, while not absolutely similar, were consistent at road features like dangerous bends and posted speed limits. Further analysis of these results by Brogan and Kaneswaran (2014) showed a correlation of 84.6% between the video and ground truth speeds [59]. This validation of the video based simulator suggested that drivers reacted reliably to the designed scenarios.

Although the simulator used in this study did not have steering capabilities, lateral movement was not a primary concern in the designed experiment. Furthermore, studies by Mars et al (2012) investigating fixation points while driving, reported no significant differences between driving with and without steering enabled [68]. Vestibular feedback was also not used, as successful eye tracking was dependent on little head movement for accurate sampling.

It is also important to note that simulation models are used as an abstraction of reality and that the primary interest of this study was in the 'validity' of the measurement tool. Validity is represented as the ability for the driving simulator to measure the trait or behaviour that it was intended to measure [56]. As participant's reactions to the video cue stream have shown high correlation to a real world measure of the same route, the simulator is proven a valid measurement tool. However, what this also suggests through validation of the results is that simulators can comprise only the necessary elements for

measuring certain factors and that the absence of a Stewart platform (allows driving platforms to simulate rotation: pitch, roll and yaw) and steering can still yield meaningful results.

2.8 Driving Simulation with Eye Tracking Integration

When attention prioritisation becomes the focus of a driving behaviour assessment, then an eye-tracking device is required to allow the recording of eye-gaze when fixating on the road. A method was developed in the current study to measure driver behaviour when a change in the visual stream was recorded. Driving Simulators that incorporate eye tracking have distinct advantages. For example, drivers can be deliberately placed in dangerous scenarios that may involve risky eye behaviours, such as treacherous bends with complicated intersections. In addition, such scenarios can be used to reduce risky eye behaviours in a controlled environment unlike that of naturalistic driving tests [69].

Comprehensive research has been carried out on the effects of attention/inattention while driving using eye movements as a primary variable [69][70][71][72][73]. These driving studies examine factors such as eye gaze, pursuit movements, eye-fixation and look-ahead fixation, all of which are various types of eye behaviours [69][70][71]. Early research from Cohen (1977) highlights the use of fixation duration as an effective information input, however, his study suggests that fixation may only be measured as an element of prior and post eye movements using variables such as prior fixations, amplitude of eye movements as well as the subjects capacity to process the information stream [74].

More recent studies have also examined fixation patterns like guiding fixations to determine 'sequences' of eye movements when steering into road curves [75]. However, further studies using eye-trackers have suggested that drivers can extract information from traffic signs and markings without fixating on them [76][77]. For this reason driving research has also been explored in topics dealing with peripheral fixation [78][79]. These dual functions of the eye and fixation sequences are amongst the many difficulties faced when designing experiments for eye movement analysis.

2.8.1 Where Do We Look When Negotiating Bends?

The tangent point on a road bend is the point where the straight line of a road meets the beginning of a road curve as discussed in *Section 2.4.1*. However, in this section the tangent point refers to the point where the driver's line of sight is tangent to the road curve as shown in Figure 2.7 (B). The tangent point has been prominent as the region on the curve that attracts significant amounts (up to 75%) of eye fixations since principal studies of visual orientation by Land and Lee (1994) [49][50][68].

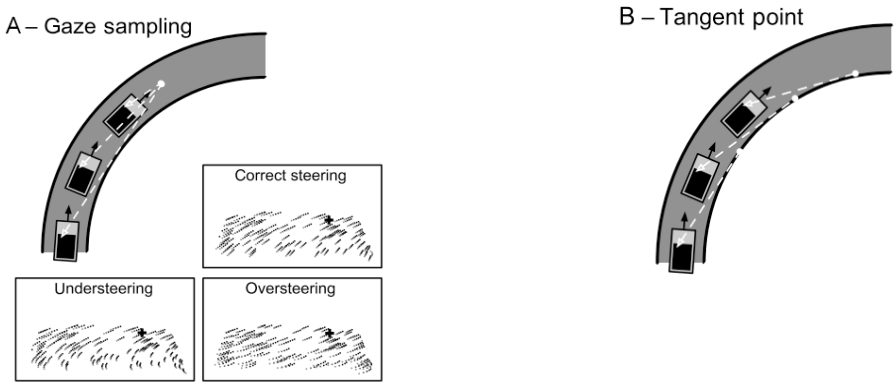

Figure 2.7 Two Strategies for Negotiating Curves [49].

In addition, other models of visual orientation have been explored. For example, figure 2.7(A) show the gaze sampling method and figure 2.7(B) the tangent method used for negotiating bends examined by Kandil, Rotter and Lappe (2009). In these studies an alternate model of visual orientation called 'gaze sampling' first introduced by Wann and Land (2000) is used to determine if the retrieval of future path points are necessary when negotiating bends [49][80]. Insets in Figure 2.7(A) show strips of gaze samples taken consecutively over 5 points to indicate forward direction of gaze. However, these studies conclude that the use of the gaze sampling caused over and under-steering errors and that the tangent point method allowed subjects to drive more smoothly through the curves. Thus, fixations on the tangent point remain the default strategy used of the two.

The use of the tangent point is undoubtedly important in curve negotiation, however, surprisingly drivers still have the ability to negotiate curves when for example a lead vehicle is occluding the road ahead. Research by Mars (2008) experiments with the lateral position of the tangent point by placing visual cues along 5 points ranging from the left and right of the original tangent point as shown in Figure 2.8 [68].

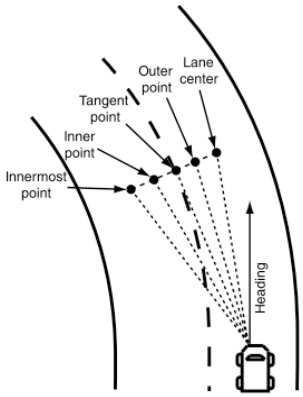

Figure 2.8 Experiments with lateral position of the tangent point [68]

Results showed that each point preserved the eye-to-steering cues needed to safely negotiate the bend. Thus indicating that once target points other than the tangent (e.g. a

leading car's break light) are at the same curvature angle as the tangent point, drivers can still successfully negotiate smoothly around a bend.

The dual functions of the eye are yet another factor considered when designing eye movement experiments as these factors support the importance of sight distance (available visible road geometry) when negotiating bends. For example, models of steering behaviour in research by Donges (1978) describe the control of steering as two parallel processes fed by dual signals of information as opposed to one [81]. The first level relies on near field information a few metres ahead of the car for lateral positioning. The second level uses distant information and is responsible for the anticipation of road curvature. Furthermore, this theory is supported by Land and Horwood (1995) in their studies on the parts of the road that guide steering [79]. By occluding near and far road sections in separate experiments, Land and Horwood (1995) were able to determine which section of the road is relied on most. Results suggested that although it is possible to still navigate with one section of the road hidden, driving tasks with the 'far section' of the road in view resulted in smoother steering [79]. This suggests that if road features somehow obstruct or decrease the drivers sight distance, poorer steering is to be expected.

The experiment developed for Chapter 4 examines the sight distance information available on a variety of open and closed bend types. The 'openness' of these bends is defined by the sight distance available to the driver at the point of entering the road curve. Gradual transitional curves associated with greater sight distances were sampled form Irish motorways and considered 'open bends'. Closed bends were more commonly found on the regional road curve samples and consisted of shorter sight distances. Research has indicated that the degree of openness on a bend can be as important as

curvature in determining where a driver is looking on a bend [82]. For example, studies from Salvucci and Gray (2004) and Kandil (2010) indicate that a driver chooses the fixation point in the scenery available necessary to the actions he/she intends to take [82][83]. If the driver wishes to stay in lane (where openness values are small), then the tangent point is used heavily. However, if the driver wishes to partially leave his lane in order to 'cut a corner' then the end of the bend is relied on heavily. This suggests that the openness of the bend also influences where the driver fixates.

Curve types have been proven to influence 'where' drivers look, however, studies have also shown that external factors such as driver experience (e.g. experienced, novice) can also help determine 'why' drivers look where they do. For example, studies by Crundall & Underwood (2002) further decipher eye behaviours while driving by considering factors such as driving experience. These studies showed that when comparing experienced drivers with novice drivers, cognitive loads for each experience level differed and as a consequence influenced visual patterns [78]. Such visual patterns involved novice drivers fixating directly ahead on the road when confronted with multiple hazards, failing to scan the surroundings of the roadway. However, experienced drivers performed better in these hazardous scenarios demonstrating greater attention capacity and situation awareness. In addition, studies by Underwood and Chapman (2003) report findings as to what can be recalled by drivers of different experience levels. These findings indicate that when presented with hazardous events, learner drivers when asked to recount on information after the event, were unable to recall details surrounding the hazard [73]. Taking this into account the behavioural demands of different geometric factors and furthermore the different levels of

experience, has indicated the important factors to be considered when analysing eye behaviours observed in simulator scenarios.

2.9 Theoretical Foundations for the Analysis of Eye Behaviour

Eye tracking research and applications have continued to grow over the last 30 years[54][84][85]. A factor of this growth can be due to technical advancements being made each year in eye tracking hardware and software [52][54][86]. While research based eye tracking has advanced from Cohen's video frame analysis of eye movements to Zang's low cost wearable video-based glasses, so too have commercial eye trackers. Commercial tracking devices have evolved so quickly, decreasing in size and price, that they too are commonly found in academic research [82][87][88][89]. Much like video-based eye trackers, commercial trackers have progressed from fixed static based monitors (similar to the one used in this research) to the most recent wireless head mounted trackers that feed back eye movement information during real time naturalistic driving scenarios [87][90]. Unlike video recordings (of the eye) these devices use multiple Near Infra-Red Light-Emitting Diodes (NIR-LEDs) to generate even lighting and reflection patterns in the eyes of the user. The advantage of using in Infra-Red sensitive CCD cameras is that they perform far better in low light conditions.

2.9.1 Eye Tracking Apparatus

This research employs the use of a standard fixed based commercial eye tracking device, the Tobii model 1750 (see Figure 2.9). This device was chosen as it was readily available for research from the Psychology Department at Maynooth University. The elements of the eye tracker software used for this experiment will be discussed in Chapter 4 with examples of data obtained by the device. A brief overview of the components and orientation follows. During eye tracking, the Tobii eye tracker (TET) uses near infrared diodes to generate reflection patterns on the corneas of the eyes of the user. Algorithms in the accompanying *ClearView* software calculate the position in space of each eye-ball, and finally the gaze point on the screen. This information is then communicated to a TET server software via USB and Firewire interfaces. The following components shown in Table 2.11 are part of the Tobii model 1750 hardware:

Table 2.11 Summarised components for the Tobii eye tracking apparatus[Tobii manual]

Component	Description
TET Display	The TET 17" display has a maximum resolution of 1280x 1024 pixels (1280 x 768 used for this study to reduce CPU workload). Response time 8 or 16 ms.
Camera	A high-resolution camera with a large field-of-view is used to capture images of the user required for eye tracking.
Near Infra-Red Light-Emitting Diodes	NIR-LEDs are used to generate even lighting and reflection patterns in the eyes of the user.
Optical Filters	Filters are used to block sun-light and to hide components from the user.
Control electronics	Connections Control electronics are built-into the device to handle communication with the computer, and to control the camera and the NIR-LEDs.
Connections	The tracker is connected to a standard PC using a USB cable, a Firewire cable (IEEE-1394) and a VGA cable (Tobii 1750 and Tobii 2150).

Figure 2.9 Tobii Eye tracker showing the default point of origin

Figure 2.9 shows the Tobii eye-tracker showing the default point of origin located in the upper left corner of the screen. During eye tracking the gaze point calculated is then scaled between 0 and 1 with the ***y*** origin at the upper left corner of the screen. For this study the origin was translated to the bottom left corner by subtracting the ***y*** values of the gaze points from the maximum ***y*** value of the resolution being used. This was done to assist in determining gaze distance from the camera view.

2.9.2 Projective Transformation Used for Translating Eye Gaze to Gaze Distance

Homogenous coordinates provide a mathematical framework to describe projective geometry. These coordinates can be used to simulate camera behaviour where 3D objects are mapped onto an imaging plane. In addition they can be used to map between projective planes.. The following homogeneous solution was used to map the eye gaze coordinates (X,Y) coordinates obtained by the eye tracking apparatus to a two-dimensional plane representing the surface of the road. Positions on the road could then be used to estimate gaze distance, the distance from the eye gaze coordinate to the gaze point on the road. This method is used in Chapter 4 to analyse and translate eye-gaze information in order to determine a look-ahead distance on the approaching roads. In order to do this, a plane projective transformation was used as illustrated in Figure 2.9.

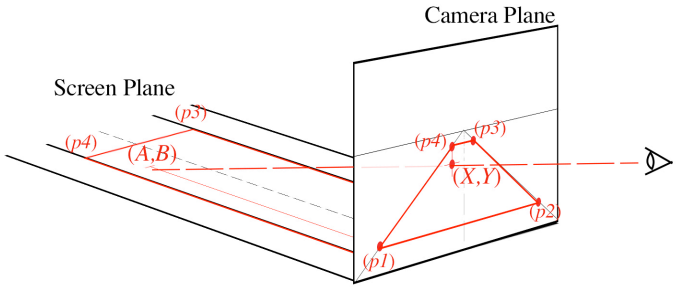

Figure 2.9 Gaze point (x,y) within the *Camera Plane* being transformed to the same corresponding points on the *Screen Plane*

Figure 2.9 shows the *Camera Plane* containing a gaze point (X,Y) being projected to a *Screen Plane* and represented as (A,B) a distance in space (or in this case, a distance along the road). This was achieved by calibrating four points on the *Camera Plane* shown in Figure 2.10. The trapesoid shown in Figure 2.10 shows the 4 initial points and

Figure 2.11 shows the four corresponding points on the *Screen Plane* shown in Figure 2.11.

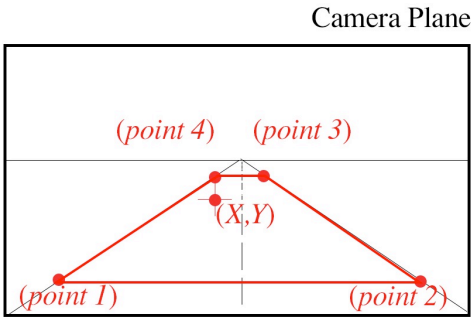

Figure 2.10 Gaze point within (x,y) within the *Camera Plane* (trapezoid) overlaying road leading to vanishing point

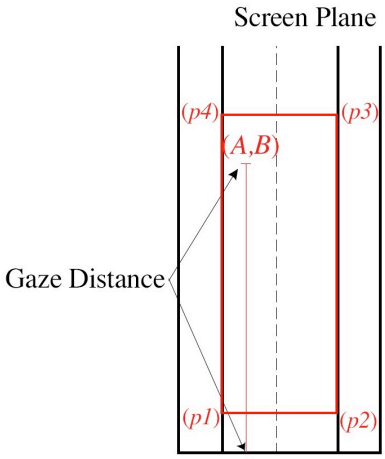

Figure 2.11 Gaze point (a,b) within the *Screen Plane* overlaying road tending to infinity. Also shows *Gaze Distance*.

Thus any Cartesian point found on the plane (or road section) between the lines (*point1 to point4*) and (*point 2 to point3*) on the *Camera Plane* can then be mapped to the corresponding area on the *Screen Plane*. The gaze distance length is then determined by measuring the distance from the ***B*** value of (A,B) shown in Figure 2.11 to the camera position point at (0,B) using a standard Euclidean distance formula (See Eq.2.6) . The projection matrix used for this translation was adapted from the following method used by Fisher (1997) [91][92].

Solving matrix $\boldsymbol{H}$ such that $(a,b) = \boldsymbol{H}(x,y)$

$$\begin{pmatrix} a_1 \\ b_1 \\ w \end{pmatrix} = \begin{pmatrix} h_{11} & h_{12} & h_{13} \\ h_{21} & h_{22} & h_{23} \\ h_{31} & h_{32} & h_{33} \end{pmatrix} \begin{pmatrix} x_1 \\ y_1 \\ w \end{pmatrix} \tag{2.7}$$

Where w is the scale factor and is assigned the value 1 if scale factor is unknown for 4 points. Each point generates two linear equations which are then divided by the scale factor generated ***w.***

$$a_1 = \frac{h_{11}x + h_{12}y + h_{13}}{h_{31}x + h_{32}y + h_{33}}, \qquad b_1 = \frac{h_{21}x + h_{22}y + h_{23}}{h_{31}x + h_{32}y + h_{33}}$$

(2.8)

Fisher's homogeneous solution for dealing with the unknown scale factor in a homogeneous matrix is solved by allowing one of the values of the matrix to have a value. Where h_{33} is equal to 1, the above equations for 4 points can be written as follows

$$\begin{pmatrix} a_1 \\ b_1 \\ a_2 \\ b_2 \\ a_3 \\ b_3 \\ a_4 \\ b_4 \end{pmatrix} = \begin{pmatrix} h_{11} \\ h_{12} \\ h_{13} \\ h_{21} \\ h_{22} \\ h_{23} \\ h_{31} \\ h_{32} \end{pmatrix} \begin{pmatrix} x_1 & y_1 & 1 & 0 & 0 & 0 & -a_1x_1 & -a_1y_1 \\ 0 & 0 & 0 & x_1 & y_1 & 1 & -b_1x_1 & -b_1y_1 \\ x_2 & y_2 & 1 & 0 & 0 & 0 & -a_2x_2 & -a_2y_2 \\ 0 & 0 & 0 & x_2 & y_2 & 1 & -b_2x_2 & -b_2y_2 \\ x_3 & y_3 & 1 & 0 & 0 & 0 & -a_3x_3 & -a_3y_3 \\ 0 & 0 & 0 & x_3 & y_3 & 1 & -b_3x_3 & -b_3y_3 \\ x_4 & y_4 & 1 & 0 & 0 & 0 & -a_4x_4 & -a_4y_4 \\ 0 & 0 & 0 & x_4 & y_4 & 1 & -b_4x_4 & -b_4y_4 \end{pmatrix}$$

[2.9]

Consequently to these series of linear equations, if the determinent ***w*** equals zero then no solution exists. Using this method the system developed in Chapter 4 was able to take eye gaze coordinates recorded by the driving simulator and translate this information to distances along the road. The purpose of this was to determine how far drivers were looking ahead as a result of varying geometry. Furthermore, analyses of these findings are discussed in-depth at the end of Chapter 4.

2.10 Chapter Discussion

This chapter presented background literature and methods related to the two research questions being discussed in this thesis. The first question relating to the effects of road geometry on accident rates began with a preliminary analysis of Irish accident data. By classifying these results into environmental characteristics such as road character, weather condition and road surface, it was possible to determine accident rates associated with these factors in an Irish context. For example, it was indicated that 70 % of accidents on bends occurred in dry weather conditions, thus implying contributing factors other than wet weather conditions. However, it was also noted that greater numbers of accidents occurred on wet road surface conditions than on dry surface conditions (46% wet to 42% dry surface). This contradiction suggests that road surfaces in dry weather conditions still contribute to accident rates as a result of road surface conditions caused by wet weather.

Crash data analysis also showed accident ratios of two fatalities on straight road sections for every one fatality on road bends (approx 2:1). However, upon investigating larger data sets from international safety reports, it was shown that continents like American show contradicting accident ratios of 1:3 (fatalities on straights: fatalities on bends) indicating greater dangers on bends. This may be due to a number of factors. For example, one possible factor could be the size of the measured fatality statistics being compared (America: 42,000 per year vs Ireland: 182 per year), therefore the greater the data set the more accurate or innaccurate the result [24]. In addition, much of the American sample road consisted of straight roadway and therefore may have been safer. These observationss further motivated the need to compare accidents rates per km on

bends with accident rates per km on straight roads and will be discussed in a dimensional analysis in Chapter 3.

Also discussed was the process in which accident data was collected and classified in relation to road character in Ireland. The current process states that the An Garda Síochána give a 'yes or no' binary decision as to whether the accident is on a bend or not. Furthermore, 15% of the Irish accident data remains unclassified for this period. These discrepancies have indicated a need to improve data acquisition both during and after collection. The current study examines how each accident can be assigned a road curvature value by using geo-data of the location of the accident and surrounding geometry.

The literature discussed in this study widely accepts that road geometry is proportionate to accident rates. Furthermore, it is suggested that in order to analyse geometry, various geometric elements must be analysed separately [26]. For example, 'horizontal curvature' was reported the most significant geometric element contributing to accident rates. In addition, horizontal curvature was also deemed more dangerous when measured consecutively, therefore the use of transition curves were discussed for improving road safety [28][29][31]. However, it is important to note that although horizontal curvature is considered an important factor in road safety, some studies show that insignificant changes in accident rates were measured when bends were replaced with straighter road sections [21]. In addition, it was suggested that the use of gradual transition curves have a negative affect on safety by encouraging the driver to maintain greater speeds unaware that they are approaching subsequent turns, thus, resulting in abrupt speed changes. Nonetheless, quantitative studies have verified that curvature remains an important factor when measuring causes of accident frequency. For

example, research highlighted in this section, showed increases in accident rates as a result of curvature beneath 200m (sharp bend)[22]. For this reason a method to measure the radius of curvature was described and is further implemented in Chapter 3.

The second question in this thesis relates to how road geometry affects driver behaviour. This topic heavily intertwines with the first question as the related studies showed that geometric changes in road features contribute to changes in driver behaviour, (such as driving speed and eye movement) resulting in decreases in accident frequency. For this reason, the second section of this chapter further examined literature and methods related to how the geometry of the road can influence different actions such as eye movements. Results of these studies show that the tangent point of the curve (where the driver's line of sight meets the point at which the road curves) was the area attended to most frequently when traversing bends. In addition, studies showed that visual cues at the same angle of curvature as the tangent point could also be used by the driver for smooth steering orientation. However, while it has been determined that the tangent point is the main area of fixation on the bend, studies have also indicated the difficulties in determining why drivers eye movements 'scan the way they do'.

When asking 'what' drivers are looking at, conclusions can be made that dual functions of the eye like peripheral vision make physiological measurements very difficult. Studies have shown that fixating on further sections on the road allow smoother negotiation while looking near field increases steering errors[79][81]. This was discovered when experiments showed that dual signals of the eye were used to monitor separate sections of the road and thus increases the need for adequate sight distance to reduce cognitive load on a bend. Similarly, studies showed how geometric features like

the ‘openness’ of bends can lead eye movements to rely on different sections of the road.

When asking ‘why’ drivers look at certain features, it was suggested that action or task based decisions be considered and also factors such as the experience of the driver. For example, research on open and closed bends has shown that the tasks or actions associated with the road may also be a key factor in understanding where the driver is looking [82][83]. In addition, models of drivers attention based on information bandwidth have indicated that drivers with higher levels of experience cope with more information including factors such as traffic level, conditions of roadways etc. while presented with hazardous situations [78].

While section one of this chapter highlighted the importance of ‘curvature’ as a causal factor to accident rates, findings from the second section of this chapter indicate ‘sight distance’ as a factor of equal importance. In order to understand how much of this sight distance was accessed during driving, a driving simulator was developed to measure eye behaviour. A brief history of the driving simulator was described in order to evaluate its use as an effective measurement tool. The use of a plane projective transformation was described as a method to transform eye gaze recorded by the simulator into look-ahead distances . This method is used in Chapter 4 to analyse data in order to assess how far ahead on the road drivers look on different variations of geometry.

Chapter 3

Analysis of Accident Data with Geometric Characteristics

The following Chapter documents the experiment undertaken to test the effects of road geometry on the rate of Irish accident occurrences. The experiment combines three large data sets in order to estimate accident occurrence rates on contrasting Irish road types specific to road geometry. The first two datasets were accident locations combined with a digital map of the Irish road network. This information produced a mapping system with the ability to allow selection of individual roads and the accidents associated with that road. A local road curvature value was then generated for each of the given accident locations to create a third dataset. The curvatures associated with each accident were then classified into size bands to compare the radius lengths of three contrasting road types (motorway '*M'*, national '*N'* and regional '*R'*). An *accident to radius of curvature* (ARC) rate was then estimated for the given road type. Findings showed highest ARC rates on the N road category.

3.1 RSA Data Acquisition

The Irish RSA provides an online GUI that allows the public to view annual crash statistics [93]. For an average user, the web interface allows access to accident information one accident at a time, however it does not facilitate the selection of a single road. For this experiment it was necessary to acquire these statistics in their default form to avail of any information that would help in identifying road environment factors. The RSA of Ireland provided a comprehensive data set spanning from 2009-2012 in the form of four separate comma separated value (CSV) files. This four-year data set consisting of over 23,000 chronologically ordered accident points included over 150 parameters and surrounding factors for each accident. Parameters such as 'pedestrians involved'; 'primary collision type', 'severity of accident', 'time of crash' and 'lighting conditions' were some of the many factors reported for each incident. Each of these parameters were also classified by many different types of severity and scale. For example 'accident type' was classified by three characteristics 'fatal', 'severe', 'minor'. The parameters primarily investigated for this experiment are shown in Table 3.1. As discussed, studies have shown that the most common type of crashes that occur at horizontal curvature are run-off-road (76%) crashes suggesting single car accidents are more likely to be due to geometry [24]. Therefore the chosen parameters in Table 3.1 specifically relate to accidents involving a single vehicle negotiating a bend under various road surface conditions. Accidents involving multiple cars while negotiating bends were also examined in this study. However with the added complication of extra vehicles involved, they were excluded as accidents likely to be caused solely by bad road geometry.

Table 3.1 Listing of the parameters used and how they are classified.

Accident Parameter	Classifier
Year	2009 2010 2011 2012
Roadchar1 (Road Characteristic)	1 Straight 2 Bend 3 Hillcrest 4 Gradient 5 Other
Surface (Road Surface)	1 Wet 2 Dry 3 Frost/Ice 4 Snow 7 Other 8 Unknown
Weat1 (Weather)	1 Dry 2 Wet 3 Frost/Ice 4 Snow 7 Fog/mist 8 High Winds 7 Other 8 Unknown
Noveh (Number of Vehicles)	Described by number of vehicles accounted for.
X,Y (Geo-Location of Accident)	*Provided in Irish Grid Reference

*Although Years 2009-2011 were provided in Irish Grid (IG) Reference, 2012 was provided in Irish Transverse Mercator (ITM). All data was made uniform to IG.

3.2 Road Network Data Acquisition

Extensible Mark-up Language (XML) files which describe the geographical layout of areas can be accessed from the Open Street Map website [94]. The information generally has three primitive data descriptors that are ‘nodes’,’ways’ and ‘relations’ [95]. Nodes consist of a single point in space measured by longtitude and latitude. ‘Ways’ are ordered lists of nodes and ‘relations’ are ordered lists that use node information to link ‘ways’ for example for the use of ‘bus routes’. It is ‘ways’ that were extracted in this study. The parsing process of extracting these primitives is discussed in Kaneswaran et al (2013) whereby the XML information between ‘way’ opening and ‘/way’ closing tags was used [66]. However, once parsed this file was converted to a file where each line represented a road. The line contained the road name followed by CSV representing the GPS coordinates of points along the road. The location data used has the format shown in Figure 3.1

M8,52.3950313:-7.9197847,52.3954123:-7.9193167,.....
M9,52.4029188:-7.1870812,52.7737473:-6.9465602,.....
N1,54.0934581:-6.3601141,52.6494020:-7.2286934,.....

Figure 3.1 Road Data Extert

The OSM data resource was used extensively in the primary stages of the experiment to generate a map of national road network of Ireland. This data was crowd sourced therefore it contained a variable quality of road information.

3.2.1 Mapping Accident Points to the Road Network

With a definitive list of over 3000 roads, a visualization of the entire Irish road network was generated. Generating the entire network rather than individual roads made it possible for concentrated accident points to be examined as a whole much like a heat map.

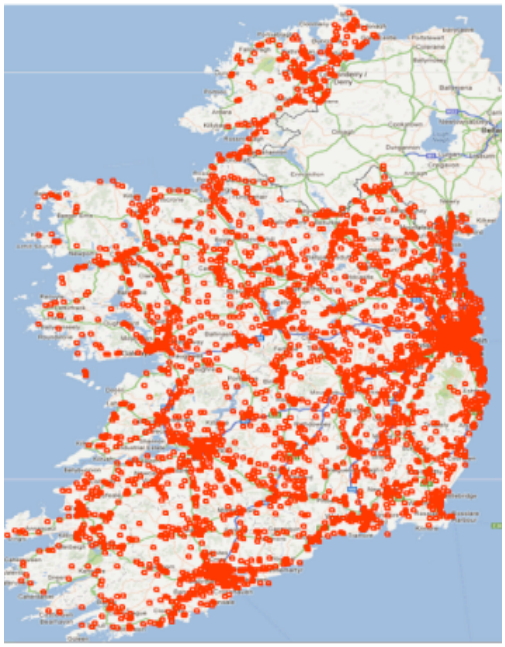

Figure 3.2 Output of mapping system GUI for 2010 accident data showing concentrated accident areas

Figure 3.1 shows a map generated using Windows Forms Application written in C# that is layered with the Irish road network and then overlaid with accident points (red circles). The software development for generating this mapping system will be described later and in more detail to include a description of the functions added after the mapping phase of the work. As expected, accident concentration was present around highly populated areas, however, the figure also shows concentration along other routes

like the ‘N25’ from Cork to Waterford. This process gave an early indication of accident-prone areas and routes, which helped to determine routes to analyse further.

3.2.2 Techniques Used to Acquire Geodetic Points and Increase Data Quality

As one of the primary purposes of this experiment was to measure road geometry, it was vital that the OSM road network geo-data used to draw road routes were adequate for use. However, upon testing it was evident that many of the roads held insufficient data. Roads points were sparse, specifically on the regional routes. Interpolation methods were developed by adding evenly spaced points between missing segments, however, some distances were too great resulting in many “straight lines” on the road segment when road points were joined. For this reason the OSM road data was abandoned and a new method to increase data quality was used. Up to this time the OSM data provided the most efficient way to view the entire map network as a whole and used only a fraction of the time necessary had the selection of over 3000 roads been done manually.

Commercial software products like Google Maps allow for routes to be generated by creating directions from for example point **a** to destination **b**. Advancements have also been made in these systems to allow a user to manually drag or manipulate the destination points and to then export these edited routes as XML based files or KML (Keyhole Markup Language) files. However, the process for adding alternate routes between departure and destination points in order to travel ‘via’ rural roads proved to be very cumbersome in Google Earth© and Google Maps©. Therefore an additional software “TyretoTravel” was used [96]. TyretoTravel © provided better route and

waypoint editing and similarly outputted KML files. Figure 3.3 shows sparse data of a segment of the M4 motorway taken from OSM and also the improved data using KML information generated from the Google Maps © database and further manipulated in TyretoTravel ©.

Figure 3.3 Arial view of M4 (20km resolution)
road segment with gaps (OSM) vs improved dense data (Google Earth)

Much like the OSM data mentioned, the KML files contained *tags* that described the structure of the document such as *headers*, *namespace declarations* and *placemarks*. For the purposes of manual road selection a list of latitude and longitude points were extracted from the *coordinate* section of the KML files.

A selection of motorway '*M'* (700km), national '*N'* (700km) and regional '*R'* (350km) roads were selected. Each road was then manually parsed to remove unwanted KML information. Figure 3.4 shows the selected roads for each road type.

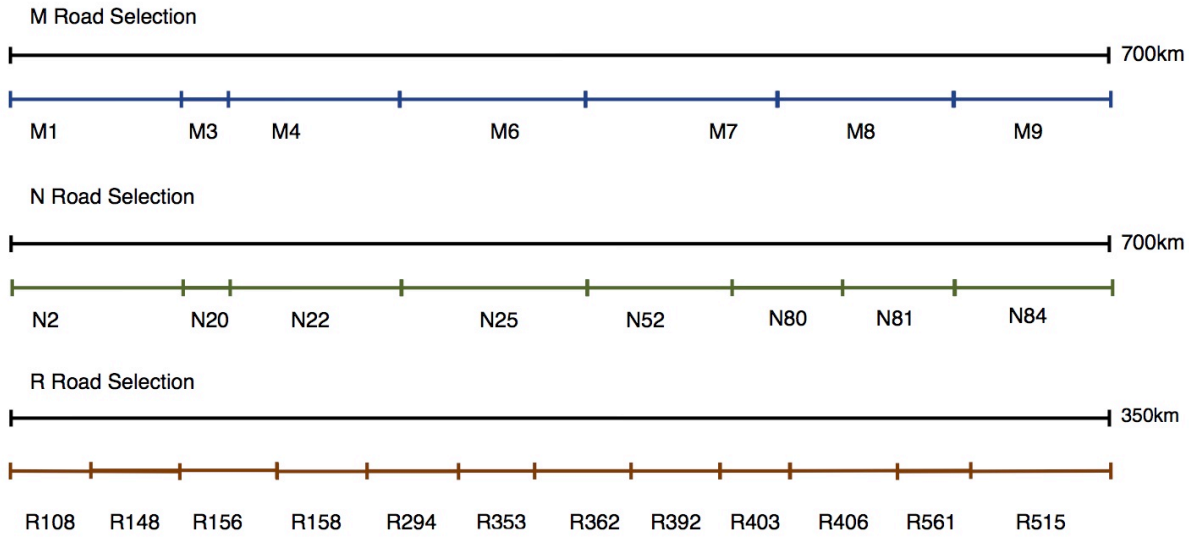

Figure 3.4 Road Type Selections

The selected M roads were chosen as they offered a contrast of high-density traffic on fixed-constant road geometry. The N roads were also chosen for high traffic ratios. The N road information was selected on the basis of a) being the primary route between two towns without the need to enter the motorway, b) for their presence of road bends and c) as some of the roads showed accident concentration in the existing mapping system. The R roads, which in general held lower ratios of traffic, were selected using the same criteria for (b) and (c) associated with N roads. The new refined road network with improved data quality was then integrated into the mapping system were a process to associate accidents with the nearest road was then developed.

3.3 Software Development

To examine the local geometric characteristics of the accident points a system was developed in C# using Microsoft's IDE 'Visual Studio 2010'. The GUI developed in *VS 2010* consisted of two form windows. The *Form1* window (default name given to form window by *VS2010*) was designed to create a visualisation map of the accident data as shown in Figure 3.5. Figure 3.5 shows the GUI for *Form1*. The left side of the figure shows the accidents overlaying a road map of Ireland. The right of the image displays the interface developed for annual data selection and a populated listbox of the predefined road types for individual road selection. Following selection of an individual road, a second Windows form panel "Form2" was then started.

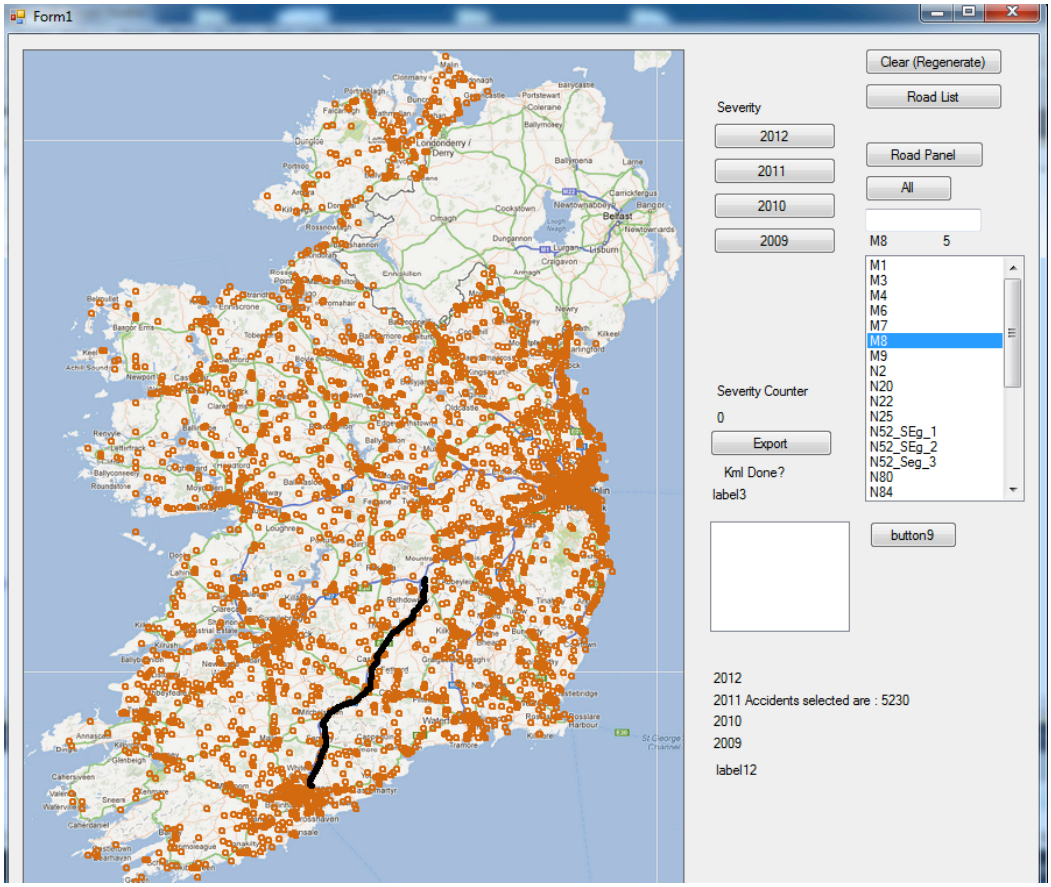

Figure 3.5 Form1 road selection tool with 2011 accident data selected.

3.3.1 Form 1 System Process Chain

Two main streams of data were processed within this form; road and accident data. The data from each file was read into the program using the *streamReader* function. Figure 3.6 shows the system chains for *Form1*.

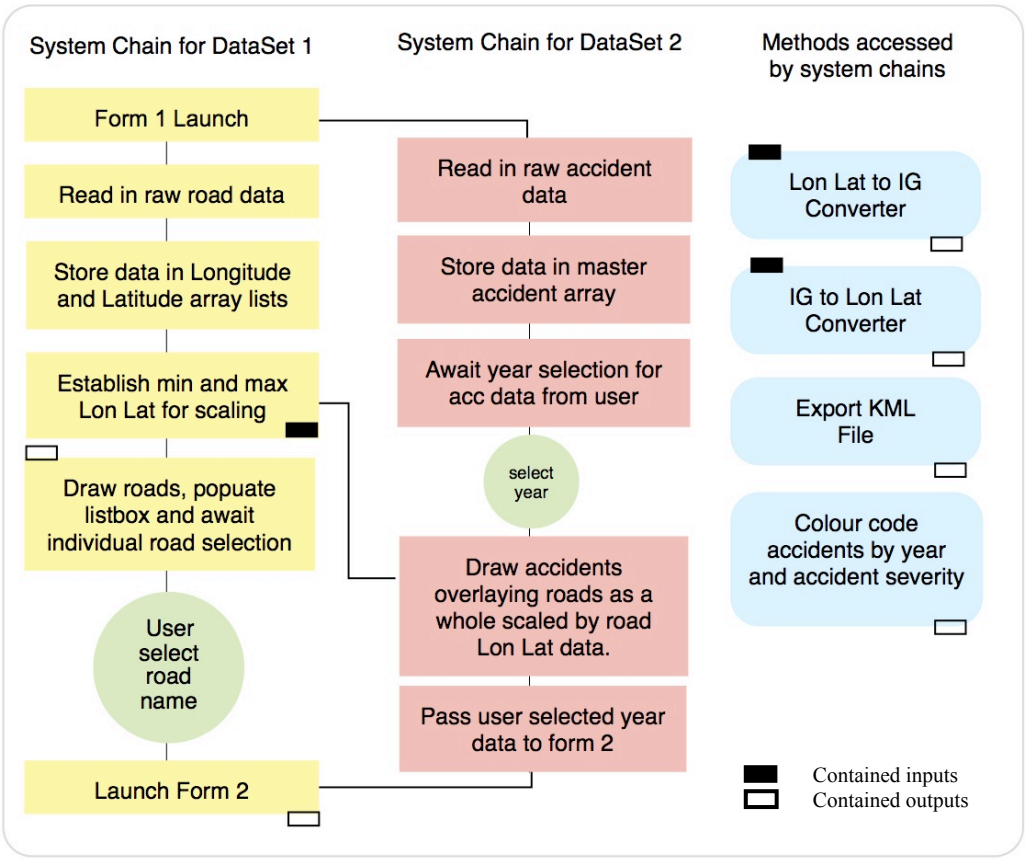

Figure 3.6 System model for Form1 mapping process for two Datasets

The road data set (see *DataSet1* in figure 3.6*)* was acquired in the UTM longitude and latitude (LL) decimal degree format. However, the accident frequency data set (see *DataSet2* in figure 3.6) was acquired in the Irish Grid (IG) format. A method for parsing from LL to IG was implemented within the code to convert to IG formats. In addition, a method was also integrated to convert back from IG to UTM LL when needed.

Typically the larger data set was left in its original state to minimise the number of points that required conversion. In *Form1* the larger dataset was the road data set, however, in *Form2* the accident data set was larger.

The points being displayed were scaled based on the minimum and maximum values of the road longitude and latitude values. Both data sets were scaled to the bounds of the Ireland land map using the below coordinates which are approximately the furthest land points on Ireland's west, east, south and north coast. This was so that the co-ordinates were in register with the map of Ireland used as a background image on the form.

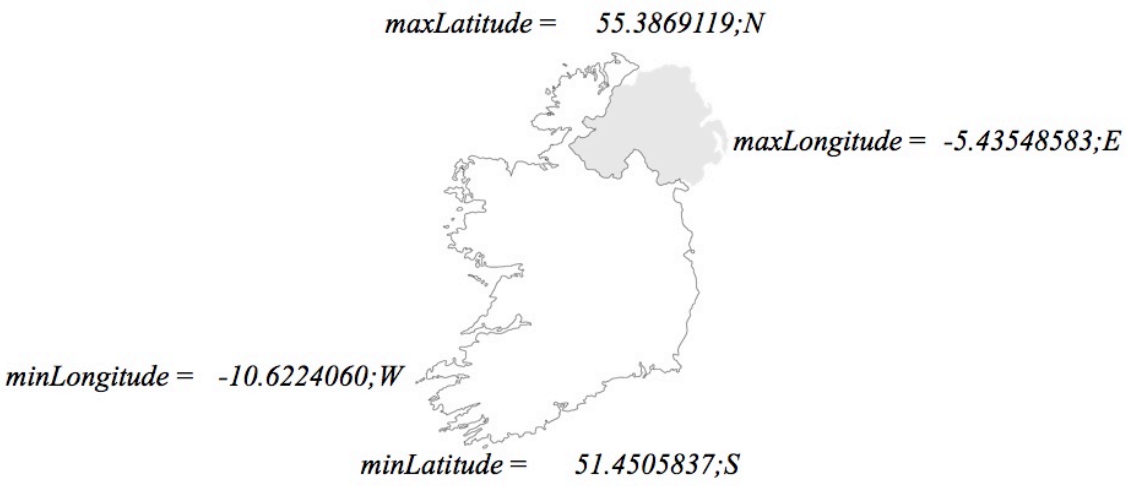

Figure 3.7 Ireland Boundary Points Used

The scaled data was then used to generate a map overlay on the left panel shown in Figure 3.5, using the *graphicsObj* function for visual verification. The 23,000+ accident points were also separated and colour coded by year of occurrence. Finally the last step in the system chain for *Form1* was to await an individual road selection from the user in order to start *Form2*. In addition, a KML export function was developed in this form so as to convert the points to a KML format for both the accident and road data. By

exporting the accident data as KML throughout the chain it allowed for the validation of accident points outside of the mapping software. An example is described in *Section 3.3.6* of how online resources were used to validate accident points.

3.3.2 Form 2 System Process Chain

Form2 was used to generate a visualisation map of the selected road on a magnified scale. The individual road selected from *Form1* was displayed showing the nearest accidents to the road. The system used in *Form2* generated the radius of curvature for each road point and the nearest accidents. Figure 3.8 shows the interface for displaying the road mapping information. List boxes were used to display normalised points (see Section 3.3.3), accident points and radius measurements, all of which were outputted to a comma separated file for statistical analysis.

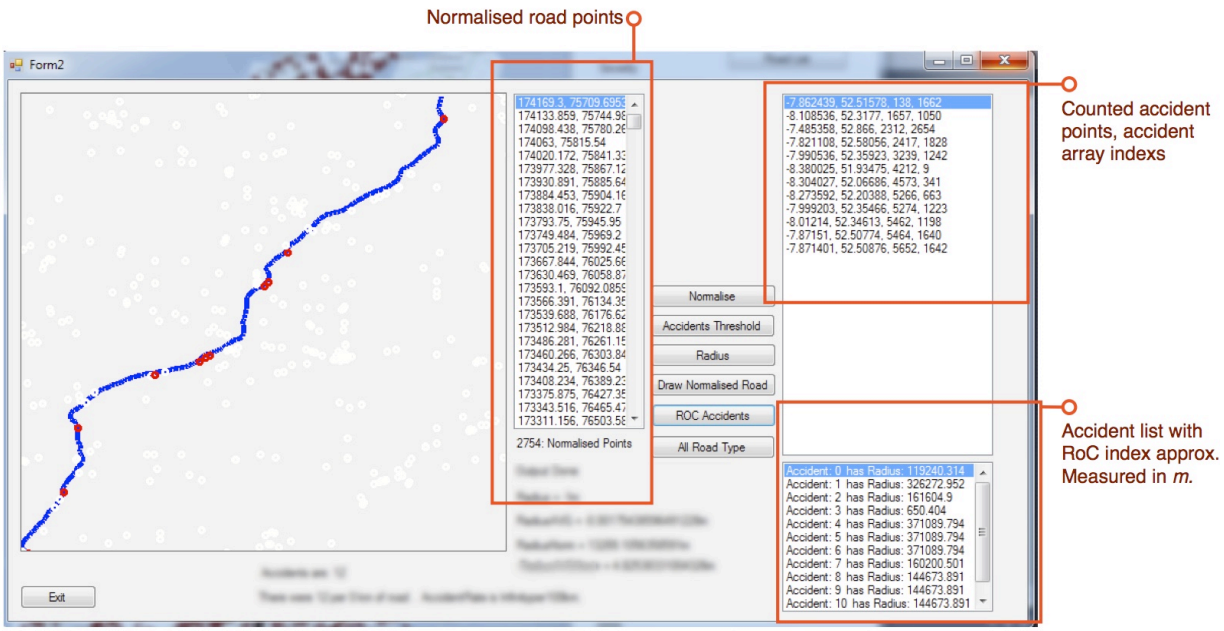

Figure 3.8 Form 2 showing accidents binding to the M8 and listboxes displaying output data.

The two data inputs for *Form2* were the *selected road* points and the accident data for the *selected year*. Figure 3.9 shows the system chain for *Form2* and the methods used to generate the result output data.

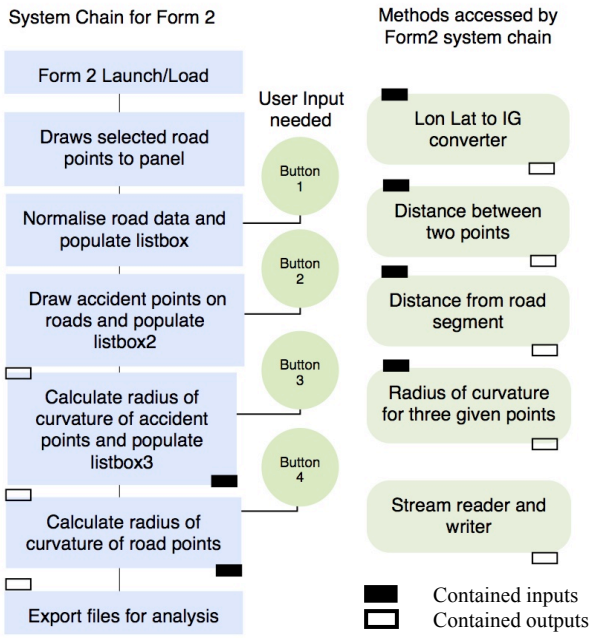

Figure 3.9 System Chain for Form2

Once launched, *Form2* automatically generates a graphical representation of the road segment in the left panel shown in Figure 3.8. This distance on the road segment between each road point was evenly spaced in order to normalise the data.

3.3.3 Normalisation

The points were normalised as some of the road data, in particular, motorway segments had bidirectional road points either close together or far apart. This un-equal distance between points caused difficulties when measuring the radius of curvature (RoC) as shown in Figure 3.10. Road points measured far apart were assumed to be long straights. If the points were gathered or clustered together then the RoC measurement assumes that the road is a very sharp bend.

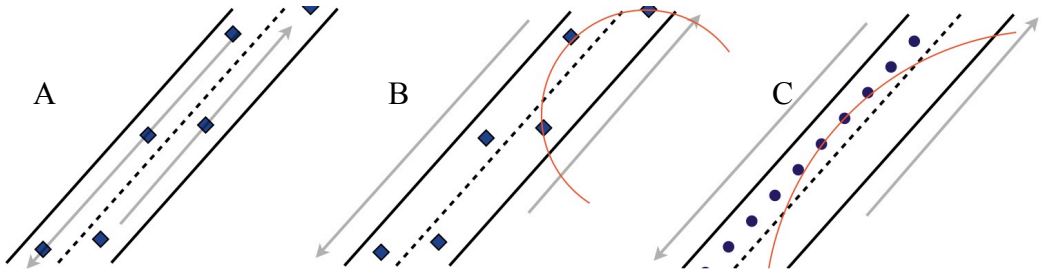

Figure 3.10 Showing the radius measurements including data from opposing lane and the normalisation solution.

Picture (A) in Figure 3.7 shows the raw data on some of the motorway road points where the road path is bidirectional. (B) shows how the road points from both lanes caused issues with measuring the radius of curvature (RoC). Picture (C) shows how normalising the points improved the RoC measurement and better represented a straighter road by having a larger arc. Note: Figure 3.10 is a mere representation of the normalisation process, curves shown in (B) and (C) are not actual measurements.

In order to remove these duplicate nodes a normalisation process was achieved by reconstructing a new list of road points starting at the first road point. A loop was used to iterate through the road points until the distance between the current point and the selected point was greater than a predefined ***d*** distance given. If the distance between

the two points was equal to ***d*** then this point was used as the next point in the normalised list. This next point became the start point for the next closed loop. If the distance between the two points was greater than ***d*** then a point is generated at ***d***. A default ***d*** of 50m was used as a minimum distance between points. This form of linear interpolation generated a new road list with points of equal distance following the natural route of the road eliminating lateral points in the opposing lane.

3.3.4 Distance to Line Segment

After normalisation occurred the distance from each accident to the local road segment was calculated. This was achieved by using a parametric equation for finding the distance from the accident point *C* to the closest line determined by points *A* and *B* [97]. The following method was used.

Where accident point ***C*** = *(Cx,Cy)*

Road segment/ Line ***AB*** = (Ax,Ay) to (Bx,By).

P is the point of perpendicular projection of ***C*** on ***AB***.

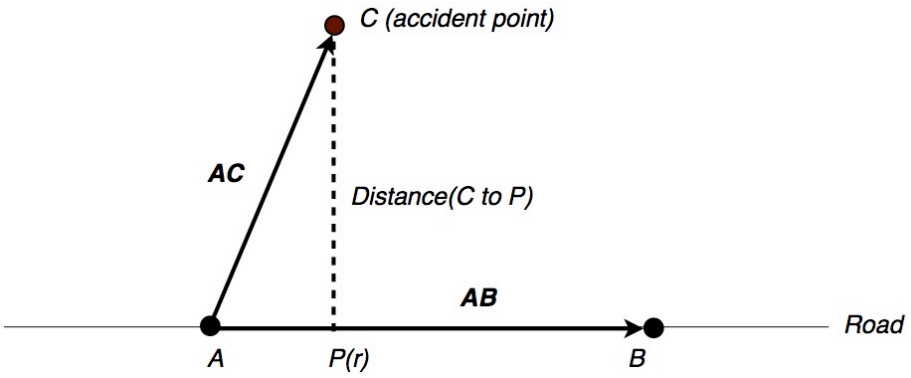

Figure 3.11 Parametric equation of the accident point *C* and its relative *vectors AC* and *AB*

The parameter ***r***, which indicates ***P***'s base position along ***AB***, is computed by the dot product of ***AC*** and ***AB*** divided by the square of the length of ***AB***:

$$r = \frac{AC \bullet AB}{|AB|} \tag{3.2}$$

Where **r** has the following meaning:

$r = 0$	***P*** = **A**
$r = 1$	***P*** = **B**
$r < 0$	***P*** is on the backward extension of **AB**
$r > 1$	***P*** is on the forward extension of **AB**
$0 < r < 1$	***P*** is interior to AB

The length of a line segment in 2 dimensions, AB is computed by:

$$L = \sqrt{(Bx - Ax)^2 + (By - Ay)^2} \tag{3.3}$$

and the dot product of two vectors in 2D, U•V is computed:

$$D = (Ux \times Vx) + (Uy \times Vy) \tag{3.4}$$

So that (3,4) expands to:

$$r = \frac{(Cx - Ax)(Bx - Ax) + (Cy - Ay)(By - Ay)}{L^2} \tag{3.5}$$

The point P can then be found:

$$Px = Ax + r\,(\text{Bx-Ax})$$

$$Py = Ay + r\,(\text{By-Ay}) \tag{3.6}$$

And the distance from ***A*** to ***P*** = ***r*** * **L**.

The local segment calculation was now achieved by binding each accident to its local road segment, however, in order to associate an accident event to a specific road and not include other nearby roads, a technique to calculate the threshold value was first developed and verified.

3.3.5 Threshold Calculation

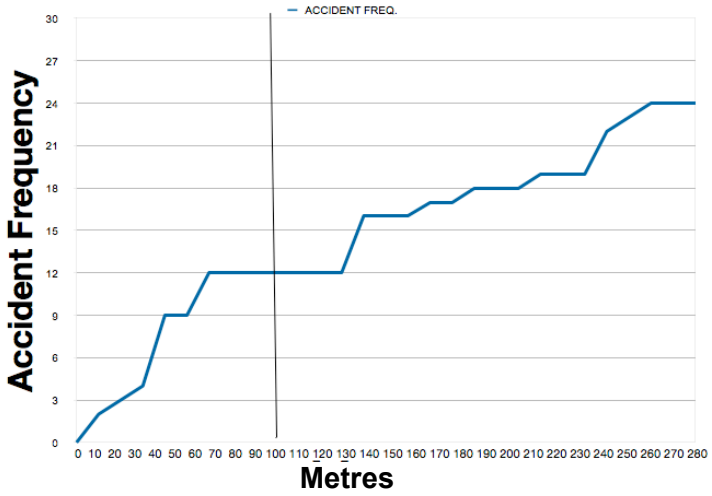

Fig 3.12 Threshold calculation of nearby accidents on the M8

Figure 3.9 shows the threshold calculation for a selected road (M8). A clear plateau, predicting a value of 12 accident occurrences on this roadway, can be seen. This gives a threshold value of approximately 100m, automating a distance limit for each accident

event for all other roads. The threshold was calculated by incrementing the distance between each accident and its local segment. If the distance between the accident and the nearby road segment was 10m then it was counted. The distance was then incremented to 20m and so on. Using a closed loop in *Form2* these increments continued for thirty steps (300m). This preliminary calculation was run as a calibration process therefore it is not included in the system chain for *Form2* mentioned earlier.

3.3.6 Validation of Nearby Accidents

In order to ensure that the correct geo-position for each accident was being generated and that the accidents were being correctly linked to their closest road without including nearby roads, two verification processes were undertaken. First, a KML export function was developed to record the accident occurrences. By encasing and exporting this accident information in a KML format it allowed verification using the Google Earth mapping system. Figure 3.13 shows 5 accidents (yellow pin drops) that were rejected by the M8 road information. Although the accidents look to have occurred along the M8 motorway, the accidents in fact belong to the R639 as shown in Figure 3.13 (b).

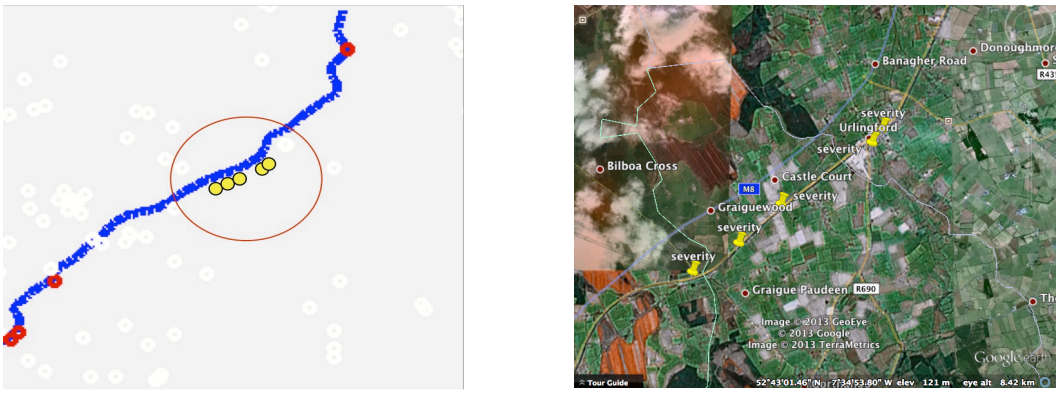

Figure 3.13 (a) Windows Form 2 displaying 5 nearby rejected accidents and (b) KML file with accident information loaded into Google Earth image confirming the rejected accidents on the R639 Road (parallel to M8)

The GUI system developed by the RSA of Ireland shown in figure 3.14 was also used as the second verification tool. A manual visual count of accident information was collected for random road types to ensure the definitive RSA of Ireland accident count matched the accidents being generated by the computer program developed for this system.

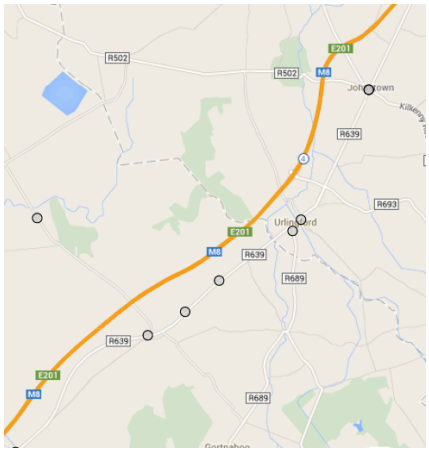

Figure 3.14 Screenshot of RSA online GUI displaying accidents close to the M8

3.3.7 Radius of Curvature Implementation

The RoC measurement was achieved by assigning a local measurement to each of the verified accidents. The two nearest road segments where chosen and the distance to each was achieved using the distance to segment formula discussed in section 3.3.4. Figure 3.15 illustrates the method used to examine local road segments between three normalised points. The normalised points before the accident, the point after and the middle point closest were used (***A,C*** and ***B*** respectively).

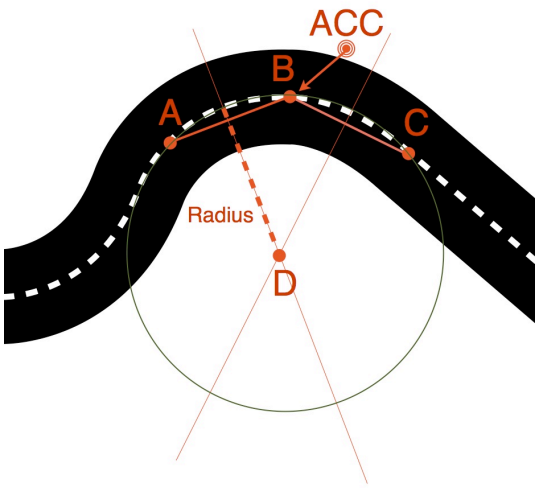

Figure 3.15 Accident (ACC) being assigned point *B*'s Radius of Curvature

The radius was calculated using the circumcentre of the three points as shown in Figure 3.15 and mentioned in Chapter 2. The distance between the circle centre and any of the three given points is the radius length for the middle point ***B*** closest to the accident ***ACC***. This radius of curvature was then assigned to the accident ***ACC*** as a value measured in meters and outputted to a comma separated file along with relevant accident data for statistical analysis. To provide environmental information for each accident, the RoC was also generated for each normalised road point and outputted to a separate file for weighted distribution and dimensional analysis. This was achieved using an identical

assignment process to the accident point but in this case the middle point for every three points examined inherited the RoC value instead.

3.4 Results of Data Analysis

The system for binding roads described in section 3.3 combined accident data and road information in order to assign each data set with RoC values. This section describes the process used to analysis the relationship between the physical quantities of these RoC values for each data set.

Data from the code developed in section 3.3 included the RoC values for each accident point and the RoC values for each road point for a distance of 700 km of motorway, 700 km of national roadway and 350 km of regional roadways. The accident counts examined for each of these selected road types are shown below in Table 3.2.

Table 3.2 Accident count per road type measured.

Road Type	Accident Count	Road Length
M Roads	439	Approx 700km
N Roads	954	Approx 700km
R Roads	316	Approx 350km

Both the road points and accident points were binned into 16 radius bands based on their RoC value. The 16 sections of each radius band consisted of 100m increments stopping at 1500 metres. Data above radius lengths of 1500m contained large values tending towards infinity, these lengths were deemed as straight roads. Othman et al (2009) deemed any curve above 1250m a straight section although it was noted that European road standards have reported gradual transitional curves for motorways as big as 1000m

on motorways for speeds of 140mph [16][98]. For this reason a maximum band value of 1500m was chosen to ensure all values about this length were almost straight if not gradual curves.

A set of 15 size bands remained under radius lengths of 1500m. By using small radius bands it was possible to analyse radius lengths of curves contributing to accident frequency the most. Results of this frequency count are shown in Figure 3.16 (a)(b)(c).

Figure 3.16 (a) Accident count per RoC band of motorway roadway measured

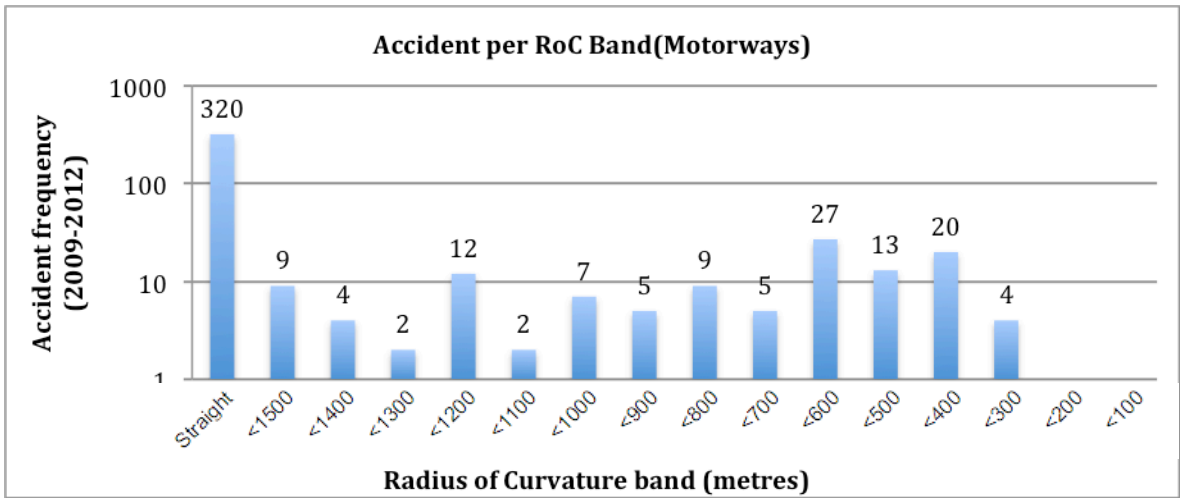

(b) Accident count per RoC band of national roadway measured.

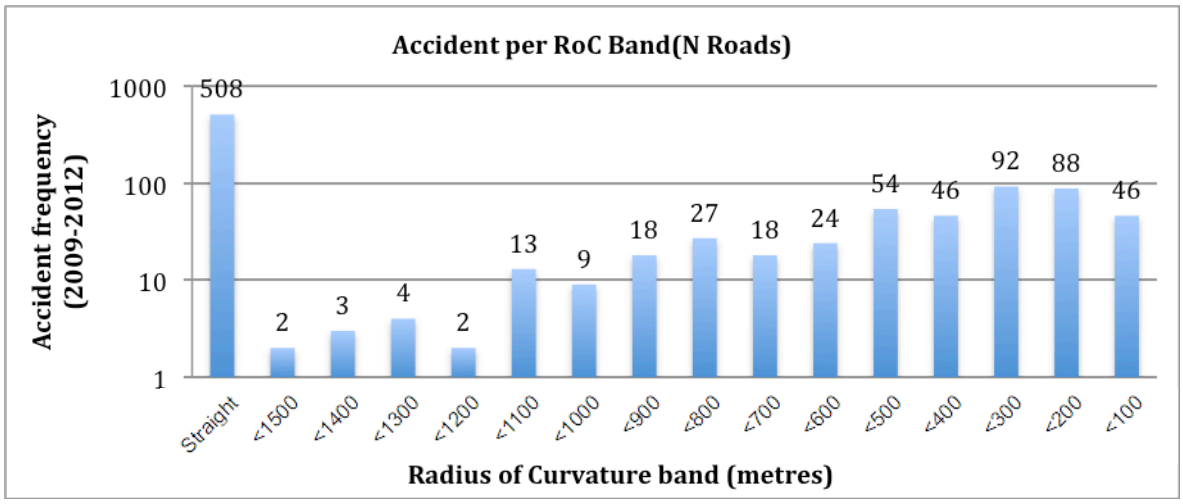

(c) Accident count per RoC band of regional roadway measured.

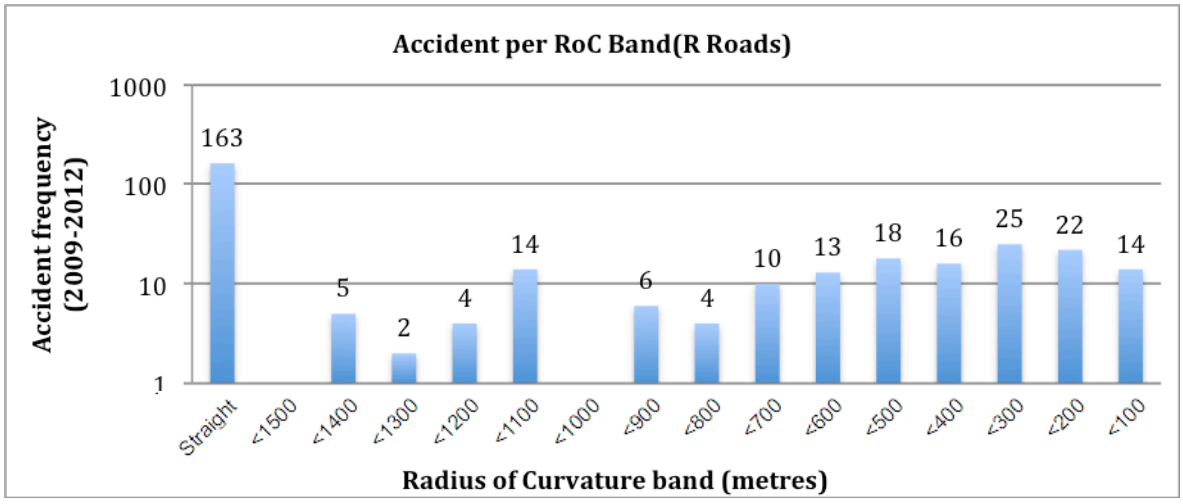

What is clearly shown in the data for all three types of road is that the majority of accidents happened on straight sections. Out of the total accidents that occurred on the given road type, 73% accidents occurred on straight sections of M motorways, 54% of accidents occurred on straight sections of N roads and 58% of accidents occurred on straight sections of R roads. With a combined average of 61.6% this value generated from the sampled road segments showed similar frequency to that of the percentage of accidents recorded by the RSA of Ireland. In Table 2.1 the RSA reported an accident frequency of 64.8% on roads with straight characteristics.

Frequencies measured amongst the remaining bands (less than 1500m) showed no accidents at motorway RoC bands less than 200m. In motorway design, values of 650m are used as the minimum horizontal radii for transitional curves for speeds of 120km/h as mentioned in *Section 1.4.2*. This may indicate why peaks of accident frequencies appear at radius lengths of less than 600m in Figure 3.16 (a) on motorways whereby drivers may not have reduced speeds to cope with the given bend.

Gradual increases on both the N and R roads were observed for RoC bands less than 1000m. Preliminary observations of these results indicated that as curvature became bigger on the N and R road types, accident rates increased in accordance with research discussed in Chapter 2. However, M roads radii lengths below 1500m on motorways show random distribution and no accidents below 200m. It was estimated that this was due to motorways not consisting of many bend sections with this radius length. At this point, observations from the M Road data indicated that in order to fairly distribute accidents amongst radius bands, a further analysis of the ‘percentage of road’ within the same RoC band was necessary.

For example, to conclude that 50% of accidents occurred on straights on a road that consists of 50% straight geometry indicated a 1:1 ratio or accident rate. The accident rates that interested this study most were higher than average accident frequencies for a given curvature per kilometre of road. To fairly distribute the accident frequency amongst radius bands, a process to include the percentage of road points in the same radius band was included.

As mentioned, the road point curvature values generated and assigned by *Form2* were also binned into 16 radius bands. The percentage of accident frequency allocated to each radius band was directly compared to the percentage of road points occupying the same bin in order to normalise the data. The percentage of frequency of both values are shown in part (a) of Figures 3.17, 3.18 and 3.19 for each road type M, N and R respectively.

In addition, using dimensional analysis an accident per road curvature (ARC) rate was then calculated by dividing the accident frequency percentage by the road point percentage in the same radius band as shown in equation 3.7.

$$\frac{\%\text{ of Accident Points } x \text{ RoC}}{\%\text{ of Road Points } x \text{ RoC}} \tag{3.7}$$

A unit of measurement is then further calculated by dividing this ARC rate by the length of the road type measured and the time period measured to produce an ARC rate *per km per year*. The results of which are also shown in part (b) of Figures 3.17, 3.18 and 3.19.

(a)

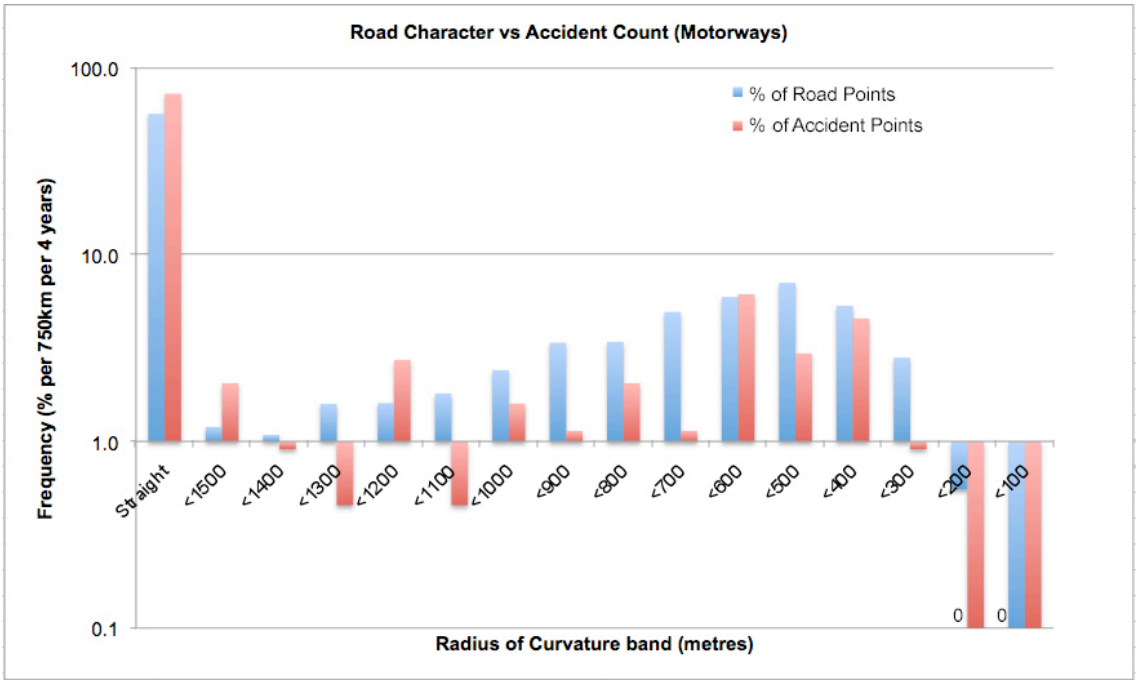

(b)

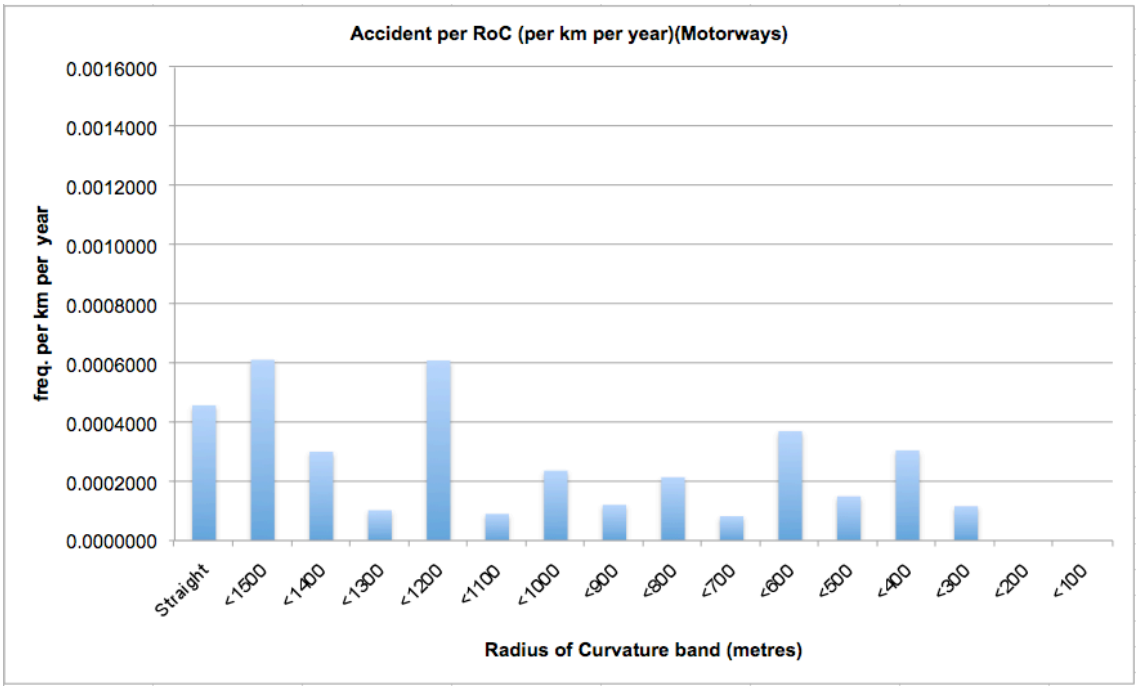

Figure 3.17 (a) shows the percentages of accident frequency and road points within the same RoC band for Motorways and Figure 3.17 (b) shows the ARC rates generated by these comparisons.

(a)

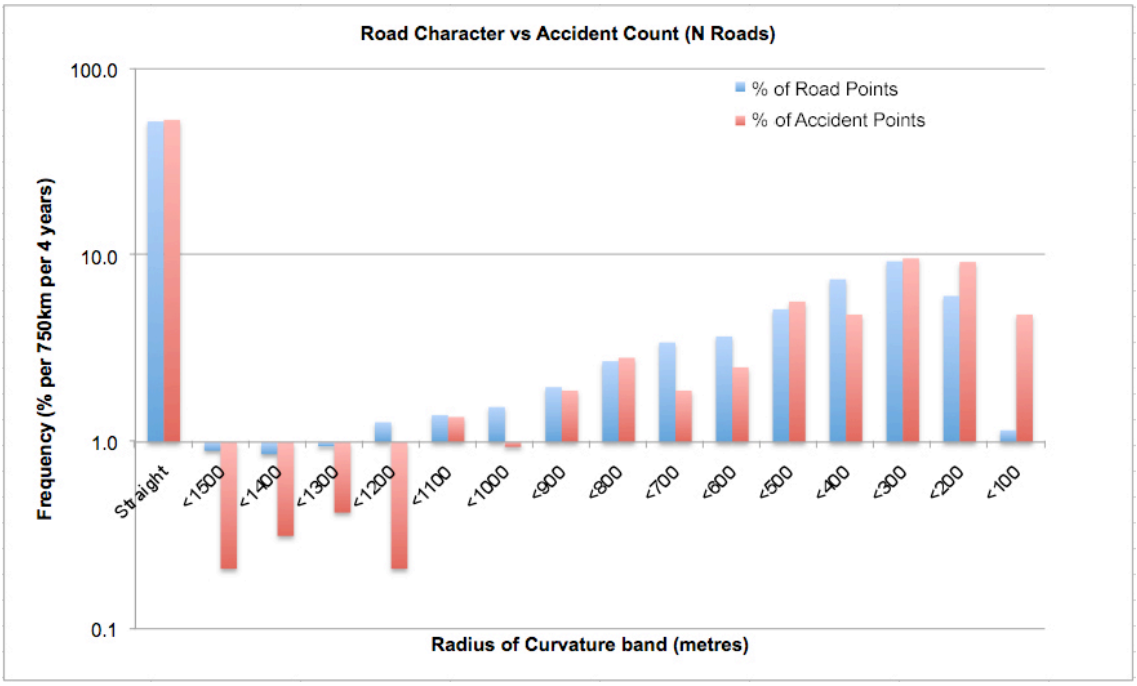

(b)

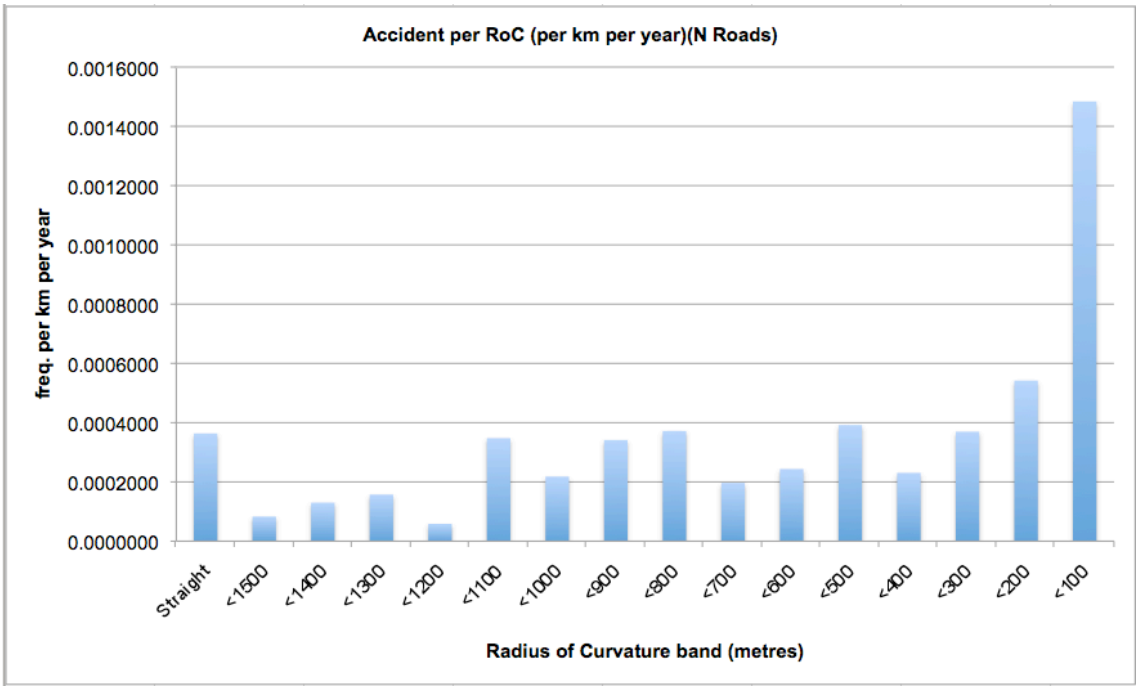

Figure 3.18 (a) shows the percentages of accident frequency and road points within the same RoC band for N roads and Figure 3.18 (b) shows the ARC rates generated by these comparisons.

(a)

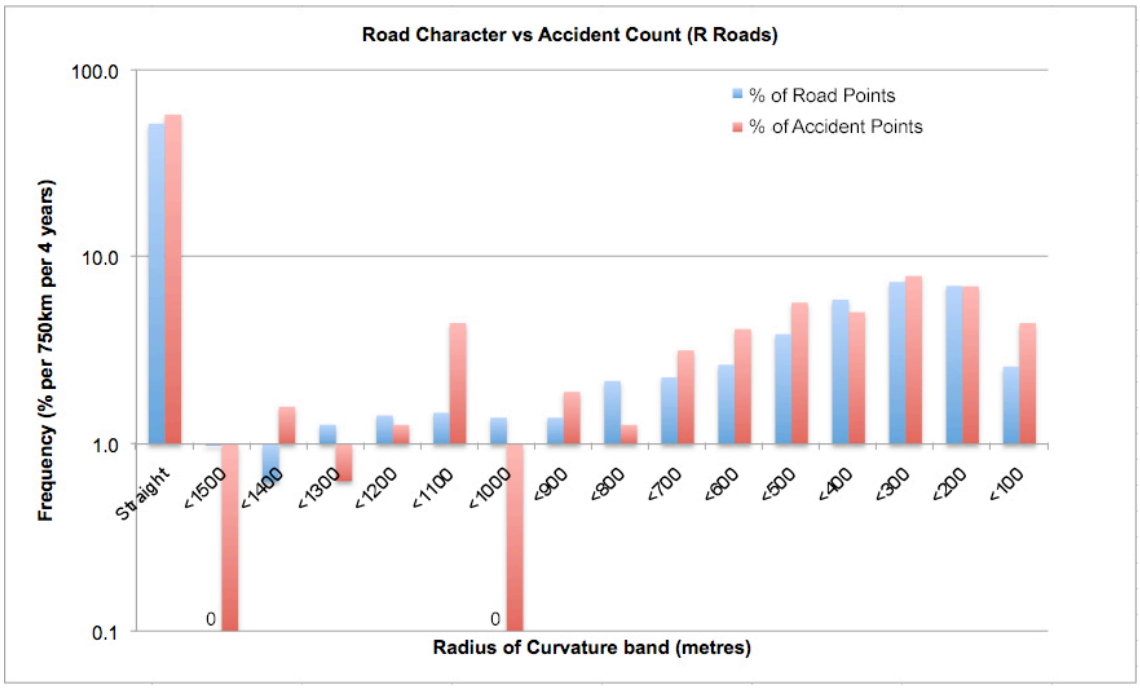

(b)

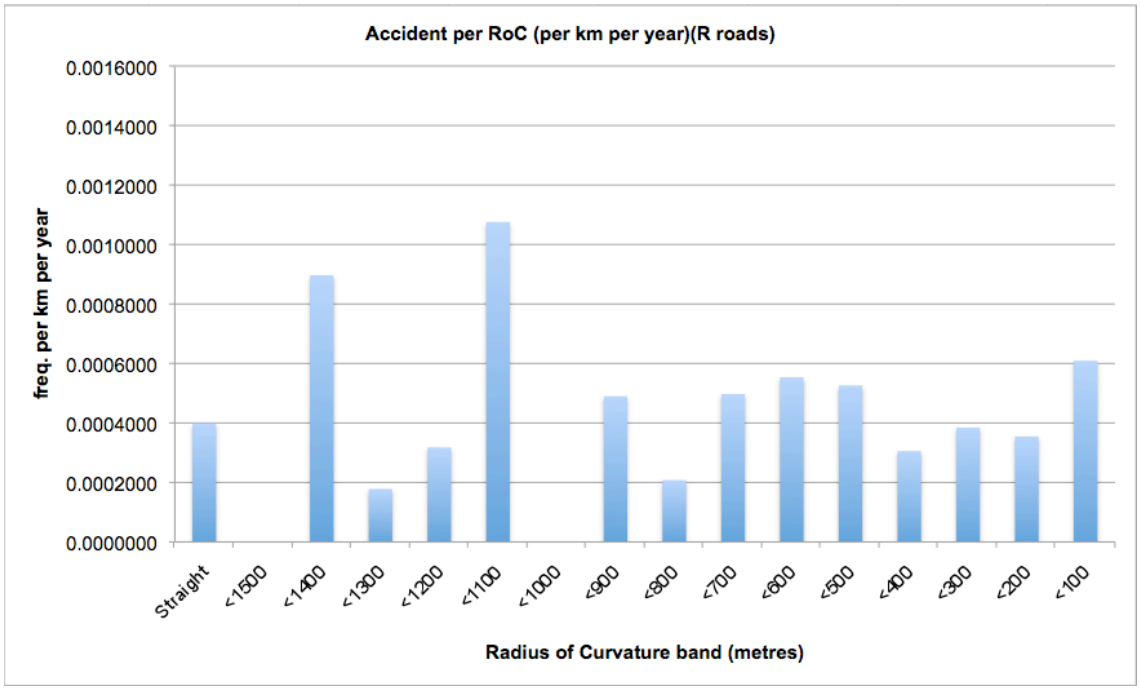

Figure 3.19 (a) shows the percentages of accident frequency and road points within the same RoC band for R roads and Figure 3.19 (b) shows the ARC rates generated by these comparisons.

M Roads

Figure 3.17 (a) shows higher accident frequency percentages on straight segments of M road, however, this road type also consists of equally high percentages of straight segments. When these accident values are normalised by their corresponding road percentage as shown in by Figure 3.17 (b) most accidents on the motorways occur on straight roads particularly above the 1200m band. Although the highest accident frequencies occurred at straight bands and bands less than 600m in Figure 3.16, Figure 3.17 (b) shows the highest ARC rates at 1500m and 1200m. The values below 1100m are considered safer than that above 1200m, However this may be due to motorways not consisting of this curvature type. For example, Figure 3.17 (b) shows no percentages of road points below 200m.

N Roads

Figure 3.18 (a) shows high accident frequency percentages on straight segments of N roads and similar to M roads, shows equal amounts of straight segments. However, when these accident values are normalised as shown in Figure 3.18 (b), ARC rates show that straight roads are relatively safe particularly at bands above 1200m. This rate is in contrast to M roads. For example, the mean ARC rate above 1200m for the N road when compared with the M road is .0001589 vs .0004162(per km per year) respectively. Curvatures between 300m and 1200m show increases in risk but are considered relatively safe ARC rates similar to M roads within these bands. However, in cases below 300m an increase in risk can be seen indicating irregular ratios of accident to road points with highest frequencies at radius lengths below 200m and 100m. These findings for N roads indicate higher accident concentration for radius lengths below 200m (sharp bends).

R Roads

Results for R roads are shown in Figure 3.19. Figure 3.19 (a) shows values consistent with M and N roads where the percentages of both values in the straight radius band are high and of almost equal percentage. Similar to N roads, R roads show a higher percentage of road that consists of lower radius bands (sharper bends) and a gradual increase in accidents below 400m. However when normalised, unlike N roads, these values in the lower bands generate lower ARC rates than that of N road segments in the same radius band. The highest ARC rates on R roads shown in Figure 3.19(b) exist at radius lengths of 1400m and 1100m, which are considered gradual developing curves. Much like the M roads, there are no consecutive increases or decreases in ARC values and no concentrations in the lower bands.

As N roads show concentrations of accidents per road type below 100m, weather conditions and road surface conditions were also analysed to consider any further environmental factors surrounding this signal. Results show 74% of these accidents occurred during dry weather with dry road surface conditions (friction coefficient $>.75\mu_s$) and the remaining 26% occurring in wet weather with road surface conditions ranging from wet to dry (frictional coefficient $>.4\mu_s$ and $< .9\mu_s$), thus indicating mainly dry conditions. No accidents for the sample of N roads were associated with snow or icy weather and road surface conditions.

3.5 Chapter discussion

This Chapter developed a new method that classifies road accident locations according to geometry. In addition, a method to map accidents onto individual roads was designed and then used to determine an *accident to radius of curvature* (ARC) rate for the given road. These individual roads were grouped into three categories of Irish roadways and a comparison was then made based on the ARC rates assigned to each road type.

The current method to assign road curvature to an accident location is made by An Garda Síochána in the form of a binary decision; whereby the accident is either on a 'bend' or on a 'straight'. In addition, no further classification is made in relation to the 'type' of curvature the collision occurred on. Furthermore, in cases where the collision location is reported as a straight segment, it is not checked after the event if the location was actually part of a larger gradual bend. The current study has developed a method whereby each accident location can be assigned a radius of curvature value based on the nearby geometry. This is important as it improves the detail associated with each curvature type. For example, using the method developed, accidents can be assigned road characteristics such as 'gentle curves' (based on RoC values close to 1000m) 'sharp curves' (based on RoC values below 200m), 'very sharp curves' (based on RoC values below 100m) and so on, thus, highlighting bends 'types' that are associated with accidents.

In addition to the An Garda Síochána reporting two primary road characteristics to determine the roads curvature, two further road characteristics are recorded, 'gradient' and 'hillcrest' for vertical alignment. These additional road characteristics currently make up less than 5% of the total accidents recorded over the 4 year period examined (as shown in Table 2.1). These low percentages may be due to the fact that currently there is

no method used by the RSA of Ireland to combine road characteristics. For example, combining horizontal curvature elements with elements such as grade may increase the number of accident frequencies reported for both road character types. Chapter two discussed American studies whereby the combinations of these characteristics increased the detail of the accidents descriptions for example "straight and grade (gradient)" "curve with grade" [19]. As altitude information was not available in the geo-data acquired, road elevation did not form part of this study. However, by successfully assigning horizontal curvature to accident locations, this technique demonstrates how vertical curvatures such as gradients can be assigned to further improve the accident description.

The method developed in this study for assigning features of road geometry to accident locations not only demonstrated ways to improve the description of the accident location but also demonstrated ways to assign geometric characteristics to accident locations that remained unclassified. For example, 15% of the accident data locations recorded by the RSA of Ireland over the four year period remained unspecified (section 2.1). The current method to assign curvature to road locations demonstrated how given an accident location, each accident could be accounted for and assigned a road characteristic.

Methods to increase the data quality of road information were also discussed in this Chapter in order to successfully map accidents onto individual roads. By assigning accidents to individual roads, it was possible to group accidents by the Irish road type on which they occurred (e.g. M, N and R roads). Within these road types, each accident was assigned a RoC value and binned into 16 radius size bands. Road points with the same RoC value were binned in the same way. By doing so, a dimensional analysis could then be carried out to determine an ARC (accident to radius of curvature) rate. Furthermore, these ARC rates were used to gain a comparison amongst the three given road types.

Results initially showed that high percentages of accidents on each road type occurred on straight segments, however, when these values were compared to the percentage of the road that contained the same radius value, results showed that most accidents occurring on straights were matched with the same percentage of straight road. ARC rates on all three road types showed that 'straight' segments were proportionate to the amount of road consisting of straight segments showing no irregularities. Irregularities that interested this study were cases in which accident frequency was high and the percentage of the associated road geometry was low, suggesting that accidents occurred as a result of the type of geometry not the magnitude of geometry.

Prior to the analysis of road types developed in this Chapter, it was hypothesised that N and R roads would show similar outcomes on curvatures due to their geometric makeup. For example, while M roads generally consist of fixed-constant geometry, it was expected that N and R roads, containing multiple bends, would show similar accident frequencies based on curvature. This was also supported by findings presented in Chapter 2 reporting accident rate increases by Cairney and Lamm as a result of increases in curvature [22][26]. In accordance with the literature findings, initial analysis (see Figure 3.16) showed accident frequency increases as road curvatures increased on both N and R roads. However, when road segments were normalised against accident rates (see equation 3.7) using the dimensional analysis discussed, ARC rates showed fewer similarities for N and R roads. For example, ARC rates on the R road types showed random distribution above the 1100m band suggesting factors other than curvature.

Although M and R roads showed some likely to be random spikes in ARC rates, it was N roads ARC rates that yielded the most significant results in radius bands lower than 200 m as shown in Figure 3.18 (b). This correspondence to the lower radius band was

the highest amongst the three road types thus indicating higher accident concentration as a result of road geometry on this road type.

One theory derived from these results was that the combination of geometry and factors such as speed limits might have afforded different driving behaviours or 'driving modes' on each road type. For example, while speed limits allow drivers to travel at high speeds of up to 120km/h based on fixed-constant geometry on motorways, in contrast, speed limits on R roads restrict drivers between 40 and 80km/h due to the presence of dangerous bends. However, although N roads can also contain dangerous bends (less than 200m) similar to R roads, drivers are warranted speed limits of up to 100km/h, thus travelling speeds more appropriate for geometry associated with motorways.

In addition to high speeds associated with curvature, another possible factor for these results and also discussed in Chapter 2 was that of consecutive curvatures particularly in cases where sharp dangerous bends are preceded by large gradual bends [29][31]. In these cases, drivers may be deceived in maintaining high speeds unable to adjust speeds in time for subsequent bends. Although consecutive curves are commonly found on N and R roads, it is N roads that may not have the necessary speed limits in place to deal with such curvature changes. Future work will target specific national and regional roadways with high speed limits paying particular interest to sharp curves situated at the end of existing transition curves.

Some of the limitations of these findings are mentioned in the data acquisition process when discussing disadvantages of crash data. For example, accident locations are estimated after the event has occurred therefore approximations of accident locations are made. By basing findings on data that may not be describing the accident location fully it has proven more difficult to consider geometry as a primary causal factor.

Furthermore, the absence of road character information in the data such as ‘grades’ or ‘superelevation’ also skews the link between other geometric factors. One possible way of improving this data is by using a similar method developed in this study to bind ordinance survey databases with accident geo-data collected at the scene. This process would provide detailed information at the accident location and details of the surrounding road segments for example elevation rates.

The method developed in this study assigned RoC values to road lengths of 100m. A further improvement could be made by grouping curvatures together based on continuous or consecutive curvatures whereby radius lengths are assessed using the beginning and end of an entire curve. This may help in deciding not only the RoC value associated with the accident but also the type of curve it was associated with (e.g. simple, reverse, compound, spiral).

Further limitations are that a considerable proportion of non-fatal collisions remain unreported as Irish accident data does not measure ‘near miss’ collisions. In other countries this is combated by using alternate methods of acquisition as demonstrated by naturalistic driving studies [19][55]. Furthermore in Ireland, accident databases are not linked to hospital or compensation claims databases to monitor accident data that may have bypassed the policing authorities. The current best estimate is derived primarily from the RSA of Ireland crash data. The data used as a basis for these studies are therefore not a complete record for all collisions. Nonetheless, crash data collected by An Garda Síochána and processed by the RSA of Ireland remain the most complete and reliable source of accident information for Irish roads, in particular for analysing crash data over time as demonstrated in this study.

This Chapter highlighted types of accident risk dependent on elements of ‘road factors’ such as road curvature on various Irish road types. The following Chapter explores changes in driving behaviours such as eye movement as a result of changes in geometry, thus ‘human factors’.

Chapter 4

Examining Interactivity Between Driver Behaviour and Road Geometry

The following Chapter presents the integration of a low-cost driving simulator and a standard eye-tracker for the purposes of monitoring driving behavior. Thirty drivers were recruited to participate in the experiment that consisted of each participant driving two contrasting Irish road routes under observation. The first route comprised of a rural road with several 'closed' bends and significant detail in the image stream while the second motorway segment contained fixed-constant geometry, 'open' bends and sparse detail in the image stream. Data collected by the driving simulator on each route was then regenerated and analysed using a purpose built visualization software. In addition, three further steps were taken to further quantify and support findings from the visual analysis software. The first measure was used to determine fixation data on road bends. The section measure was used to further classify where in the visual field participants were looking when traversing straight segments. Finally, in order to determine look-ahead distances on straight segments a calculation was used to translate eye gaze coordinates to distances along the road plane. A comparison was made using the contrasting routes for the three measures and is presented in the results section. The chapter concludes with a discussion of results obtained by the experiment.

4.1 Data Acquisition and Video Integration

This section describes the data acquisition devices used to record the video sequences and preparatory measures undertaken before this data was integrated into the simulator. Although the simulator used in this study was considered 'low fidelity' in terms of cost and components, the use of high-resolution cameras and high-resolution video playback were utilised in order to create realistic driving surroundings in order to match the capabilities of higher fidelity driving simulators.

4.1.1 Video and GPS Data Acquisition

The video sequence used for the driving simulator was generated from a data set acquired by a commercial witness-camera, as shown in Figure 4.1. The camera used was mounted to the car dashboard on the inside of the vehicle's windscreen behind the rear view mirror. The camera was selected for the benefits of its full color high definition video output (HD 1920x1080), its Global Positioning System (GPS) data and inertial measurements.

Figure 4.1: Data acquisition camera MiVue 388

The camera was then used to record the data along two separate road types measuring 6km each; the R406 (Straffan road) regional road and a segment of the M3 motorway. The R406 measured from the M7 exit northbound to the approach into Straffan town. The M3 measured from exit 6 on the M3 and traveled northbound for 6km. The two routes were chosen as they offered a contrast between rapidly changing geometry with a wide range of road signage (R road) and fixed-constant geometry with intermittent signage and gradual curvatures (M road). These differences in geometry offered a contrast in sight distances on open and closed bends. As mentioned the 'openness' of these bends was defined by the sight distance available to the driver at the point of entering the road curve. For example, regional roads contained many hazardous closed bends with road-side features obstructing the outcome of the curve, while the motorway contained open gradual bends with little to no obstructions blocking the curve exit. In addition, the rural video also contained added hazards such as pedestrians on roads, trucks crossing lanes and cars reversing on dangerous bends.

In both cases the vehicle was driven at normal road speeds suitable for the category of road. The rural road was driven at 60km/h for rural and the motorway was driven at 100km/h. Although motorways allow for speeds of up to 120km/h, a lower speed 100km/h was chosen to improve data acquisition by collecting more frames per distance traveled. The acquisition speed fluctuated on both routes resulting in a non-constant video playback speed. To combat this, a spacing algorithm was then used to interpolate the data to ensure an evenly spaced playback system.

4.1.2 Generation of GPS and Video Data

Although three data types were generated from the witness camera, only two were used for this experiment; the GPS and video data. The time-stamped GPS log collected the speed and position of the vehicle at a rate of 1 Hz, in contrast to the video, which was acquired at a rate of 30 Hz. The GPS information was in the National Marine Electronics Association (NMEA) format. NMEA is a GPS receiver communication protocol that allows navigational data to be interpreted by other data input devices [99]. The NMEA file was outputted with an accompanying .MOV video compression (e.g. FILE001.MOV, FILE001.NMEA). As each frame of the video was not geo-tagged, but the video was recorded at 30 frames per second, each 1 Hz GPS sample was interpolated into 30 equal sections, allowing an estimated geo-tag to be associated with each inter-GPS sample video frame.

4.1.3 Generating Evenly Spaced Video

In order for the subject to drive the simulator at a speed that was not a representative of how it was recorded originally, a spacing process was necessary. Spacing the video, based on GPS points of equal distance, allowed the user to advance through the video stream at a pace independent of the speed at video acquisition. Relevant data was extracted from the GPS file, namely the time, latitude, longitude and altitude. The distance between these points were then divided by the frame rate to create interpolation points (one for every 10 cm traveled). A look-up table was then created in order to have a searchable array of evenly distanced (10cm) GPS points corresponding to its nearest geo-tagged video frame. This process is modeled in Figure 4.2.

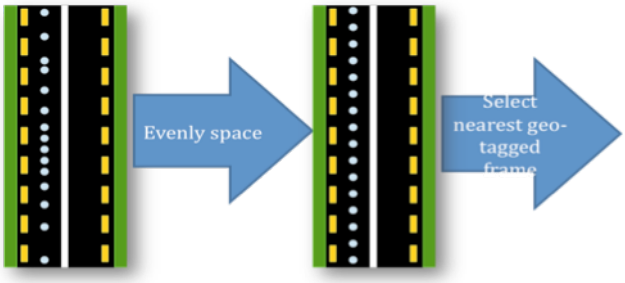

Figure 4.2: Generating evenly-spaced video

4.1.4 Integration of Video Sequence

The media player *Mplayer* provided with the Ubuntu OS was used to generate the visual stream because of its ability to deal with high-resolution video inputs and because of its real-time diagnostic abilities. By redirecting standard input from the command line it was possible to record data including a time-stamp and simulator state to a disk-file. A typical line from mplayer reads as follows where *A* is the audio position in seconds, *V*, the video position in seconds. This data is discussed in detail in Section 4.3.2.

A: 251.8 V: 251.8 A-V: 0.001 ct: 0.006 0/0 48% 2% 1.4%

Acceleration was achieved by linking the frame rate speed directly to the pressure applied by the driving simulator's accelerator pedal. A fully-pressed accelerator pedal was interpreted as full playback speed, and a fully released accelerator pedal was interpreted as a paused playback speed. An onscreen speedometer overlay was designed and used to display the driving speed to the user. This is shown in Figure 4.3.

Figure 4.3: Example of speed being relayed to user

4.2 Hardware and Software Development

A static, fixed-base driving simulator was used for the experiment as shown in Figure 4.4 consisting of two PCs. The first PC was used as a server for the Tobii 1750 eye-tracking display, together with its ClearView software. The Tobii 1750 embodies a 17-inch flat-panel monitor with in-built stereo cameras used for tracking a subject's eye movements. The Tobii server PC used was a standard 32-bit Microsoft Windows 7-based PC, with an Intel Dual Core 2 Duo processor (2.33 GHz) with 2 GB of RAM.

Figure 4.4: Driving simulator overview of the system, particpant media stream and evaluator hardware components used in this experiment.

The second computer, with the Ubuntu operating system, ran the driving simulator software. This simulator PC used an Intel® Xeon E5606 quad core processor (2.13 GHz) with 6 GB of RAM. For display purposes, a Matrox TripleHead2Go was used to output the driving simulator's visual stream across three monitors; the Tobii eye tracking screen and two standard 17-inch 1280 x 1024 monitors. This formed a single

3840 x 1024 display. Integrating the Tobii eye-tracker as the center monitor allowed for the tracking of eye-movement on the video being played on the simulator PC. An additional standard display was used to monitor the Tobii server feed and eye-tracking status while displaying the simulator on the 3840 x 1024 display.

A Thrustmaster Ferrari GT 2-in-1 Rumble Force Racing steering wheel and pedals were chosen as a sufficient tool for simulating a real-life car-control surface. As the simulator image stream used was real-world video, the steering wheel was disabled as the ability to navigate in a three-dimensional space is not yet possible. Pedals were used to control the playback speed of the video frame rate as mentioned. These simulator components are also shown in Figure 4.4.

4.2.1 Engineering the Simulation Environment

As the primary input for this experiment was eye data, the use of high resolution video was necessary for the simulator. This was decided in order to improve the visual detail of road surroundings and sign legibility. Although previous iterations of simulators had been constructed using the Windows VS2010 IDE [100], Ubuntu's MonoDevelop IDE was chosen for this project to control and read from the *Mplayer* media player.

Four threads were generated in the program using the Monodevelop IDE multi-threading ability. These threads are illustrated in Figure 4.5. An *eyeTrack* thread was used to create a local network between the two PCs to synchronise the eye track data with the video data. An *mplayer* thread was responsible for reading and playing back the evenly spaced image stream and for writing the video diagnostic line (containing

frame-rate and time) to a framevstime.txt file. The *speedo* thread was used for displaying a speedometer overlay graphic to show the estimated speed being traveled along the route. Finally, a *joystick* thread was used to control the frame-rate of the image stream thus simulating the cars acceleration.

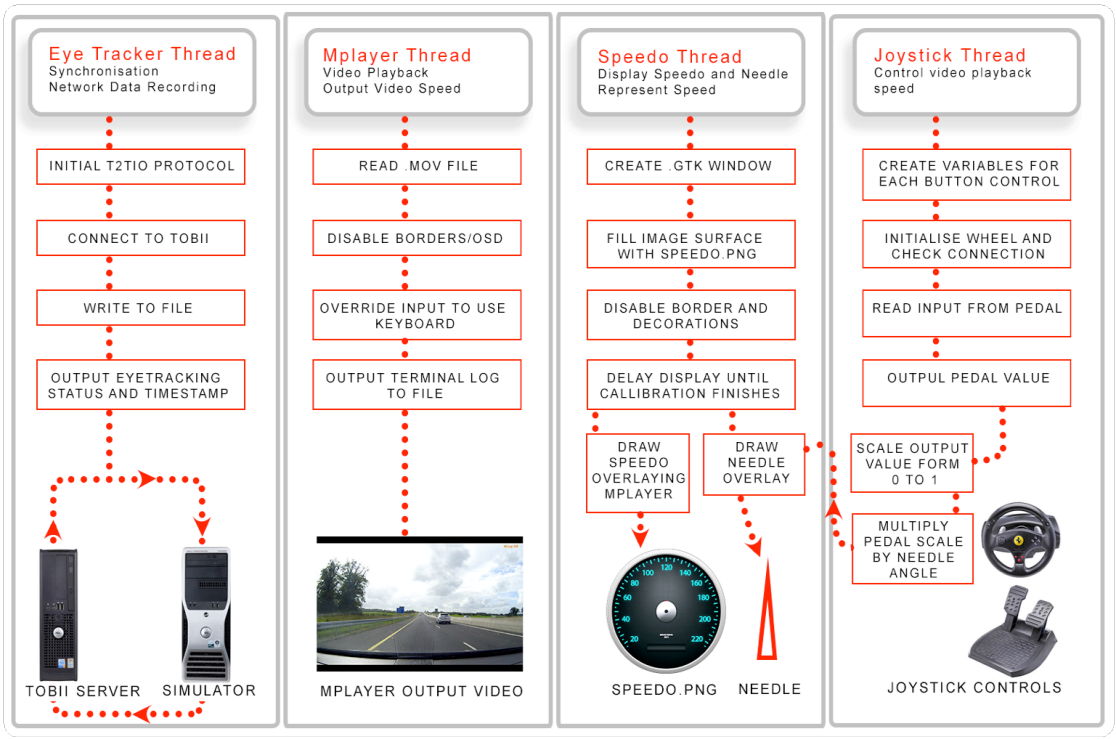

Fig 4.5: Shows four main thread processes for simulator development

The multi-threading process triggered different elements of the program simultaneously and allowed the interface to stay responsive to user input in real time. The program generated a time stamped log and frame rate (acceleration) of the video being displayed in the format of a .txt file. Accompanying this log was a second .txt file generated by the Tobii server PC containing time stamped eye-gaze coordinates. The combination of the two data sets allowed for the synchronization of corresponding eye-gaze data.

4.3 Method used for Eye Data Acquisition

Thirty drivers took part in the study that consisted of the two contrasting driving routes. Although accelerator pedal information was collected, the primary variable being examined was the eye-fixation data. The participants (12 males and 18 females), aged between 19 and 58 with a mean age of 29 +/- 2.02 years, took part in the study. Participants were recruited via an *ad hoc* sampling method of convenience from the student population of Maynooth University. Each participant was instructed to "*travel each route at a speed adhering to the road signs and to react to road geometry as if in a real world vehicle*". Participants were not informed of hazardous bends prior to their experiment and for most of the participants; it was their first time driving both of these routes. Twenty-six out of 30 participants had a full Irish driving license. Of the remaining participants only 1 had less than 6 months driving experience. Therefore our participants would be generally be classified as being experienced drivers.

The simulator allowed the participants to drive at an independent pace through the two video segments. The rural road video, 'R', was video acquired of the R406 rural road and the motorway video, '***M,***' was a section of the M3 motorway on the Navan bypass. Three calibration videos (video ***Ca***) were placed within the video, the sequence of which varied. Fifteen participants drove through the sequence Ca-**R**-Ca-**M**-Ca and 15 drove Ca-**M**-Ca-**R**-Ca. M and R road video sequences varied so as to help verify if a training phase occurred at the start of using the simulator for the first time. The variation also eliminated bias in data that may have been caused by starting with the segment containing more stimulation, in this case video ***R***.

4.3.1 Synchronisation of Video Frames with Eye Gaze and Control Data.

Initially, eye-tracker networking software "t2tio" was used to obtain synchronization from the eye-tracker. In practice this was not done as server/network delays led to inconsistent results. Instead, each video sequence was preceded with the calibration (***Ca***) video clip of a red dot traversing a white screen in a "Z" pattern (see Figure 4.6). A time offset value associated with each experimental run was then adjusted so that the eye-gaze followed accurately the "Z" when the video was played back. The offset measured the time between eye-tracking starting acquisition and *mplayer* starting video playback. A final check on calibration was to observe the eye gaze on the calibration "Z" at the end of each video sequence. The calibration and data set was considered correct when eye gaze tracked the three calibration sequences available in each video.

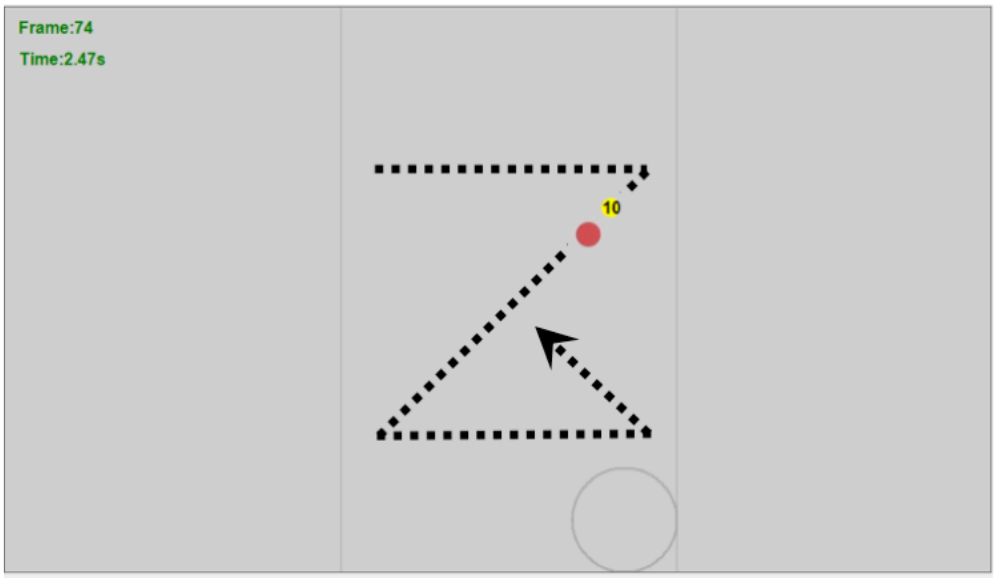

Figure 4.6 Synchronisation of eye-tracker and video clocks, dotted line shows path of red dot displayed in video, yellow dot shows subject 10's eye gaze.

The data collected for each participant was parsed and written to three text files, as shown in Table 4.1.

Table 4.1: First three lines of the three data files used in the analysis of a single subject.

1. timeoffset.txt	**2. framevstime.txt**				**3. tracker.txt**		
Subject data	*Frame*	*Simulator time*	*Accelerator pedal*	*Speed Index*	*Tracker time*	*Gaze X*	*Gaze Y*
Participant1	0.000	3412.0	0.1082	7	0.00	526	357
9650*	0.749	3432.0	0.1082	6	19.88	401	441
RM Sequence**	1.499	3452.0	0.1082	5	39.85	183	748

* Offset frame number(ms) where subject began following "Z" pattern
** Rural-Motorway Video Sequence (e.g. Ca-R-Ca-M-Ca)

4.3.2 Description of Data Acquired by the Video Playback Thread

The Mplayer outputted a diagnostic line of text which was normally directed to the standard output (console). By redirecting standard input within the Mplayer thread it was possible to record the line of data including a time stamp and simulator state to a disk file. As mentioned a typical line from Mplayer reads as follows and is further described,

A: 251.8 **V**: 251.8 **A-V**: 0.001 ct: 0.006 0/0 48% 2% 1.4%

where **A** is the audio position in seconds, **V**, the video position in seconds, **A-V**: audio-video difference in seconds (delay), ct, the total A-V sync correction done, frames played (counting from last seek), frames decoded (counting from last seek), video codec cpu usage in percent (for slices and DR this includes video_out), video_out cpu usage, audio codec cpu usage in percent, frames needed to drop to maintain A-V sync, current level of image post processing (when using -autoq) and current cache size used (around 50% is normal). If the video contained no audio stream then a simpler string was produced.

The V: value was used to estimate the frame being viewed; however only read to a resolution of 0.1seconds. Typically each line was created by the Mplayer every 0.033 seconds. Linear interpolation was used to create a unique frame number for each line produced by the Mplayer program. This enabled the simulator state (accelerometer and speed) and real time to be correlated with a specific frame of video as shown in Table 4.2.

Table 4.2 Data contained in video.txt and the corresponding estimate of frame number,

Line	V: Time	V x fps	Time stamp	Accelerator	Speed index	Frame No.
1	0	0	3.236	0.19072	4	0
2	0.1	3	3.264	0.22165	5	1.499
3	0.1	3	3.291	0.28349	6	2.997
4	0.2	6	3.319	0.31958	7	3.996
5	0.2	6	3.348	0.31443	8	4.995
6	0.2	6	3.376	0.30412	7	5.994
7	0.3	9	3.405	0.30412	8	6.993
8	0.3	9	3.433	0.30412	7	7.992
9	0.3	9	3.462	0.30412	8	8.991

Frames per second =30.

The video player had 35 discrete play back speeds which could be set by use of the accelerator pedal. The following table (Table 4.3) was used to convert from playback speed to frame rate. For the motorway sequence a speed factor of 1.0 corresponds to 100km/h (the speed at data acquisition) and 60km/h for the rural road, see Table 4.3.

Table 4.3 Mplayer playback speed as a function of speed index.

Index	Factor	Index	Factor	Index	Factor	Index	Factor	Index	Factor
0	0.17	**7**	0.32	**14**	0.62	**21**	1.23	**28**	2.36
1	0.18	**8**	0.35	**15**	0.68	**22**	1.36	**29**	2.59
2	0.2	**9**	0.39	**16**	0.75	**23**	1.49	**30**	2.85
3	0.22	**10**	0.42	**17**	0.83	**24**	1.64	**31**	3.14
4	0.24	**11**	0.47	**18**	0.91	**25**	1.81	**32**	3.45
5	0.26	**12**	0.51	**19**	1	**26**	1.99	**33**	3.8
6	0.29	**13**	0.56	**20**	1.12	**27**	2.18	**34**	4

4.3.3 Description of Data Acquired by Eye-Tracker

The Tobii 1750 running the *ClearView* software was executed on a PC separate to the simulator. The video output from this PC was split so that it could be displayed on an independent monitor at all times and when required on the Tobii screen via one input of a KVM (keyboard,video and mouse) switch box connected to the Tobii monitor input (see Figure 4.4). The Tobii monitor was placed in the central monitor position of the simulator. The screen resolution of this computer was set at 1024x768. The TSV log file created by the software contained useful information about eye-gaze and system time (see Table 4.4). System time was divided by 1000 to convert from eye-tracker units (μS) to simulator units (mS).

Table 4.4 Fields in each line of TSV file, each line is recorded every 20mS. Fields used for analysis software highlighted in grey, microsecondtimestamp, Gazepoint X and Gazepoint Y.

Timestamp	3	Event	0
DateTimeStamp	38:33.6	EventKey	0
DateTimeStampStartOffset	00:00.0	Data1	0
Number	0	Data2	0
GazePointXLeft	470.0494	Descriptor	0
GazePointYLeft	377.2332	StimuliName	No media
CamXLeft	0.8227536	StimuliID	0
CamYLeft	0.6311249	MediaWidth	1024
DistanceLeft	660.6461	MediaHeight	768
PupilLeft	5.538805	MediaPosX	0
ValidityLeft	0	MediaPosY	0
GazePointXRight	475.3902	MappedFixationPointX	469
GazePointYRight	368.9937	MappedFixationPointY	375
CamXRight	0.5735529	FixationDuration	182
CamYRight	0.6409533	AoiIds	0
DistanceRight	662.9463	AoiNames	Content
PupilRight	5.658517	WebGroupImage	0
ValidityRight	0	MappedGazeDataPointX	473
FixationIndex	0	MappedGazeDataPointY	373
GazePointX	473	MicroSecondTimestamp	2730
GazePointY	373	AbsoluteMicroSecondTimestamp	92566485019

4.4 Data Analysis Process

In order to analyse gaze information collected by the Tobii eye tracker, a visualization software was developed to bind the gaze information (GazepointX, GazepointY) to the road video sequence. The analysis software used for the experiment result data was developed as part of a group effort to facilitate ongoing multi disciplinary research based on driving simulation at Maynooth University. The code for this visualisation software was inherited and adaptations were made to process the necessary information for this study.

Figure 4.7 shows features of the visualisation GUI including a *Visual Panel*, an *Acceleration Panel*, a *Video Playback* and *Target Panel*. The *Visual Panel* displayed each subject's gaze information (numbered) and also areas of interest (AOI) inputted by the user for example *Dog Walkers* and the *Speedometer* (highlighted in blue).

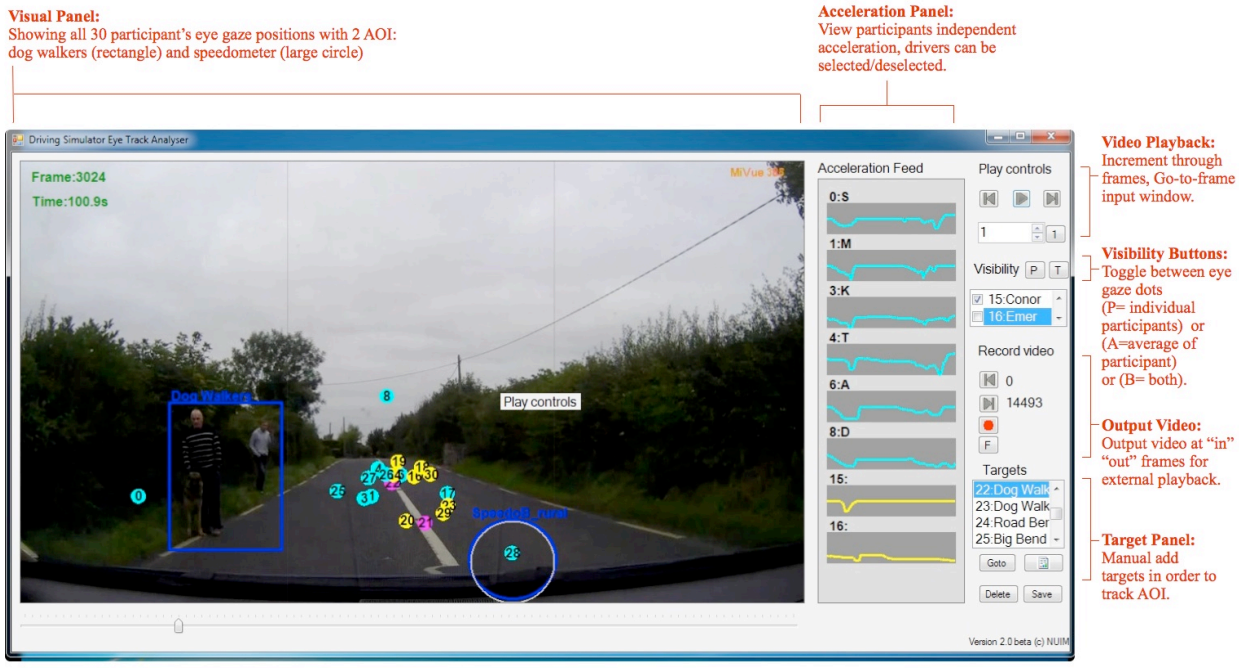

Figure 4.7: Analysis software showing driver's eye gaze and acceleration behavior when presented with a hazardous situation.

A feature for visualising acceleration pedal data is shown in the *Acceleration Feed* and can be seen relaying independent acceleration data for each participant. In this particular frame the independent acceleration graphs can be seen dipping as the dog walkers are approached. A *Play Controls* panel is also shown and was used to navigate through video frames in addition to outputting video segments. A target panel is also shown which allows users to populate and track targets such as road signage or lane obstructions. By combining video playback with eye gaze data from participants the

system allowed for real time analysis as to where drivers were looking both individually and as a group. This analysis is discussed in the results section of this chapter.

In addition to visual observations from the video playback, further quantitative analysis was needed in order to calculate where participants were looking at a given moment in time. A method was added to the analysis software to extract gaze data for the 30 participants at selected road segments such as road bends and straights segments. Three approaches were taken to analyse this extracted data further. The first approach sampled four video frames along the two routes in order to better understand eye behaviour on variations of 'openness' on bends. Two of the samples chosen were closed bends on the R road segment and 2 were open bends on the Motorway segment. In order to determine where participants looked on these bends, a measure was used to determine the mean distance (in pixels) from each fixation to the tangent point on the road bend as shown in Figure 4.8. Additional pixel coordinates were used such as the 'outer lane' point as a contrasting point of fixation.

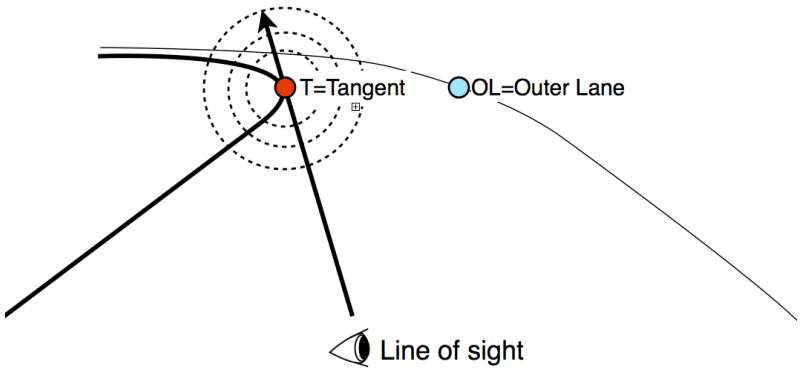

Figure 4.8 Schematic of tangent point data analysis method. The tangent point (T) (red circle), the pixel area around the T (dotted circle) and the outer lane (blue circle) used to measure lateral gaze deviations from the T are represented.

The second analysis method used was a measure of where participants were looking while traversing straight road segments. This was done to determine if the drivers were accessing the additional sight distance associated with straight geometry or more open curvatures. In this case, a method to classify the road segments was used to measure if users were looking on or above the road and if so, any differences between the contrasting routes. Four regions were selected to classify the road further based on visual fields inside and outside the drivers given lane. These regions were 'above the road', 'on the road', along the 'margin or outer lane (opposite lane for R roads)' and within the 'speedometer' target. By restricting the visual field to one lane this allowed for a fair comparison between the regional (one lane) and motorway (two lanes) segments. The four options used to classify the road are shown in Figure 4.9. For this process a sample of straight R road and Motorway were compared and are presented in the results section.

Figure 4.9 shows a video frame of the motorway road segment containing eye gaze data overlaid with 4 colour regions representing a classification of visual fields.

Finally, the third process used for further data analysis uses the calculation process discussed in Chapter 2, Section 2.9.2. This calculation was used to translate eye fixation pixel coordinates into distances along the road plane. While fixations above the road were considered too difficult to measure (as these fixations were deemed as tending towards infinity), fixations on the road area were measured for 6 samples of both routes, 3 x R road and 3 x Motorway. For each frame a calibration process was created that allowed the mapping of points from a drivers perspective to a birds eye-view. This made use of a projective transformation (homography) from the road plane as recorded by the camera to an overhead view of the road plane allowing for distance measurements. Horizontal lines on the road were used as markers to determine the four points needed for the plane transformation process described in Chapter 2, Section 2.9.2. An example of this calibration process is shown in Figure 4.10 (a) and a representation of the area being translated is shown in Figures 4.10 (b).

(a) (b)

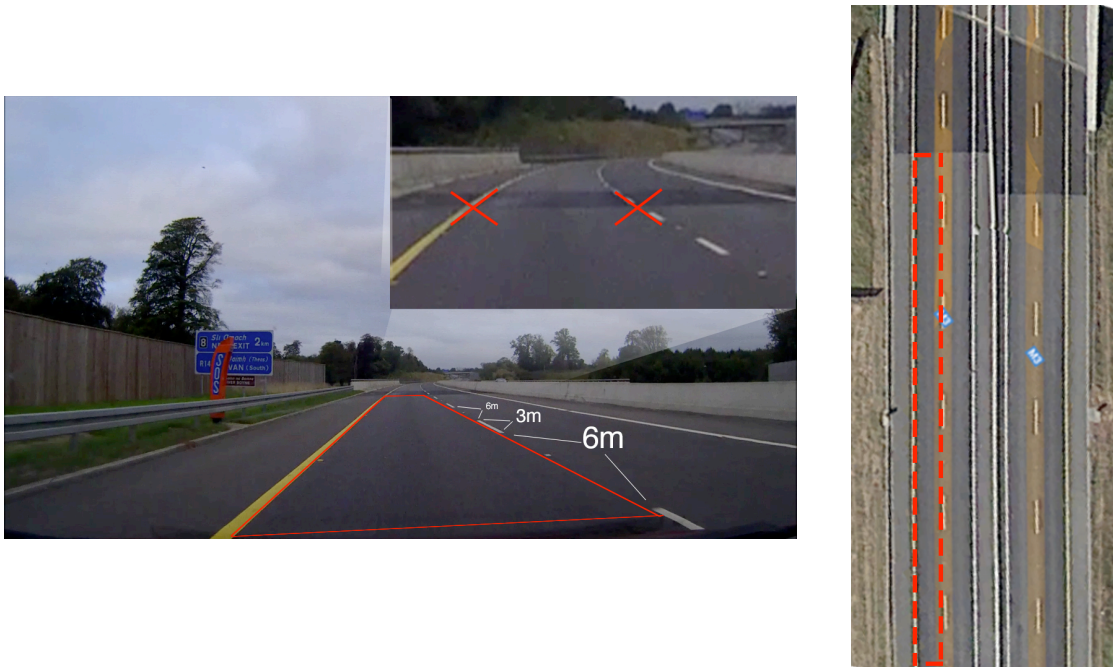

Figure 4.10 (a) Calibration process demonstrating the acquisition of four points (trapezoid) for plane transformation. Gaps in broken white line are measured as 6m and white lines measured as 3m. Inset shows an example of a distant horizontal line on the roads surface used to reference the angle of the road. Red x marks are 2 furthest points used.

Figure 4.10 (b) Shows a representation of the translated area taken from birds-eye view courtesy of Google Maps©. Broken red rectangle is a projective homography of the trapezoid from (a) translated to a 2D plane for distance calculation. Y value of this rectangle is estimated using sum of white road markings (3m) and gaps between (6m).

Using this transformation method the area (trapezoid) shown in Figure 4.10 (a) was then translated to a road plane allowing for a distance calculation (rectangle with four corresponding points shown in Figure 4.10 (b). The y value of the rectangle was scaled in meters and was determined by counting the broken white road markings on the centre lane of the road and summing them with the gaps between the roads markings (see Figure 4.10 (a)). By doing so, a look-ahead distance was estimated for on-road fixations for the 30 participants.

4.5 Results of Data Analysis

The following section presents the results of initial observations from the visual analysis software and combines these with tangent analysis at road bends and region and look-ahead analysis on straight sections of road. To do so, samples of road taken from the analysis software are further quantified using the 3 processes described in Section 4.4. Equal amounts of samples were taken of both routes and in cases where bends are being examined, equal amounts of left and right turns were chosen.

4.5.1 Tangent Analysis

The visual analysis software described in Section 4.4 successfully regenerated the data for 30 subjects and provided real-time insight as to where subjects were looking while driving both routes. In addition to individual fixations, eye movement patterns were also observed as a group allowing for a cluster analysis. Much like a heat map, groups of eye movements flowed in tandem to show areas of the road the group fixated on. For example, using visual analysis alone, it was evident that drivers were using the road tangent point to anticipate curvature on bends. In accordance with research from Land and Lee (1994) and Mars (2008), eye behaviour collected in this experiment showed that the tangent point of the curve was the area attended to most frequently when traversing Irish road bends. Samples of these observations are presented in Figure 4.11 (A), (B), (C) and (D) showing subject's gaze data concentrated at the tangent on a variation of open and closed bends. In addition to analysing video frames, the gaze data for each sample are also being represented using x,y scatter graphs in Figures 4.11 (A1), (B1), (C1) and (D1). Using this representation it was possible to select and analyse individual gaze data values particularly gaze data being hidden by other data points. For

example, Figure 4.11 (A) shows a concentration of points on the tangent making it difficult to gain information on points being concealed. The graph representations also show markers (red and blue circle) representing the tangent and outer lane points, which can be seen in Figure 4.11 (A1) (B1) (C1), and (D1).

(A)

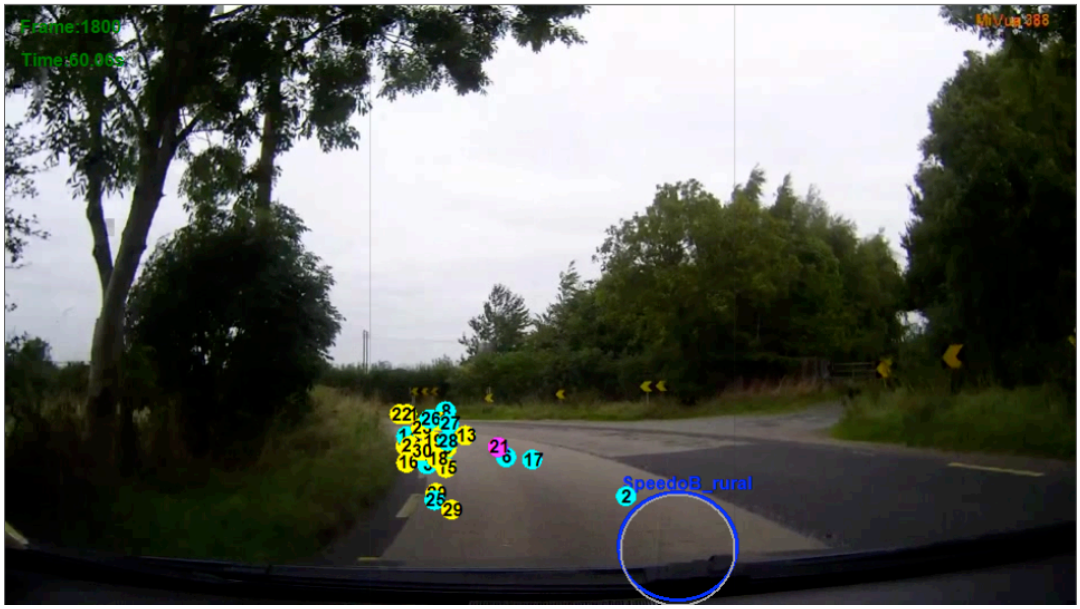

Figure 4.11 (A) shows frame 1800 sampled from the R road segment. The sample shows participant gaze data for a closed left turn on the R406. The larger blue circle at the bottom of the image represents the area where the speedometer was displayed.

(A1)

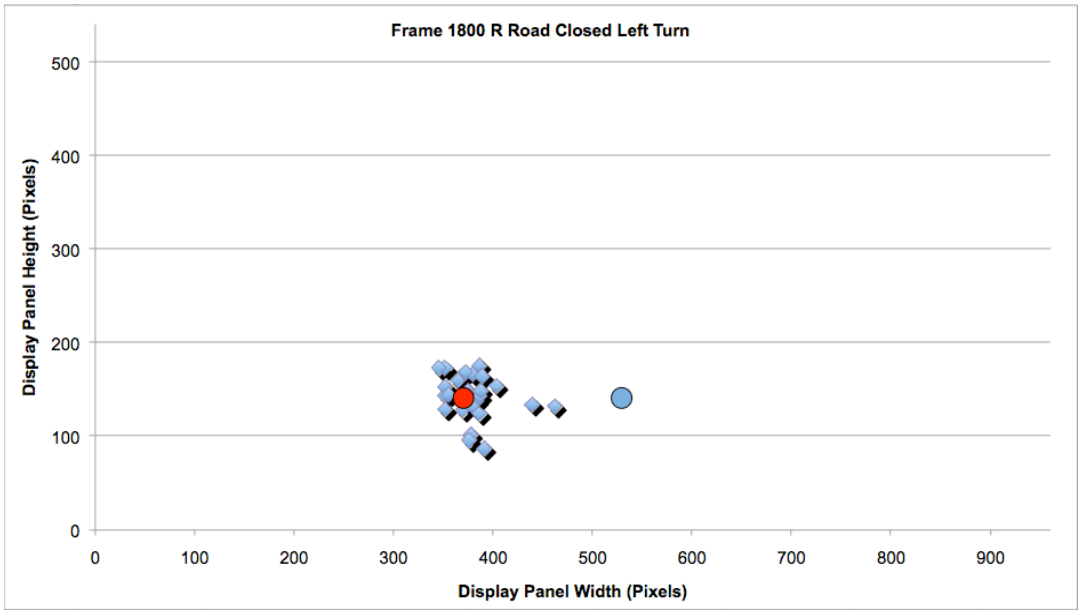

Figure 4.11 (A1) shows a representation of gaze data from frame 1800 and their proximity to the tangent point (red circle) and the outer lane point (blue circle). Blink data (pink circled numbers shown in previous image) and gaze data found at the speedometer target were classified as disparate data and removed.

(B)

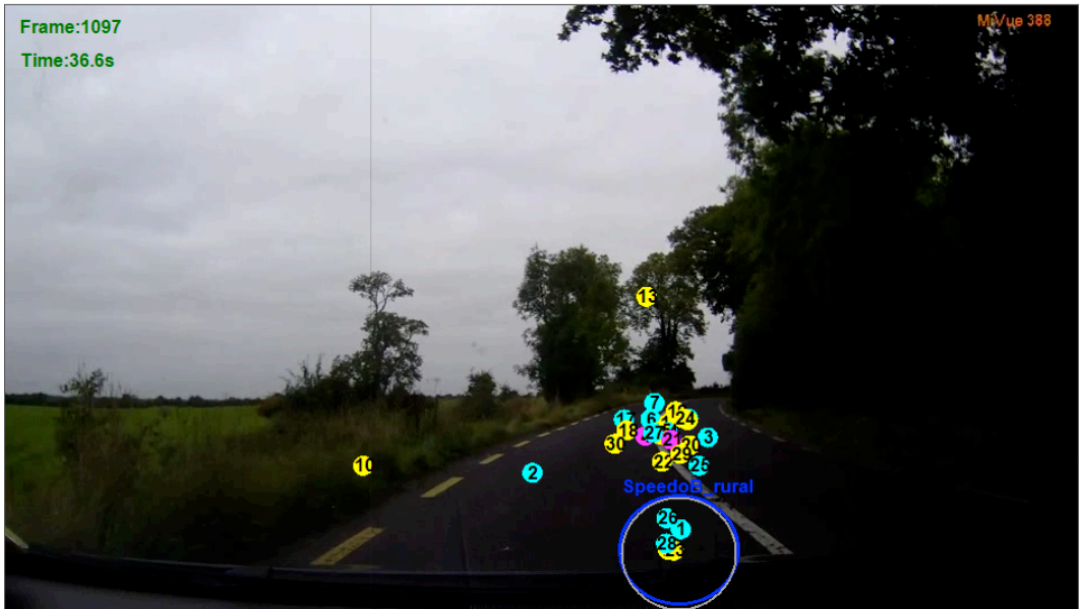

Figure 4.11 (B) shows frame 1097 sampled from the R road segment. The sample shows participant gaze data for a closed right turn on the R406. The larger blue circle at the bottom of the image represents the area where the speedometer was displayed.

(B1)

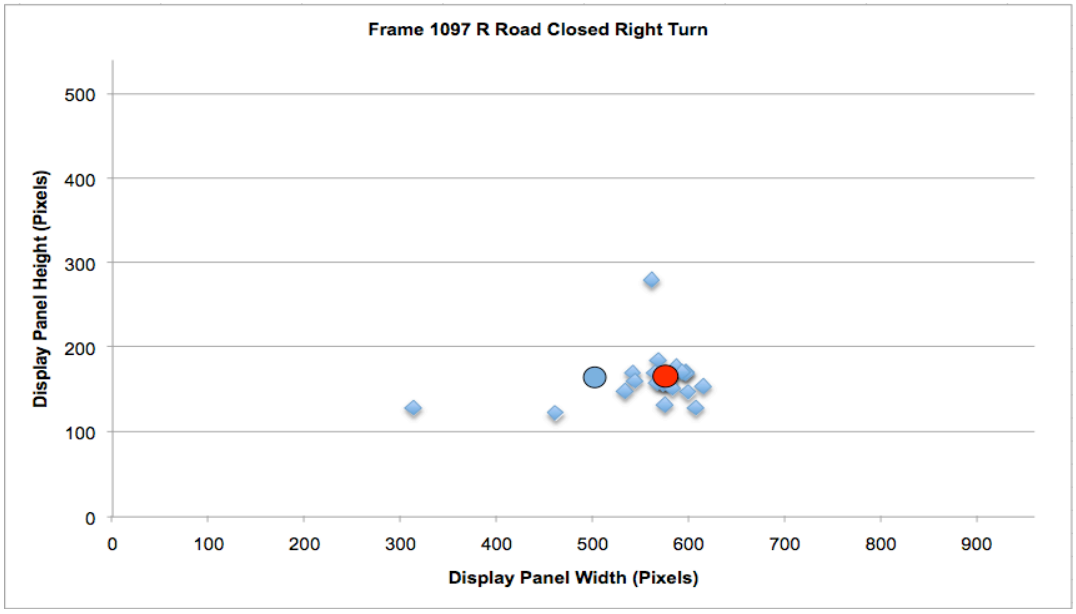

Figure 4.11 (B1) shows a representation of gaze data from frame 1097 and their proximity to the tangent point (red circle) and the outer lane point (blue circle). Blink data (pink circled numbers shown in previous image) and gaze data found at the speedometer target were removed.

(C)

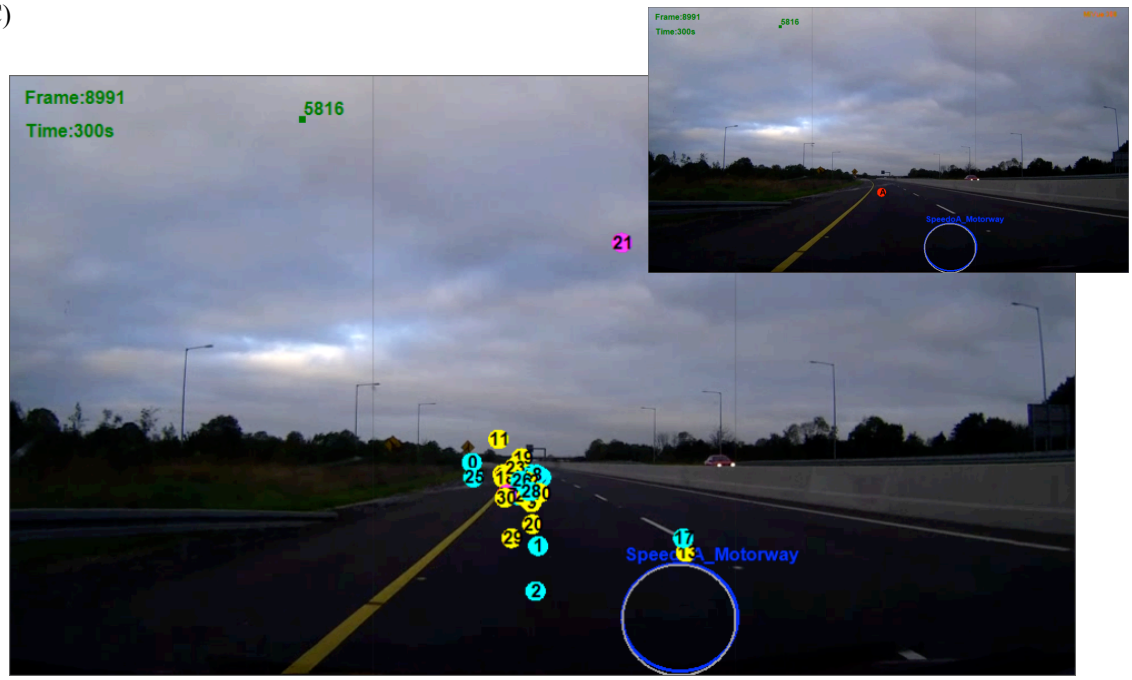

Figure 4.11 (C) shows frame 8991 sampled from the Motorway road segment. The sample shows participant gaze data for an open left turn on the M3. Insets are included to show the open curve being occluded by the gaze data.

(C1)

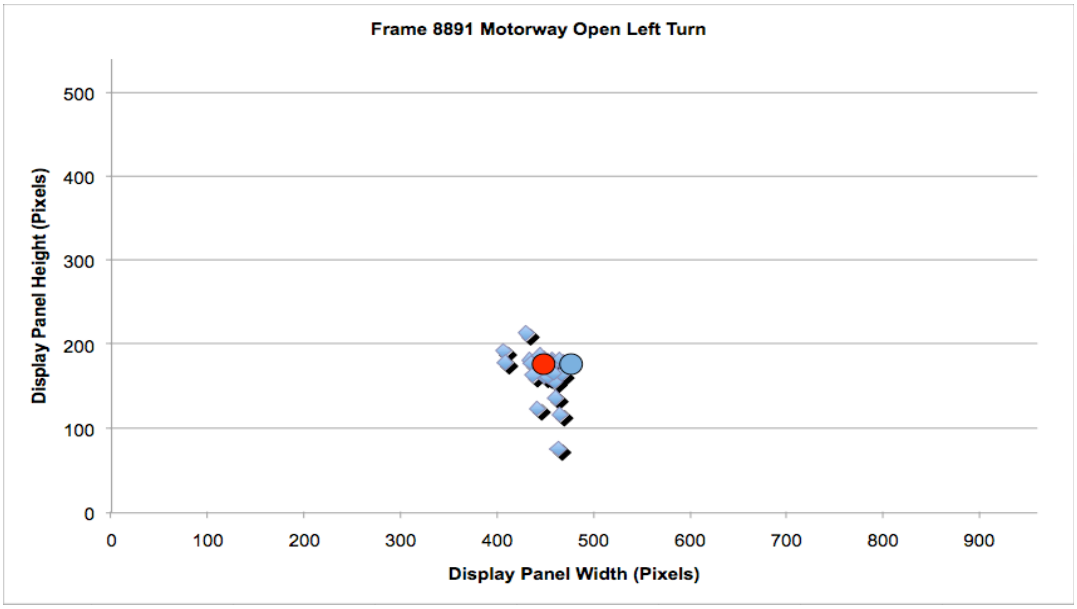

Figure 4.11 (C1) shows a representation of gaze data from frame 8991 and their proximity to the tangent point (red circle) and the outer lane point (blue circle). Blink data (pink circled numbers shown in previous image) and gaze data found at the speedometer target were removed.

(D)

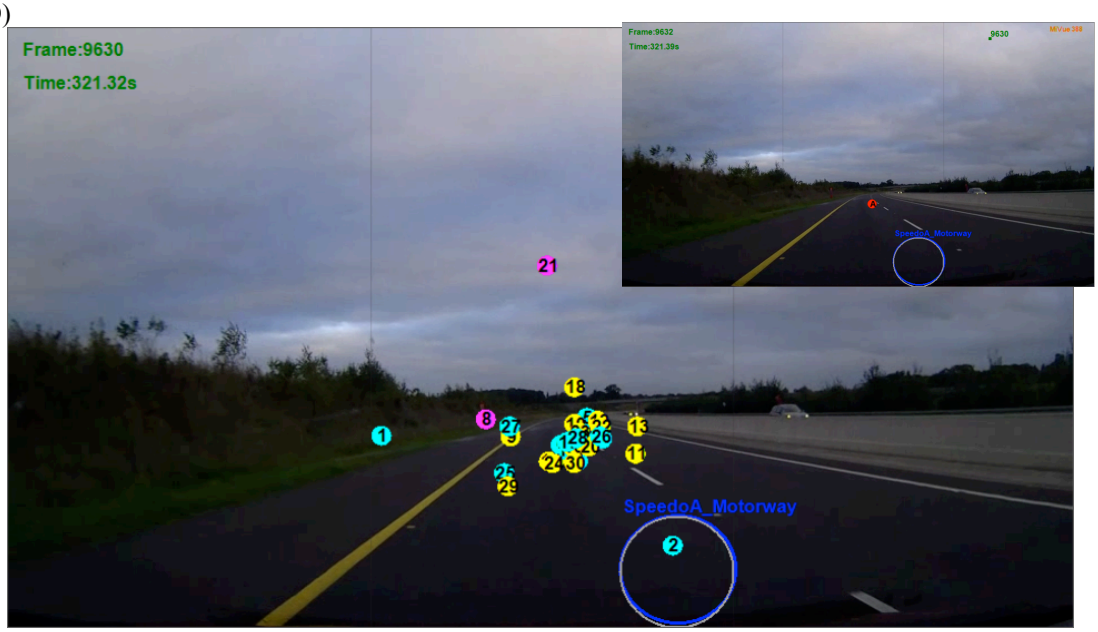

Figure 4.11 (D) shows frame 9630 sampled from the Motorway road segment. The sample shows gaze data for an open right turn on the M3. Insets are included to show the open curve being occluded by the gaze data.

(D1)

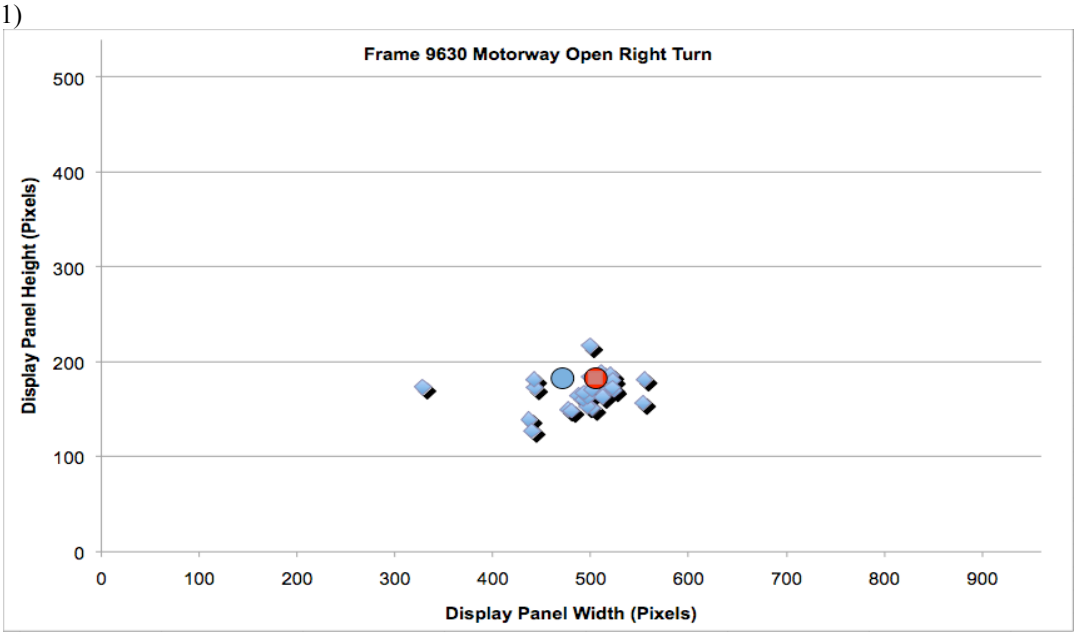

Figure 4.11 (D1) shows a representation of gaze data from frame 9630 and their proximity to the tangent point (red circle) and the outer lane point (blue circle). Blink data (pink circled numbers shown in previous image) and gaze data found at the speedometer target are removed.

For all samples, speedometer fixation and blink data were classified as disparate data and removed. Table 4.5 shows the mean distance (measured in pixels) from the tangent point for all 30 participants. The mean distance from the outer lane point is also shown along with the halfway point between the two (lane centre point). Note: Pixel ratio for the screen in which the video frame was analysed is 960px x 540px. Also as perspective occurs in these images, points examined further down the road naturally have smaller distances between them (see C and D) than those closer to the car (A and B).

Table 4.5 shows the mean distance from the participant's gaze data to three lateral points assigned to the road (tangent point, middle of lane point and the outer lane point).

Sample Description		**Gaze Fixations** Mean Distance to Road Points Below (Unit: pixels) 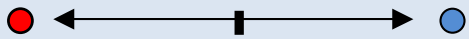		
Figure	**Frame Number**	**Tangent Point**	**Lane Centre Point**	**Outer Lane Point**
(A) R Road Closed Left Turn	1800	28px±	72px±	149px±
(B) R Road Closed Right Turn	1097	41px±	56px±	84px±
(C) Motorway Open Left Turn	8991	30px±	42px±	67px±
(D) Motorway Open Right Turn	9630	38px±	42px±	48px±

For R road samples (A) and (B) shown in Table 4.5 the tangent point shows the lowest distance to gaze information, thus suggesting the tangent point as an area attracting fixation on closed bends where sight distance is obstructed. Sample (B) shows people tending slightly further away from the tangent point on right closed turns as opposed to left. Samples (C) and (D) from the motorway route also show shorter distances to the tangent point on gradual bends where sight distance is higher indicating the use of the tangent point for 'open' bends also. All four sample frames in Table 4.5 show increases in mean fixation distances at the outer lane point supporting the tangent as the area used

most frequently on bends as an eye-to-steering cue. It is important to note again at this stage that steering was disabled for the experiment yet these results yielded by the system further validate the effectiveness of the visual cue stream by showing similar behaviours expected by those required for steering maneuvers.

4.5.2 Region Analysis

While the previous method was very useful for analysing bends, it did not offer much information by way of analysing straights stretches of road where visual analysis showed eye movement gathering above and around the lane centre. Therefore, the second process used for analysing straights involved classifying the road into 4 regions of visual exploration in order to determine where in the vicinity of the road each driver was looking. This method of analysis also included a temporal factor as shown in Figure 4.12 in accordance with early research mentioned in Chapter 2 from Cohen (1977) highlighting the use of fixation 'duration' as an effective information input. This was achieved in the experiment by analysing elements of prior and post eye movements for a duration of 4 seconds. Sequences of 12 frames (3 per second) were sampled on both routes at straight segments of road where sight distance was not obstructed. A duration factor was not applied to measuring gaze data on road bends in the first analysis process due to rapidly changing geometry.

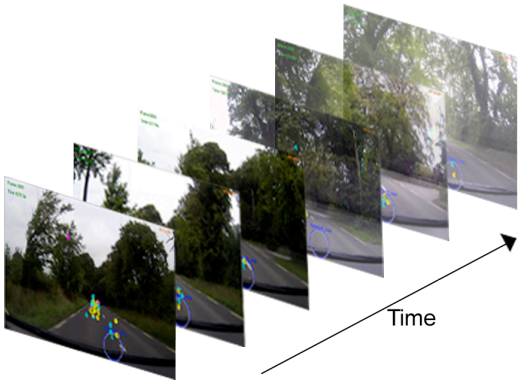

Figure 4.12 shows sequence of frames containing gaze data over time (2 seconds). 3 frames are sampled for every second measured.

Results from this analysis of both routes are listed below in Table 4.6 (A) and (B). Each row represents 30 participants in both tables and is segmented into frame description and gaze location.

Table 4.6 (A) shows the number of fixations on each region for a 4 second duration of the R406 road. Primary measurements are shown in the vertical blue columns and a participant average is shown in the bottom row. Inset is Figure 4.9 showing 4 classified regions.

R Road Segment						
Frame Description		**Gaze Location**				
Frame Number	Time Stamp	On the Road	Above the Road	Margin/Outer Lane	Speedometer	Bad Data points
3810	127.13s	19	3	1	4	3
3820	127.46s	16	6	0	5	3
3830	127.79s	20	3	1	3	3
3840	128.13s	20	5	2	0	3
3850	128.46s	18	6	1	5	0
3860	128.83s	18	4	0	2	6
3870	129.13s	21	4	2	1	2
3880	129.46s	22	3	1	3	1
3890	129.83s	19	8	0	1	2
3900	130.13s	22	1	3	3	1
3910	130.46s	23	0	5	1	1
3920	130.83s	22	3	0	2	3
	Average	**20**	**4**	**1**	**3**	**2**
	SD	**2**	**2**			

Table 4.6 (B) shows the number of fixations on each region for a 4 second duration of the M3 motorway. Primary measurements are shown in the vertical blue columns and a participant average is shown in the bottom row.

Motorway Road Segment						
Frame Description		**Gaze Location**				
Frame Number	Time Stamp	On the Road	Above the Road	Margin/Outer Lane	Speedometer	Bad Data points
5510	183.85s	21	5	3	1	0
5520	184.18s	23	3	2	0	2
5530	184.52s	23	3	3	0	1
5540	184.85s	17	6	4	2	1
5550	185.19s	17	3	2	5	3
5560	185.52s	15	4	2	4	3
5570	185.85s	17	5	4	2	2
5580	186.18s	22	2	4	2	0
5590	186.52s	15	3	3	4	5
5600	186.85s	20	2	3	4	1
5610	187.18s	18	4	3	3	2
5620	187.52s	16	7	3	3	1
	Average	**19**	**4**	**3**	**3**	**1**
	SD	**3**	**1**			

A comparison of both routes indicated that participants behaved similarly on both the R and M roads. For example, Table 4.6 (A) shows an average of 20 drivers fixating on the R (Stan. Deviation: 2) road surface region in comparison to an average of 19 drivers fixating on the motorway (Stan. Deviation: 3) road surface region. In addition, an average of 4 drivers fixated above the-road region for both routes. This result disagreed with the hypothesis formed at the beginning of this study that expected more drivers to fixate 'on the road' surface of R road type based on higher expectations of dangerous geometry. This result will be deliberated further in the discussion section at the end of this chapter in combination with the results from the third and final process used to examine fixation distances. As fixations above the road were deemed as 'tending towards infinity', these fixation points were considered too difficult to measure for gaze

distances. However, the final process in this experiment was used to measure distances that could be estimated, the fixations on the road surface.

4.5.3 Look-Ahead Distance Analysis

Fixations on the road surface were further analysed by sampling and comparing video frames from straight segments on both routes. The following 6 video frames in Figure 4.13 Samples 1-6 show 3 separate straight segments on the R road (S1-S3) route and 3 on the Motorway route (S4-S6). In each sample, video frames are preceded by graphical representations of relevant gaze data above the road (red markers) and on the road surface (blue markers). A third graphical representation for each sample then displays gaze distances calculated for each 'on the road' fixation using the projective transformation discussed in Section 2.9.2. In this analysis process gaze data was also manually excluded for speedometer fixations, blink information and data considered not in the vicinity of the road.

Sample 1

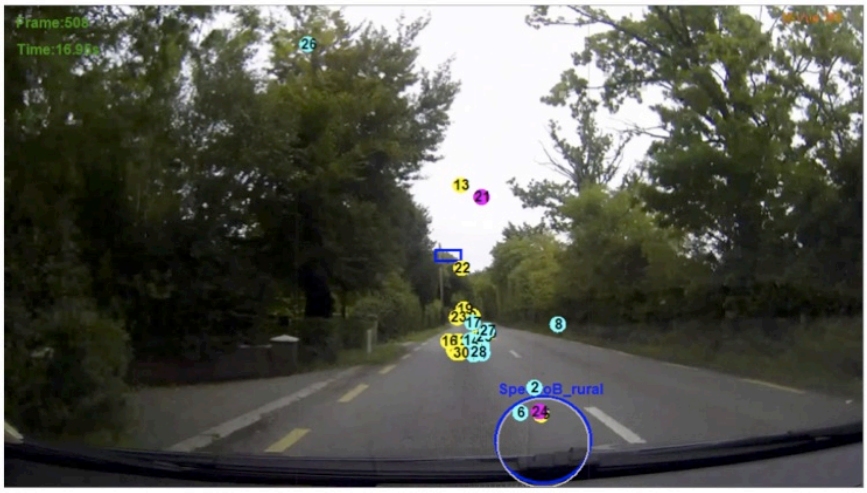

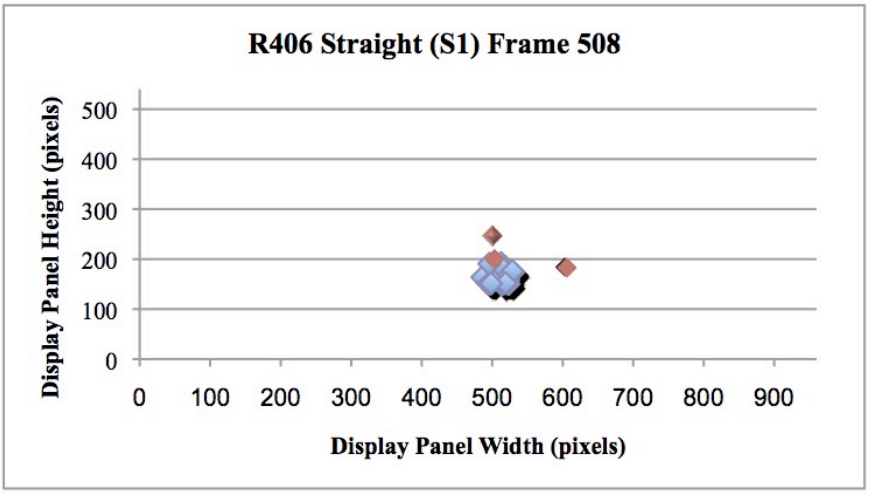

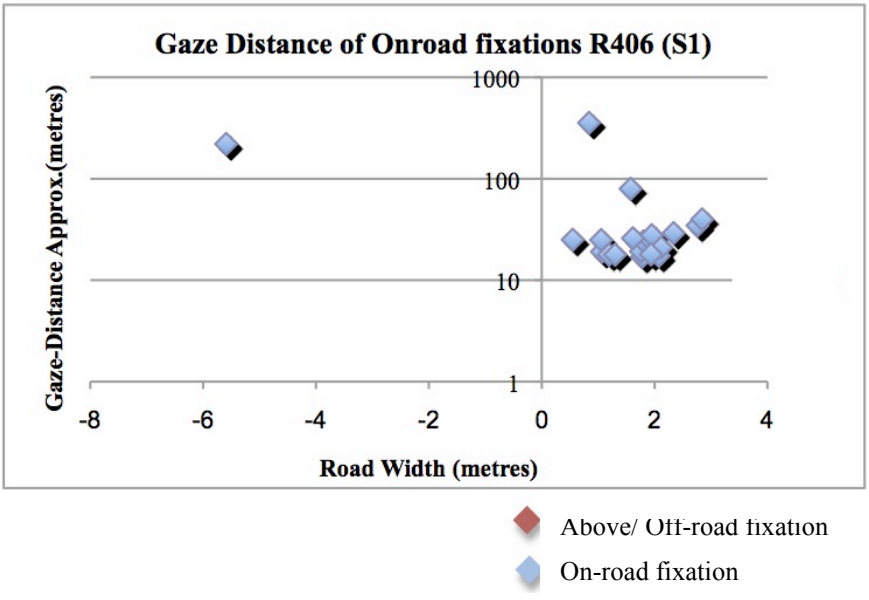

Figure 4.13 (S1) shows gaze data for video frame 508 preceded by a graphical representation of the gaze data. On the road fixations are then represented as gaze distances and scaled in metres.

Sample 2

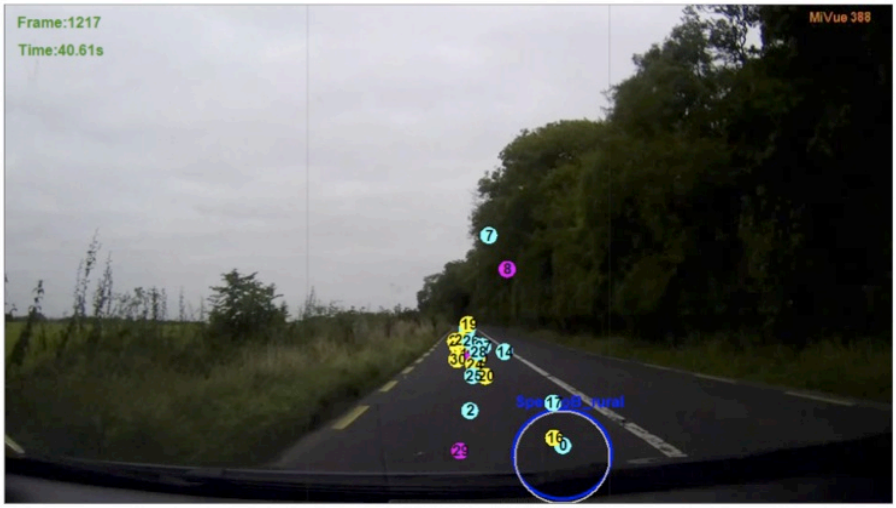

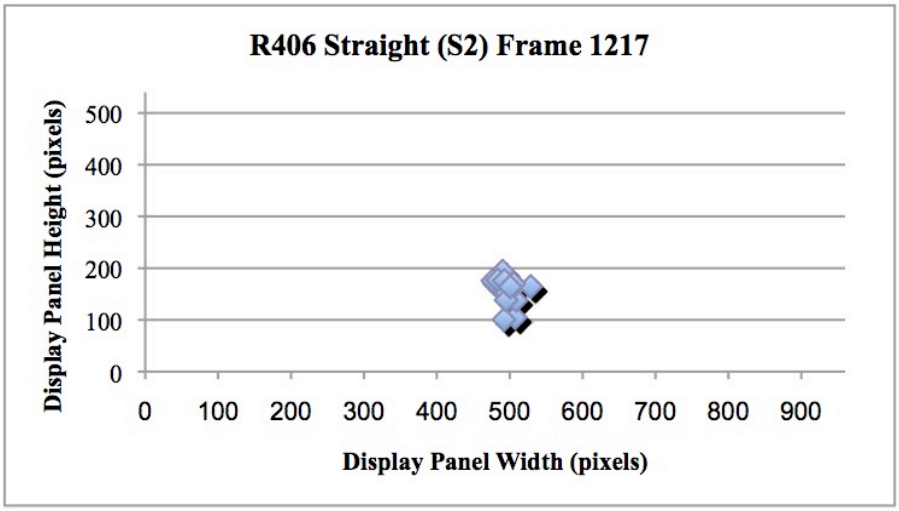

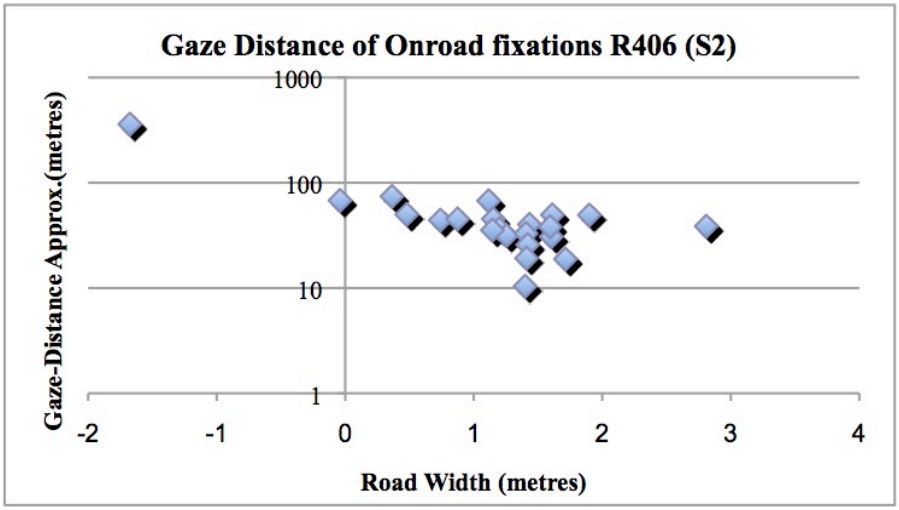

Figure 4.13 (S2) shows gaze data for video frame 1217 preceded by a graphical representation of the gaze data. On the road fixations are then represented as gaze distances and scaled in metres.

Sample 3

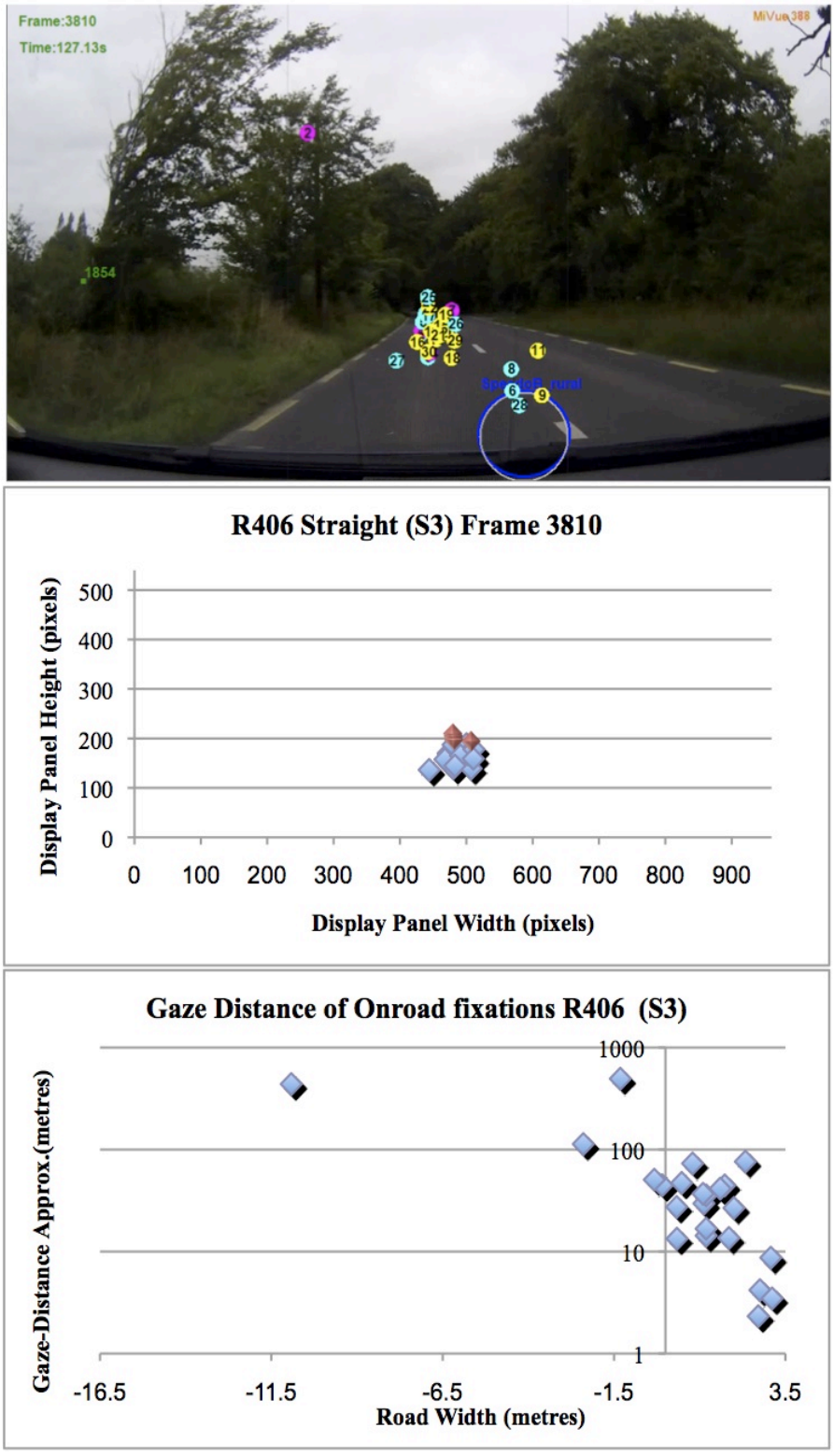

Figure 4.13 (S3) shows gaze data for video frame 3810 preceded by a graphical representation of the gaze data. On the road fixations are then represented as gaze distances and scaled in metres.

Sample 4

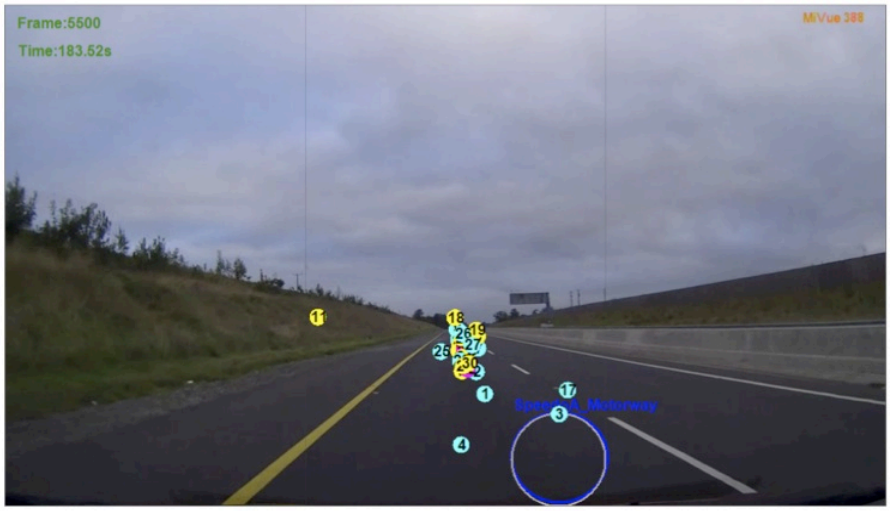

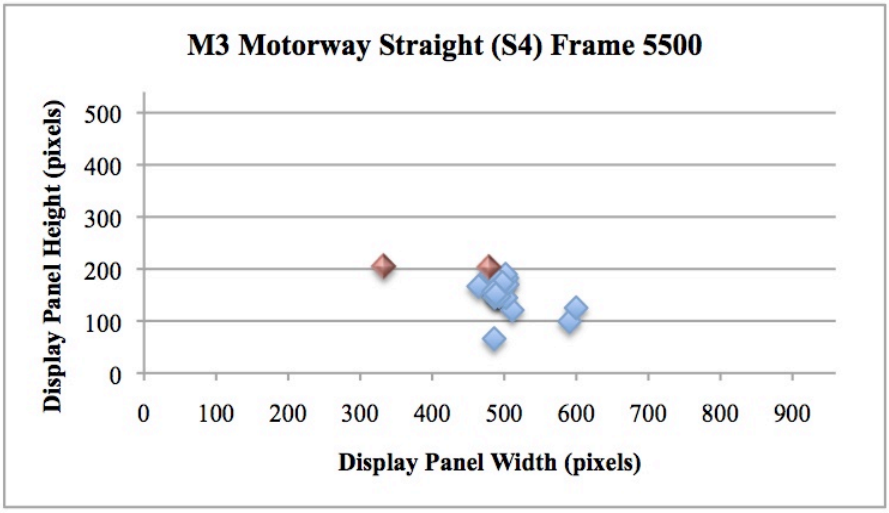

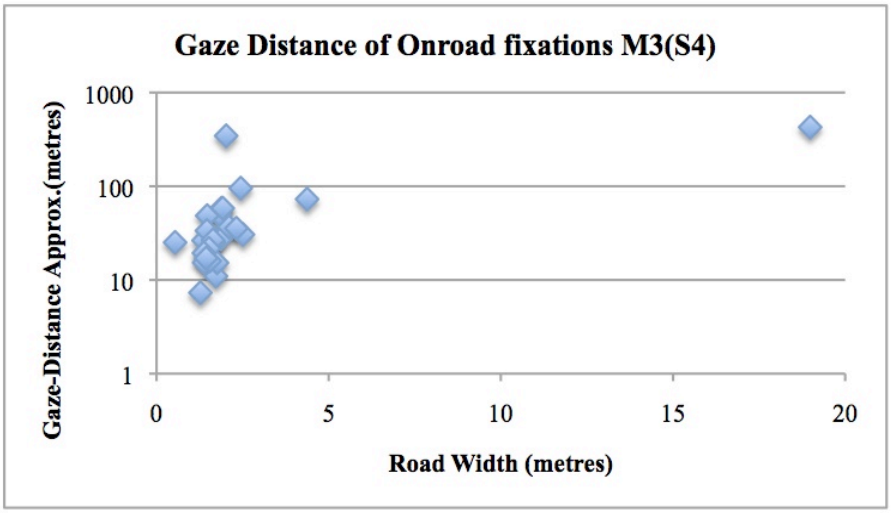

Figure 4.13 (S4) shows gaze data for video frame 5500 preceded by a graphical representation of the gaze data. On the road fixations are then represented as gaze distances and scaled in metres.

Sample 5

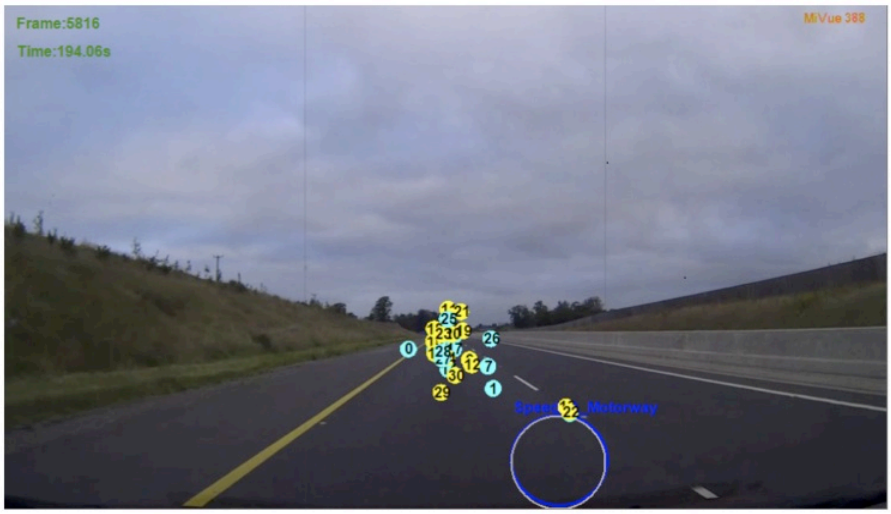

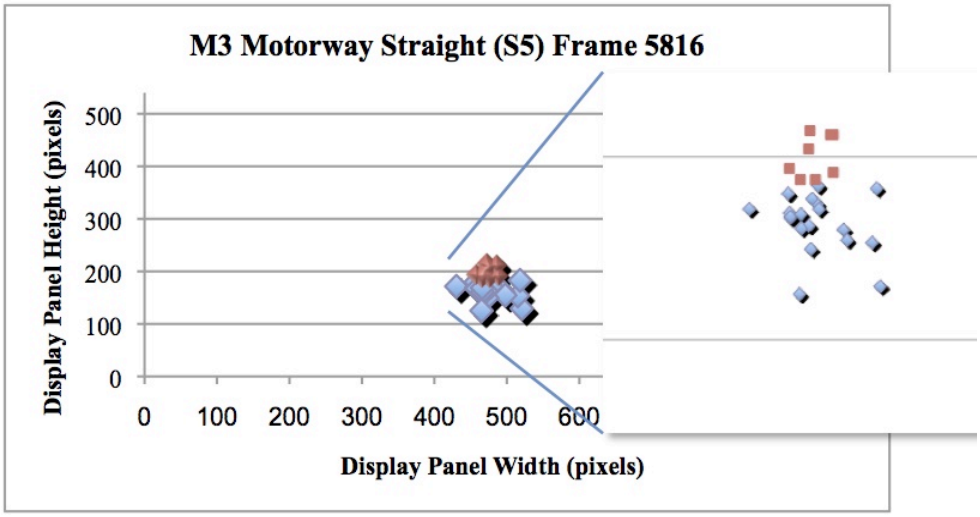

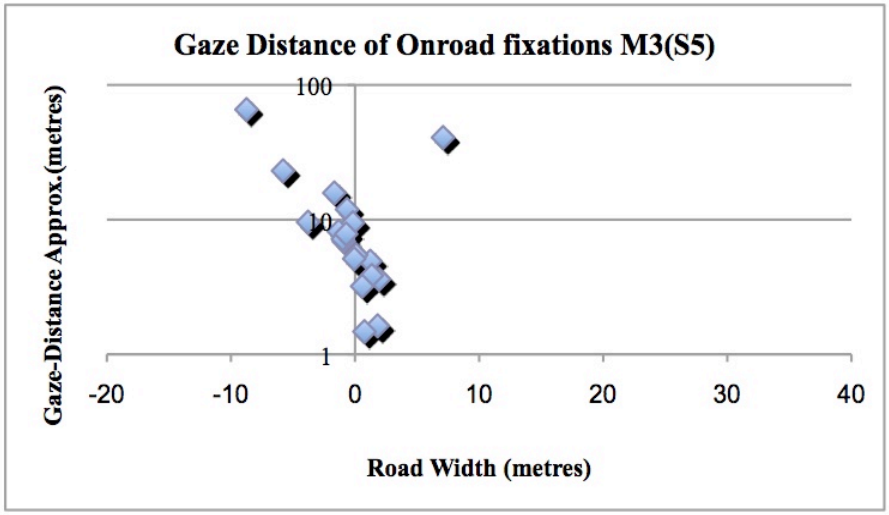

Figure 4.13 (S5) shows gaze data for video frame 5816 preceded by a graphical representation of the gaze data. Inset is used to enlarge condensed data. Red markers indicate above road fixations. On the road fixations (blue markers) are then represented as gaze distances and scaled in metres.

Sample 6

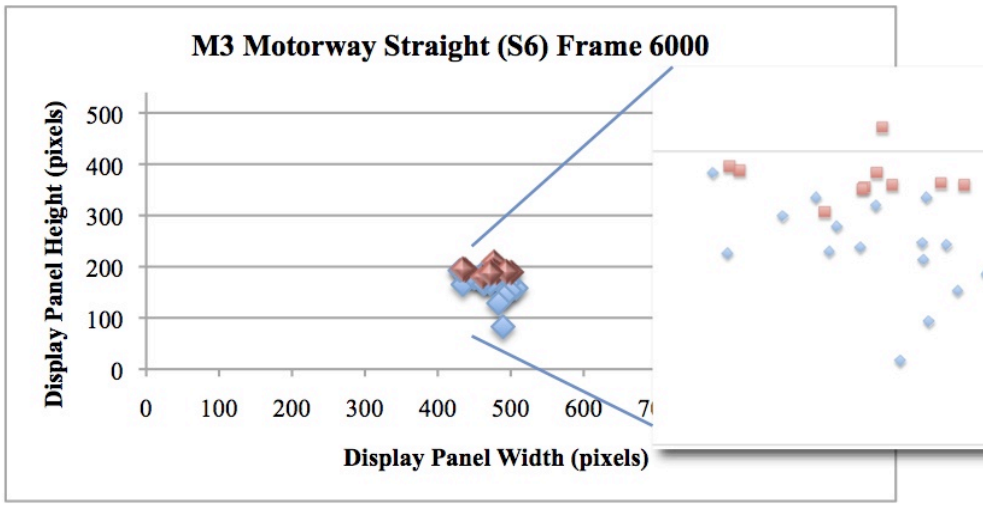

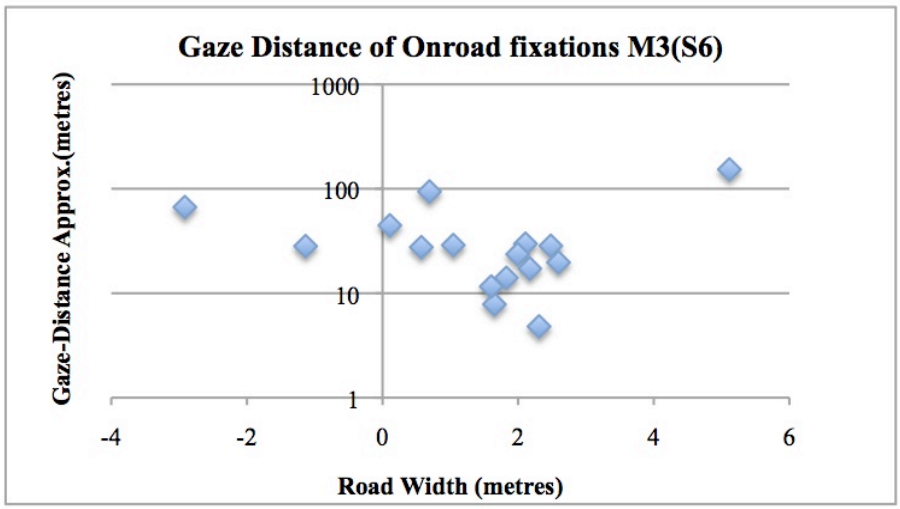

Figure 4.13 (S6) shows gaze data for video frame 6000 preceded by a graphical representation of the gaze data. Inset is used to enlarge condensed data. Red markers indicate above road fixations. On the road fixations (blue markers) are then represented as gaze distances and scaled in metres.

Insets for Figure 4.13 samples (S5) and (S6) are used to clarify high numbers of fixations above the road. Results of the 6 samples shown in Figure 4.13 (S1-S6) are further quantified in Table 4.7. Mean participant distances were calculated for valid gaze data for each sample. Furthermore a mean distance for each road type was calculated by combining the three samples for both routes. Results showed that the mean gaze distance ($\bar{x}$) on the R road segment showed higher measurements (49.1m) than that on the M road segment (39.9m).

Table 4.7: Gaze Distance calculations for R road vs M road

Rural			**Motorway**		
Sample	**Mean Distance (metres)**	**S.Deviation (metres)**	**Sample**	**Mean Distance (metres)**	**S.Deviation (metres)**
1	52.9	84.4	4	60.9	98.9
2	55.0	69.8	5	19.8	15.1
3	39.6	27.4	6	39	38.15
$\bar{x}$	**49.1**	61.8	$\bar{x}$	**39.9**	50.7

Lowest mean distances measured in Table 4.7 occur in sample 5 (19.8m) on the motorway segment, however, insets for this video frame also show a number of fixations above the road. In addition to sample 5, sample 6 (see Figure 4.13 S6) also showed fixation data numbers above the road which in turn caused lower averages of gaze distances due to less drivers fixating on the road surface. Nonetheless, it was expected at the start of this study that fixation distances on R road types would be lower (nearer to the area in front of the car) than that of M road types due to dangerous bends

associated with R road geometry. These results were unexpected and are discussed further in the discussion section.

4.6 Chapter Discussion

This Chapter has described the acquisition system and analysis processes developed to collect and analyse driver behaviours. The experiment involved thirty participants driving contrasting routes in order to determine if features of road geometry affected driving behaviour. Gaze information for each participant was recorded and combined with video frames of the routes driven. Samples of this combined data were extracted of left and right 'open' and 'closed' bends along with samples of straight road sections. Equal samples were taken of bends and straights on both contrasting R and M routes and a comparison was made.

Currently, there are many ways to measure driver behaviour including naturalistic driving and real-time video observation as discussed in Section 2.1. However, as these methods involve real-time observation of drivers everyday behaviours, they are often uncontrolled and can be both timely and costly when using multiple vehicles instrumented with video and sensor devices (naturalistic)[19]. This study chose the use of a low fidelity fixed base driving simulator for measuring driving behaviour not only for the availability of its low-cost components but also for the advantage of observing drivers while deliberately placing them in controlled scenarios involving dangerous road geometry. In addition, the integration of an eye-tracking device with a fixed base simulator added physiological advantages. For example, eye movement was steadily recorded as no lateral or longitudinal forces acted on the driver causing the body (head) to move from a fixed position, allowed for more focused recordings of eye behaviour.

The method developed in this study also demonstrated the effectiveness of the use of a low-fidelity simulator for measuring driving behaviours. By combining low cost data acquisition systems such as the witness camera with software based driving scenarios, meaningful measurements were achieved based on drivers reacting similar to how they would normally on a real world route. This was validated in relation to speed as discussed in Chapter 2, Section 2.7 (*Driving Simulator Fidelity and Purpose Validation*), whereby drivers reacted to road geometry by breaking appropriately and was also validated in relation to eye movement in Chapter 4, Section 4.5 (*Results of Data Analysis*), where drivers eye movements followed road geometry for steering cues even though steering was disabled.

Methods to analyse the data generated by participants driving these simulator scenarios were also discussed in this chapter. The first method used to analyse data from the experiment was interactive visualisation software allowing for the regeneration and observation of eye movement overlaying video streams of both routes. This allowed for visual observations to be made and showed eye gaze data overlaying oncoming road geometries. However, in order to further analyse this gaze data in relation to road features such as road bends, samples of these video frames were extracted to measure and compare eye behaviour on both routes. As discussed in chapter 2 road behaviour has been measured in the past using driving simulators on American and other European roads[88], however, little to no studies have been reported on Irish roads whereby road types such as R roads and M roads are being compared.

Results drawn initially from the visual analysis software gave a clear indication that behaviours on Irish road bends were in accordance with research related to bends from other countries reporting the tangent point as the region on the curve that attracted the

most amounts of eye fixations [51][54][82]. These frequencies were observed in video playback when clusters of eye movements fixated on the tangent point before and during bend negotiation. An example of this is shown in Figure 4.11 (A) when eye gaze concentration was observed at the curve tangent to the drivers line of sight on a closed left bend. However, as studies suggested in Chapter 2, drivers still have the ability to negotiate curves when using lateral points at the same angle to the tangent point [51]. In addition, at open bends where tangent points were further away from the car (see Figure 4.11 (*C*)), it was difficult to determine the point of the road lane drivers were fixating on due to distance and perspective causing the gap between the tangent and outer lane point to look very small. To combat this, further analysis was used to measure each fixation and its relation to the tangent on 4 sampled curves, 2 from the R road and 2 from the M road. All 4 sample frames showed increases in mean fixation distances from the tangent at the outer lane point further supporting the use of the tangent point as the most frequented point of fixation when negotiating curves.

Although similar results were gained for bends on both R and M road types, an observation made on the samples containing open bend showed fixation data scanning above and around the road as the geometry gradually straightened indicating that as sight distance became more available, drivers accessed additional regions of the road. To examine these straight sections of geometry, a process was used to further classify regions of the road to determine where drivers were looking in the vicinity of the road lane. To do this, the average fixation for the participants was achieved by measuring data for 12 consecutive video frames (approx. 330ms apart). Results of these measurements showed that at a given time on straights on R roads, an average of 4 out of 30 drivers were fixating ‘above the road’ in comparison to 20 of the 30 drivers

fixating ‘on the road’. Motorway regions measured similar frequencies averaging 4 of 30 drivers fixating ‘above the road’ and 19 of the 30 drivers fixating ‘on the road’ at a given time. Measurements on the M road showed more fixations on the margin of the road (avg. 3 of 30 vs avg. 1 of 30 on R road). An observation made from this measurement is that lateral sight distance may have been more available to motorway drivers as opposed to vision being ‘tunneled’ by surrounding foliage on R roads. The hypothesis formed at the beginning of this study estimated that the number of driver’s gaze fixations ‘on the road’ on the R road would be significantly more than that of M Roads due to higher expectations of danger/hazardous geometry. However, this measurement has shown that regardless of road type, drivers fixated on regions of the road based on the road geometry.

Furthermore, the hypothesis formed prior to this investigation also expected that fixations ‘on the road’ surface would be ‘near of field’ on R roads due to expectations of danger, narrower road margins (room for error) and higher risks of obstructed hazards. To measure this, a calculation was used to translate gaze fixation to look-ahead distances. Results showed that the mean gaze distance on the R road segment showed higher measurements (49.1m) than that on the M road segment (39.9m). This result however does not include ‘above the road’ fixations which were more common in the sampled M road frames, thus, less fixations on the road surface. Regardless of the difference between the two road types, the results failed to show fixations close to the car or ‘near of field’ as expected on the R roads. This further supports drivers fixating on regions of the road based on the road geometry by suggesting that the fixation area within the road surface region was also based on road geometry.

Hardware and environmental limitations of this experiment are indirectly highlighted at the start of this discussion having chosen a driving simulator tool to measure driving behaviour. Much like naturalistic and video observation measurement methods discussed, simulators so too have their inherent disadvantages. By merely asking a driver to participate in this 'lab-based' experiment there were indications that the input data was subject to environmental factors. For example, subjects may have performed better or worse under observation as opposed to the naturalistic driving approach where subjects are semi-unaware of being observed. In addition, some of the components of the simulator were also similar to that of gaming tools such as the steering wheel and pedals which may have also influenced how users perceived the experiment. Drivers were asked in advance if they had had experience on driving games on gaming consoles in order to highlight this influencing factor. In addition, lighting situations introduced errors in eye tracking particularly in cases where drivers wore glasses or room lighting interfered. To combat some of these issues, sample gaze data points showing connection errors due to lighting were extracted before analysis.

Limitations in the measurement of the raw gaze data were that suggested by Donges (1978). As discussed Donges (1978) reported eye movement as a process fed by dual signals of information as opposed to one [81]. For example, the first level relying on near field information for lateral positioning and the second level using distant information for the anticipation of road curvature. This experiment based its findings on the measurements capable of being measured by the Tobii eye tracker, therefore peripheral vision was not measured for this study.

Further limitations were present in some of the processes used to analyse data post-video analysis. The first process of analysis used to measure bends could not

incorporate the same temporal factor as that that applied to the second process measuring straights (duration of 4s) due to rapid changes in geometry. For the bends used in this study, there was limited time before the drivers exited each curve therefore samples of individual frames (as opposed to consecutive frames) were chosen instead. The process used to calculate look-ahead distances also presented limitations. This distance measurement was initially applied to bends also, however as calibration for this particular method was only permitted on the plane of the road, results for distances on bends scaled incorrectly due to curvature and the perspective of the road. Subsequently, as this measure of distance was not the primary focus for bend analysis it was therefore abandoned.

An additional difficulty associated with measuring look-ahead distances was presented when measuring distances of fixations above the horizon as these fixations were considered as 'tending towards infinity'. For example, as these fixations were above the horizon, a finite point could not be determined due to the absence of any physical surface. In addition, as the fixation distance increased towards infinity, the margin for error increased exponentially. For example, as minute changes in the fixations pixel position at these distances could possibly equate to hundreds of kilometres in real-world metric measurements. For this reason the look-ahead distance method proved more useful for calculating distances on the road surface as fixations in this case were referenced using corresponding road markings (broken white line) during the calibration process. This allowed distances to be crosschecked against physical properties of the road. However, similarly with measuring fixations on the road surface, errors were also expected as distances increased. Therefore the confidence of using this method for accurate look-ahead distance calculation was reliant on measuring fixations for closer

distances (of up to approx. 200m), thus proving appropriate for this experiment primarily measuring ‘near of field’ fixations.

The simulator developed in this experiment has proven an effective tool for measuring driver’s eye behaviours on contrasting Irish routes. The data generated from participants will be further analysed to measure additional measurements taken during testing such as speed and sustained attention. This will be discussed in the future work section of the next chapter. The following chapter will also combine findings from experiments documented in Chapters 3 and 4.

Chapter 5

Conclusions and Future Work

This body of work has investigated the effects of road geometry on Irish accident rates and driver behaviour. The study has also sought to examine different categories of Irish roadways particularly those containing dangerous geometric characteristics. Although the RSA of Ireland promotes many aspects of safe driving including speed awareness, drink driving etc. through many successful campaigns and the National Roads Authority is generally charged with designing, building and maintaining roads, research on road geometry, accident rates and driving behaviour within an Irish context is generally limited. This study sought to answer the following two research questions in order to investigate accidents and driver behaviour at contrasting features of road geometry.

1. Does a relationship between road geometry and Irish accident rates exist?

2. Does road geometry affect driver behaviour?

To examine these two questions, two experiments were developed. Although findings related to each specific question have been discussed in the two relevant chapters (Chapter 3 and 4), This chapter will try to bring the results together and show how these combined observations suggest work for the future.

5.1 Summary of Achievements

1. Relationship between road geometry and Irish accident rates.

a. Key literature findings: Literature from European transportation bodies have shown conflicting results as to whether changes in geometry can affect accident rates, however, what is generally accepted is that certain 'elements' of geometry can play a pivotal role. For example, factors such as 'horizontal curvature' has been shown to be related to accident rates particular at sharp bends of less than (200m). In addition, 'types of curvature' such as consecutive curves have also been reported as contributing to abrupt speed changes and therefore increases in accident rates [31].

b. Classification method: The method developed in this study for assigning road character to accident location demonstrate a possible technique to improve the road description of the accident location. For example, where accidents are normally assigned a curvature based on a subjective decision by policing authorities, the method in this study assigns curvature based on GPS information and further classifies these curvatures into categories of curvatures bands. Furthermore, as 15% of the 23,000+ accidents recorded by the RSA of Ireland over the four year period remained unspecified, this study has also demonstrated ways to assign geometric characteristics to accidents that currently remain unclassified. Currently the RSA of Ireland use geo-locations as a description for accidents but do not assign road names to an accident . The method developed in this study investigated ways in which these individual accident locations may be bound to individual road names or routes. Future applications of this technique can be used to apply accident weights to particular roads.

c. Dimensional Analysis and ARC rate: An analysis of the three Irish road types has shown that the N road category agrees with literature relating to accidents on horizontal curvature the most. Following the new classification method and assignments of accidents, the study reveals an interesting pattern of results with high concentrations of accidents on roads of high curvature (<200m) particularly on the N roads. Bends less than 200m seemed to be particularly affected, agreeing with other studies [22]. In this case, the correspondence to the lower radius band was the highest amongst the three road types. This was unexpected as typically R road types have similar geometric make-up to N roads in that they both contain a combination of straights and hazardous bends. Therefore it was hypothesised that similar accident concentrations would be present in the same band of curvature on N and R road types. However, as shown this was not the case. The R road can be differentiated to N road types in that it contains a lower speed-limit (approx.40-80km/h). An observation made from the analysis was that accident concentrations on the N road may be as a result of a combination of geometries. For example, a combination of geometries such as a straight (allowing higher speeds of up to 100km/h) followed by curvature or consecutive curvatures (causing abrupt changes in speed), and further offering less time to react to hazardous bends.

2. Effects of road geometry on driver behaviour.

a. Key literature findings: Research has suggested various ways in which drivers eye behaviours interact with road bends. These studies widely accept the tangent point of the curve (where the driver's line of sight meets the point at which the road curves) as the area used most frequently as an eye-to-steering cue [49][50]. Other research has shown that dual signals of the eye are used during steering and that areas further down

the road are relied upon heavily in order to reduce steering error, thus demonstrating the importance of available sight distance [81].

b. Driving Simulator with Eye Tracking Integration: In order to better understand driver fixation points across various road geometries, a reality-based driving simulator with physiological and cognitive assessment capabilities was developed. Initial tests were carried out on the simulator to validate its use as an effective measurement tool using a video model. With correlations above 84% these validations of the video-based simulator suggested that drivers reacted reliably to the designed scenarios based on speed when compared. Further validation was determined during eye measurement analysis when drivers tracked geometry and targets on screen.

c. Experiment Method: Thirty participants were asked to drive two contrasting route scenarios using the driving simulator (motorway and a rural road). Eye fixation co-ordinates were analysed to measure where particpiants looked when driving. The output of this experimental tool was a data set for each participant that included parameters such as eye fixation co-ordinates. The data set for each participant was integrated into a GUI to display visualisations of eye movement.

d. Tangent and Look-ahead distance Analysis: Findings demonstrated that participants eye behaviour on Irish road geometry was in accordance with literature showing eye gaze concentration on the tangent point of the curve at road bends [49][50][51]. As curvature increased, participants focused directly on the road surface at the tangent of the curve, however as curvature gradually decreased, a number of participants frequented other regions of the road surroundings. To investigate this further, straight segments of the road were classified into various regions of interest. Comparisons of

both the motorway and the rural road showed almost equal amounts of fixations 'above the road' and 'on the road surface'. In addition, fixations on the road surface were further examined to calculate 'look-ahead distances' on the contrasting routes. Results showed similar mean look-ahead distances for both road types with drivers looking slightly further ahead on R road segments. These results for region analysis and look-ahead distances on the straight segments did not agree with the hypothesis at the start of this study expecting drivers to fixate on areas closer to the car than those reported based on dangerous geometries associated with R road types. However, a positive result from these data analysis processes showed that drivers did react to the road environment based on road geometry regardless of the road type, thus demonstrating road geometry affecting driver behaviour.

5.2 Contributions

The two principal contributions of this study were the development of a system to further classify Irish accident data and the commissioning of a reality-based driving simulator with integrated eye tracking accompanied with purpose-built visual analysis software. In developing these two systems the following contributions were made:

(i) Validate the purpose of the data.

This study began by examining a data set of over 23,000 accident points spanning a 4 year period. In the past, this collision data has been used primarily for compiling safety reports on Irish accident occurrences. However, by using the accident data for road

geometry analysis, this abstract study has further validated the purposes of such data acquisition.

By further classifying road accident locations, this study has introduced a possible technique to cross check road accident descriptions so that all accidents can be accounted for. It has also demonstrated ways in which other curvatures such as 'vertical curvature' and 'consecutive curvature' could be applied to accidents post-acquisition based on a given GPS location.

(ii) Commissioning of the reality-based driving simulator.

This study successfully developed and tested a driving simulator integrated with eye-tracking features. Measurements drawn from this tool validated its use as an effective assessment tool. In addition to recording drivers eye behaviours, this simulator has simultaneously recorded other physiological behaviours such as acceleration pedal and blink information to name a few. Therefore future applications of this simulator system are countless.

A technical achievement for the research group at Maynooth University was to develop visual analysis software in order to synchronise, regenerate and analyse the eye movement data for the 30 participants. Additions to the visual software allowed for the tracking of targets such as road signs, monitoring acceleration data and highlighting areas of interest such as hazards. Furthermore, plane projective transformations were integrated to features of the software that managed the output data of the system so as to provide limited range information. This system also has many uses and will be used for future behaviour analysis such as measuring sustained attention.

(iii) Investigation of Irish Roadways

This study has analysed driver behaviour and accident rates based in an Irish context. Throughout both of the experiments in this thesis, a comparison of contrasting Irish road types have been assessed in order to gain a better understanding of how geometry can affect Irish accident rates and driver behaviours in this context. What Irish accident analysis shows is an increase in risk when roads with dangerous /consecutive curvatures are combined with high speed profiles. Furthermore, driver behaviour analysis is showing that as sight distances increase and straighter geometry becomes more available, drivers eye movements are accessing regions above the road and regions ahead on the road (approx 40m) suggesting geometries that are perceived as safer. While transportation studies have shown human error as a leading contributing factor in crashes, the current studies combined suggest that road geometry if designed correctly can contribute to reducing human error. For example, based on findings from this study, eliminating the need for abrupt changes in speed and increasing sight distances at road geometry may reduce the risk of driver error. These findings are in accordance with French reports discussed that show that consistent road geometry can ease the task of the driver therefore dramatically reducing the risk of driver error [20]. It is hoped that these assessments may help to inform policy makers of some of the dangers associated with Irish road types based on geometry in order to improve Irish road safety.

5.3 Future Work

Although there are many numerous environmental, human and vehicle factors that contribute to road accidents including weather, journeys, vehicle condition etc, this thesis has focused on just two, geometry and driving behaviour. Furthermore, within these categories there are many more factors to consider e.g. different road design elements, different types of behaviours, different types of drivers, thus further complicating accident analysis and prevention. Future work will analyse some of these additional factors with the tools and techniques developed in this study.

A further addition to accident data analysis in this study will be to consider the risk associated with a journey or route. This experiment will estimate the 'risk to a driver' based on a start and destination point. In addition, it will combine geometric characteristics for this route with its traffic information for the same time period of the day the trip is intended. Preliminary work for this experiment has commenced by analysing the NRA's journey data acquisition for the same 4 year period as in this study and will form the basis of future work [102].

In addition to developing accident data analysis, further driver behaviour analysis could be determined by analysing secondary data recorded by the driving simulator such as driving speeds and reaction times. Reaction times in the form of acceleration pedal data were collected in this experiment. Additional information from this data may provide insight as to reaction times when interacting with various geometries in the visual stream. However further quantitative analysis is needed to link eye behaviours to this speed information. Future work will also examine accelerator data before and after hazardous areas of interest, in this case bends. Figure 5.1 demonstrates a hazardous

situation involving a car reversing on a bend on the R406. In these cases, experiments can be further designed to measure driver behaviours such as sustained attention when presented with geometric features as shown.

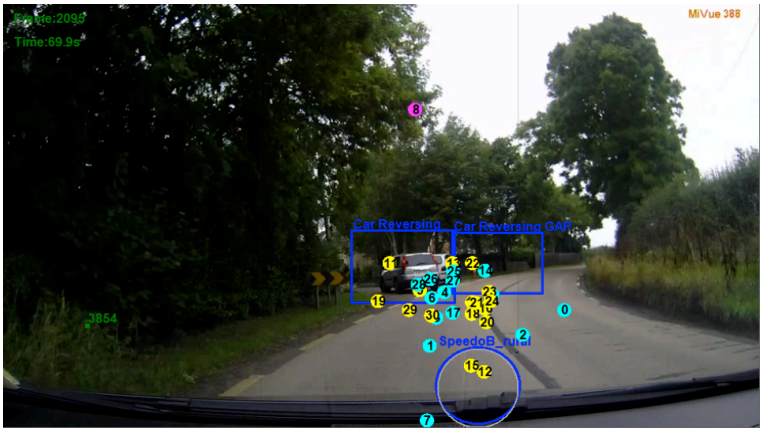

Figure 5.1 Shows hazardous situation as car reverses on dangerous closed right bend

As discussed, both of these experiments have demonstrated many measurements that can be achieved when using assessment tools such as driving simulators. The ultimate future aim of this study is to combine accident data analysis with driving behaviour analysis to design future driving scenarios that further measure how correct road design can reduce human error.

5.4 Concluding Remarks

This thesis has investigated how geometry can affect Irish accident rates and driver behaviour. Results from accident data analysis have shown that road types (N roads) that combine high speed limits with dangerous or consecutive geometry produce the most significant signal at sharp bends. What is shown in driver behaviour analysis is that drivers react to geometry as a result of available sight distance. Where drivers are presented with straights, most are not anticipating geometry far ahead, in fact 4/5 drivers are concentrating on areas 40 metres ahead, therefore the faster a curve approaches, the less time the majority of road users have to react. Further work could target specific national and regional roadways with high speed limits paying particular interest to transition curves that are situated at the end of straight sections of road.

References

[1] Road Safety Authority (2012) '*Road Collision Facts 2012'*, Available at: http://www.rsa.ie/Documents/Road%20Safety/Crash%20Stats/2012_Road_Collision_Facts.pdf [Accessed 16 Feb 2014].

[2] Road Safety Authority (2009-2012) '*Road Collision Data Set from 2009-2012'*, Data Acquired via Personal Communication [Accessed February 2013, updated February 2014]

[3] Mc Elhinney, C. et al (2010) '*Initial Results from European Road Safety Inspection'* (EURSI) MOBILE International Archives of Photogrammetry, Remote Sensing and Spatial Information Sciences, Vol. XXXVIII, Part 5 Commission V Symposium, Newcastle upon Tyne, UK.

[4] NCAP (2014) '*European New Car Assessment Program',* [online] Available: http://www.euroncap.com/results.aspx [Accessed 16 Feb 2014].

[5] NCT (2014) '*National Car Test Ireland',* [online] Available: http://www.ncts.ie/index.html [Accessed 16 May 2014].

[6] ECORYS Transport (2005) '*Impact Assessment Road Safety Action Programme'*, [online] (p 32) Available at: http://ec.europa.eu/transport/roadsafety_library/rsap_midterm/rsap_mtr_impact_assmt_en.pdf. [Accessed 16 Feb 2014].

[7] Road Safety Authority (2012) '*Road Collision Facts 2012'*, (pp. 4) Available at: http://www.rsa.ie/Documents/Road%20Safety/Crash%20Stats/2012_Road_Collision_Facts.pdf [Accessed 16 Feb 2014].

[8] National Roads Authority *NRA* (2012) '*Road Link Design'*. , 6 (NRA TD 9/12), p.1/6. Available at: http://nrastandards.nra.ie/road-design-construction-standards/dmrb/volume6/nra-td-9-road-link-design-incorporating-ta-43-where-applicable. [Accessed January 2014]

[9] World Health Organization (2009) '*European status report on road safety'(pp.12-14)*, Available at: http://www.emro.who.int/violence-injuries-disabilities/information-resources/rti-countries.html [Accessed 16 Feb 2014].

[10] Road Safety Authority (2011) '*Road Safety Strategy 2011'*, (pp. 27) Available at: http://www.rsa.ie/en/RSA/Road-Safety/Our-Research/Collision-Statistics/ [Accessed 16 Feb 2014].

[11] Road Safety Authority (2010) '*Road Safety Strategy 2010'*, (pp. 15) Available at: http://www.rsa.ie/en/RSA/Road-Safety/Our-Research/Collision-Statistics/ [Accessed 16 Feb 2014].

[12] Hauer, E. (1982) '*TRAFFIC CONFLICTS AND EXPOSURE'. Accident Analysis and Prevention*, 14(5), pp.359–364.

[13] Young, W. et al (2014) '*Simulation of safety: a review of the state of the art in road safety simulation modelling'*. Accident; analysis and prevention, 66, pp.97. Available at: http://www.ncbi.nlm.nih.gov/pubmed/24531111 [Accessed May 16, 2014].

[14] Kaneswaran, D. (2014) *Telephone Conversation with An Gardai Siochani,Traffic Corp*. Personal Communication (February 2013, July 2014)

[15] World Health Organization (2009) '*European status report on road safety'*. (pp11) Available at: http://www.emro.who.int/violence-injuries-disabilities/information-resources/rti-countries.html[Accessed 16 Feb 2014].

[16] Othman, S., Thomson, R. & Road, S.N. (2009) 'Identifying Critical Road Geometry Parameters'. (pp.157, 53) Annals of Advances in Automotive Medicine / Annual Scientific Conference.

[17] Brownfield, J., Graham, A. & Eveleigh, H. (2003) '*Congestion and Accident Risk*' for the Department of Transportation London. (pp 10-12) DoT London.

[18] Vlakveld, W. et al.(2011) '*Do Crashes and Near Crashes in Simulator-Based Training Enhance Novice Drivers' Visual Search for Latent Hazards?'* Transportation Research Record: Journal of the Transportation Research Board, 2265, (pp.153–160) Available at: http://www.pubmedcentral.nih.gov/articlerender.fcgi?artid=3472432&tool=pmcentrez&rendertype=abstract [Accessed May 12, 2014].

[19] Feng Guo, Sheila G. Klauer, Michael T. McGill, and T.A.D., 2010. '*Evaluating the Relationship Between Near-Crashes and Crashes : Can Near-Crashes Serve as a Surrogate Safety Metric for Crashes ?'* (pp 33) Available at :http://www.nhtsa.gov/DOT/NHTSA/NVS/Human%20Factors/Safety%20Problem%20Identification/DOT%20HS%20811%20382.pdf [Accessed May 14th]

[20] Dupré, G., Floris, O. & Patte, L. (2009) '*Improving the Safety of Bends on Major Rural Roads – Understand and Act'*.pp.7-10 SETRA Reports Collection. Translation of 2002 publication.

[21] Department for Transportation United KIngdom. (2002) '*Highway Link Design*,pp1/4'. Available at: http://www.dft.gov.uk/ha/standards/dmrb/ [Accessed January 2014]

[22] Cairney, P. & McGann, A. (2000) '*Relationship between Crash Risk and Geometric Characteristics of Rural Highways'*, pp.22 .Available at: https://www.onlinepublications.austroads.com.au/items/AP-R162-00. [Accessed January 2014]

[23] Persaud, B, AR Retting and Lyon, C. (2000) '*Guidelines for identification of hazardous highway curves'*. Paper no.00-1685, Transportation Research Record 1717: 14–18. PIARC.

[24] Torbic, D. J. et al (2004) NCHRP Report 500: '*Guidance for Implementation of the AASHTO Strategic Highway Safety Plan*'. (p 35) Volume 7: A Guide for Reducing Collisions on Horizontal Curves. Transportation Research Board of the National Academies, Washington, D.C. http://onlinepubs.trb.org/onlinepubs/nchrp/nchrp_ rpt_ 500v7.pdf. [Accessed March 27, 2013].

[25] Lyinam, T.F., Lyinam, S. Ergun M. (2008) '*Analysis of Relationship between Highway Safety and Road Geometric Design Elements:Turkish Case'*.(online) [Accessed online March 27, 2013].

[26] Lamm, R, EM Choueiri and T Mailaender (1988) '*Accident rates on curves as influenced by highway design elements: an international review and in-depth study*'. Pp37–55 in VTI Rapport 344 A, International Conference on Road Safety in Europe, 12–14 October, Gothenburg, Sweden.

[27] Lamm R., Koeckner, J.H. (1980) '*Safety Evaluation of Highway Design Parameters'* Road and Construction. Vol.10, pp. 14-22.

[28] Ahmed, M. et al (2011) '*Exploring a Bayesian hierarchical approach for developing safety performance functions for a mountainous freeway*', Accident Analysis & Prevention, Volume 43, Issue 4, Pages 1581-1589. Available at: http://www.sciencedirect.com/science/article/pii/S000145751 1000728. [Accessed January 2014]

[29] Stewart, D. Chudworth, CJ. (1990) '*A remedy for accidents at bends. Traffic Engng and Control*'. v31 n2 pp88-9,92-3. Printerhall Limited, London.

[30] U.S. Naval Education and Training (2003) '*Engineering Aid 2'*, Naval Education and Training Professional Development and Technology Center. Chapter 11 (p1-20)

[31] LIPPOLD, Ch. (1997) '*Weiterentwicklung ausgewählter Entwurfsgrundlagen von Landstraßen Dissertation'* segment; Fachbereich Wasser und Verkehr der technischen Hochschule Darmstadt; Darmstadt, Germany in Gatti et al(2005) Safety Handbook for Secondary Roads pp.23 available at: http://ec.europa.eu/transport/roadsafety_library/publications/ripcord_d13_secondary_roads_safety%20_handbook.pdf.

[32] Gatti, G. et al (2005) '*Safety Handbook for Secondary Roads'*, SIXTH FRAMEWORK PROGRAMME PRIORITY 1.6. Sustainable Development, Global Change and Ecosystem 1.6.2: Sustainable Surface Transport. Available at: http://ec.europa.eu/transport/roadsafety_library/publications/ripcord_d13_secondary_roads_safety _handbook.pdf.pp.21

[33] Torbic, D. J. et al (2004) '*NCHRP Report 500: Guidance for Implementation of the AASHTO Strategic Highway Safety Plan*'. (p 36) Volume 7: A Guide for Reducing Collisions on Horizontal Curves. Transportation Research Board of the National Academies, Washington, D.C. http://onlinepubs.trb.org/onlinepubs/nchrp/nchrp_rpt_ 500v7.pdf. [Accessed March 27, 2013].

[34] Karlaftis, M.G. & Golias, I. (2002) '*Effects of road geometry and traffic volumes on rural roadway accident rates*'. Accident, Analysis and Prevention, 34(3), pp.357–65. Available at: http://www.ncbi.nlm.nih.gov/pubmed/11939365.

[35] UNECE (2002) '*TEM STANDARDS for United Nations Economic Commission for Europe*', (p14-16) Available at: http://www.unece.org/fileadmin/DAM/trans/main/tem/temdocs/TEM-Std-Ed3.pdf. [Accessed January 2014].

[36] Hallmark, S., Hsu, Y. -Y., Boyle, L., Carriquiry, A., Tian, Y., Mudgal, A. (2011) *'Evaluation of data needs, crash surrogates, and analysis methods to address lane departure research questions using naturalistic driving study data*'. SHRP 2 Report S2-S01E-RW-1, National Academy of Sciences, USA.

[37] Szabo, S. Norcross, R. J. (2006) '*Recommended Objective Test Procedures for Road Departure Crash Warning Systems'*. NHTSA Report. NIST Interagency/Internal Report (NISTIR) – 7288

[38] Gatti, G. et al (2005) '*Safety Handbook for Secondary Roads'*, Available at: http://ec.europa.eu/transport/roadsafety_library/publications/ripcord_d13_secondary_roads_safety _handbook.pdf.pp.136

[39] Wilkie, D., Sewall, J. & Lin, M.C. (2012) '*Transforming GIS data into functional road models for large-scale traffic simulation'*. IEEE transactions on visualization and computer graphics, 18(6), pp.890–901. Available at: http://www.ncbi.nlm.nih.gov/pubmed/21690653.

[40] TRB (1998) '*Managing Speed*; *Review of current Practice for Setting and enforcing Speed Limits'*. Transportation Research Board.

[41] Cafiso, S. et al (2005) '*Identification of Hazard Location and Ranking of Measures to Improve Safety on Local Rural Roads':* pp.20 Mid Term Research Report. European Project Report. Published by University of Catania. Dept. of Civil and Environmental Engineering. Project Tren-03-ST-S07.31286

[42] Watter, P. and O'Mahony, M. (2007) '*The relationship between geometric design consistency and safety on rural single carriageways in Ireland.'* European Transport Conference, Noordwijkerhout, Netherlands.

[43] Cairney, P. and Bennett, P. (2008) '*RELATIONSHIP BETWEEN ROAD SURFACE CHARACTERISTIC AND CRASHES ON VICTORIAN RURAL ROADS' Rural network*. In *23rd ARRB Conference – Research Partnering with Practitioners, Adelaide Australia,*. pp. 1–9. Available at: http://www.arrb.com.au/admin/file/content13/c6/6-relationship between road surface characteristics and crashes on Victorian rural roads.pdf.

[44] Michigan Tech (2014) '*Calculating Stream Sinuosity in Arcview GIS and ArcMap'*. (Online) Available at: http://forest.mtu.edu/faculty/hyslop/gis/sinuosity.html. [Accessed July 9th].

[45] O' Connor, D. (2011) '*A network scan of horizontal road geometry'*. In Proceedings of the ITRN. pp. 3–5. Available at: http://www.itrn.ie/uploads/sesB2_ID124.pdf Accessed [Jan 2014].

[46] Iannaccone, P. M., Khokha, M. K. (1996) '*Fractal Geometry in Biological Systems.An analytical approach'*. Boca Raton, FL: CRC Press.

[47] Markham, C. (2013) *'Fractal dimensions'*, CS426: Graphics, 7 Feb, National University of Ireland, Maynooth, unpublished.

[48] Bourne, M. (1997-2014) '*Interactive Maths'* Chapter8:Radius of Curvature. (online) Available at:http://www.intmath.com/applications-differentiation/8-radius-curvature.php Accessed [Accessed Sep 2013]

[49] Kandil, F.I., Rotter, A. & Lappe, M. (2009) '*Driving is smoother and more stable when using the tangent point'*. vol 9, pp.1–11 Journal Of Vision. Available at: http://www.journalofvision.org/content/9/1/11.full [Accessed Jan 2014]

[50] Land, M.F. & Lee, D.N.(1994) '*Where we look when we steer'*. Nature. 369(6483), pp.742–744. Available at: http://dx.doi.org/10.1038/369742a0.

[51] Mars, F.(2008) '*Driving around bends with manipulated eye-steering coordination'*. Journal of Visio*n*, 8, pp.1–11. Available at: http://journalofvision.org/8/11/10/.[Accessed Jan 2014]

[52] Fu, X., Zang, Y. & Liu, H. (2012) '*A REAL-TIME VIDEO-BASED EYE TRACKING APPROACH FOR DRIVER ATTENTION STUDY'*. Computing and Informatics, 31, pp.805–825. Available at http://www.cai.sk/ojs/index.php/cai/article/viewFile/1106/460

[53] Tokunaga, R. (2005) '*EFFECTS OF CURVE DESIGNS AND ROAD CONDITIONS ON DRIVER'S CURVE SHARPNESS JUDGMENT AND DRIVING BEHAVIOR'*. Journal of the Eastern Asia Society for Transportation Studies, Vol. 6, pp. 3536 - 3550, 2005

[54] Land, M.F. & Lee, D.N. (1994) '*Where we look when we steer'*. Nature, 369(6483), pp.742–744. Available at: http://dx.doi.org/10.1038/369742a0.

[55] Brownfield, J., Graham, A. & Eveleigh, H. (2003). '*Congestion and Accident Risk*' for the Department of Transportation London. Available at : http://citeseerx.ist.psu.edu/viewdoc/download?doi=10.1.1.219.1945&rep=rep1&type=pdf

[56] Käppler, W. D. (2008) '*Smart Driver Training Simulation: Save Money. Prevent'*. Berlin, Heidelberg, Springer-Verlag, pp.24

[57] Allen, R. W., Rosenthal T. J., and Cook, M. L. (2011) '*A short history of driving simulation'* in Handbook of driving simulation for engineering, medicine and psychology, D. L. Fisher et al., Eds. Boca Ranton, Florida, USA: CRC Press, ch. 2, pp. 1-16].

[58] Hulbert and Wojcik (1960) '*Driving Simulator Research*'. In 39th Annual Meeting Highway Research Board , pp1-13.

[59] Brogan, M. et al (2014) '*Automatic Generation and Population of Graphics-based Driving Simulator using Mobile Mapping Data for the Purpose of Behavioral Testing of Drivers*'. In pp. 1–15 in proceedings of the 93rd Annual Meeting of the Transportation Research Board.

[60] Meister. (2008) '*Smart Driver Training Simulation: Save Money. Prevent*'. Berlin, Heidelberg, Springer-Verlag, pp.24

[61] VTI (2014) '*The Swedish National Road and Transport Research Institute'* (Online) Available at: : www.vti.se/en . [Accessed March 2013].

[62] NADS (2014) '*The National Advanced Driving Simulator*' (Online) Available at: : http://www.nads-sc.uiowa.edu/ [Accessed: 12 March 2013].

[63] Toyota (2009) *'Telegraph Report: Toyota's $30 million driving simulator review'* (Online) Available at http://www.telegraph.co.uk/motoring/road-safety/6598418/Toyotas-30-million-driving-simulator-review.html) [Last Accessed 10 April 2013].

[64] Zeeb, E. (2010) *'Daimler's New Full-Scale, High-dynamic Driving Simulator – A Technical Overview'*. Proceedings of the Driving Simulation Conference Europe 2010, Paris, France .

[65] TRL berkshire (2009) '*Toyota's $30 million driving simulator review*' (online) Available at http://www.telegraph.co.uk/motoring/road-safety/6598418/Toyotas-30-million-driving-simulator-review.html) [Accessed 10 April 2013]

[66] Kaneswaran, D. et al (2013) *'Replicating reality: The use of a low cost driving simulator for design and evaluation'* in Proceedings of the 24th IET Irish Signals and Systems Conference, Letterkenny, Donegal, Ireland, (pp. 29-35)

[67] Caird,.(2011) *'A short history of driving simulation'* in *Handbook of driving simulation for engineering, medicine and psychology*, D. L. Fisher et al., Eds. Boca Ranton, Florida, USA: CRC Press, ch. 2, pp. 1-16].

[68] Mars, F. & Navarro, J. (2012) '*Where we look when we drive with or without active steering wheel control'. PloS one*, 7(8), p.e43858. Available at: http://www.pubmedcentral.nih.gov/articlerender.fcgi?artid=3425540&tool=pmcentrez&rendertype=abstract [Accessed May 29, 2014].

[69] Fisher, D. L., Pollatsek, A. and Horrey, W. (2011) '*Eye Behaviors: How Driving Simulators Can Expand Their Role in Science and Engineering*'. In D. Fisher, M. Rizzo, J. Caird and J. Lee (Eds), *Handbook of Driving Simulation for Engineering, Medicine and Psychology*. Boca Raton, FL: CRC Press.

[70] Pollatsek, A. et al (2006) '*Using eye movements to evaluate a PC-based risk awareness and perception training program on a driving simulator'*. Human Factors 48,447-464.

[71] Liu, B., Sun, L. & Rong, J. (2011) '*Driver's Visual Cognition Behaviors of Traffic Signs Based on Eye Movement Parameters'*. Journal of Transportation Systems Engineering and Information Technology, 11(4), pp.22–27. Available at: http://www.sciencedirect.com/science/article/pii/S1570667210601298 [Accessed Feb 15, 2014].

[72] Salamati, K. et al. (2012) '*Simulator Study of Driver Responses to Pedestrian Treatments at Multilane Roundabouts'. Transportation research record*, 2312(2012), pp.67–75. Available at: http://www.pubmedcentral.nih.gov/articlerender.fcgi?artid=3863904&tool=pmcentrez&rendertype=abstract [Accessed Feb 12, 2014].

[73] Underwood, G. et al. (2003) '*Driving experience, attentional focusing, and the recall of recently inspected events*'. Transportation Research Part F: Traffic Psychology and Behaviour, 6(4), pp.289–304. Available at: http://www.sciencedirect.com/science/article/pii/S1369847803000500 [Accessed Feb 13, 2014].

[74] Cohen, a S. (1977) *'Is the duration of an eye fixation a sufficient criterion referring to information input?' Perceptual and motor skills*, 45(3 Pt 1), p.766. Available at: http://www.ncbi.nlm.nih.gov/pubmed/600631.

[75] Lehtonen, E. (2013) '*Look-ahead fixations in curve driving: Theory and Practice'*. Ergonomics: an international journal of research and practice in human factors and ergonomics. Taylor & Francis.

[76] Inman, V.W. (2013) *'Traffic Sign Detection and Identification':* Proceedings of the 7th International Driving Symposium on Human Factors in Driver Assessment, Training, and Vehicle Design : driving assessment 2013*,* The Sagamore on Lake George, Bolton Landing, New York, USA, June 17-20, 2013. Iowa City, Iowa: The University of Iowa, Public Policy Center, 2013. Print.

[77] Duchowski, A. T. (2007) '*Eye Tracking Methodology: Theory and Practice'*. Springer-Verlag New York, Inc, Pages 179-180.

[78] Crundall, D., Underwood, G. & Chapman, P. (2002) '*Attending to the Peripheral World While Driving'. Applied Cognitive Psychology*, 475(March), pp.459–475.

[79] Land M.F., Horwood J. (1995) '*Which parts of the road guide steering*?' Nature 377: 339–340.

[80] Wann, J. Land, M. (2000) '*Steering with or without the flow: Is the retrieval of heading necessary?'* Trends in Cognitive Sciences, 4, 319–324. [PubMed]

[81] Donges, E. (1978) '*A two-level model of driver steering behaviour'*. Human Factors, 20, 691–707.

[82] Kandil, F.I., Rotter, A. & Lappe, M. (2010) '*Car drivers attend to different gaze targets when negotiating closed vs . open bends*' . Journal of Vision, 10, pp.1–11. [PubMed]

[83] Salvucci, D. D. Gray, R. (2004) '*A two-point visual control model of steering'*. Perception, 33, 1233–1248. [PubMed]

[84] Cohen, A. S. (1983) '*Informationsaufnahme beim Befahren von Kurven*', Psychologie für die Praxis 2/83, Bulletin der Schweizerischen Stiftung für Angewandte Psychologie

[85] ETRA (2014) '*Announcement of 15th Biennial Meeting*'. (online) Available at http://www.etra2012.org/.

[86] Tobii (2014) '*Creating the Future Before Your Eyes With Leading Eye Tracking Innovations'*. Available at: www.tobii.com

[87] Martens, M.H. (2011) '*Change detection in traffic: Where do we look and what do we perceive? Transportation Research Part F':* Traffic Psychology and Behaviour, 14(3), pp.240–250. Available at: http://linkinghub.elsevier.com/retrieve/pii/S1369847811000052 [Accessed May 2, 2012].

[88] Knodler Jr, M. & Noyce, D. (2006) *'Tracking driver eye movements at permissive left-turns'*. PROCEEDINGS of the Third International Driving Symposium on

Human Factors in Driver Assessment, Training and Vehicle Design, pp.134–142.

[89] Taylor, T. et al (2013) '*The view from the road: the contribution of on-road glance-monitoring teclnologies to understanding driver behavior'*. Accident; analysis and prevention, 58, pp.175–86. Available at: http://www.ncbi.nlm.nih.gov/pubmed/23548549 [Accessed April 30, 2014].

[90] Tobii (2014) '*Tobii Glasses'* [online] Available at (http://www.tobii.com/en/eye-tracking-research/global/landingpages/tobii-glasses-2/)[Accessed June 2014]

[91] Hefferon, J. (2000) '*Linear Algebra'* . Projective Geometry (Pp 333) University Press, Cambridge.

[92] Fisher, B. (1997) *'Computing Plane Projective Transformations'* (Online) Available at: http://homepages.inf.ed.ac.uk/rbf/CVonline/LOCAL_COPIES/EPSRC_SSAZ/node11.html

[93] RSA (2014) '*Irish road Collisions*' (online) Available at:http://www.rsa.ie/RSA/Road-Safety/Our-Research/Ireland-Road-Collisions/

[94] Open Street Map (2013) *'Export Function.'* [online], available: http://www.openstreetmap.org/export#map=9/53.6430/-6.4449 [Accessed 16 Jan 2013].

[95] Open Street Map Wiki (2014) *'Nodes.'* [online], available: http://wiki.openstreetmap.org/wiki/Node [Accessed 1 Jan 2014].

[96] Tyretotravel (2014) *'Homepage'* (online), Available at: http://www.tyretotravel.com [Accessed 1 Jan 2014].

[97] Lennox, S. C., Chadwick, M. (1977) *'The Scalar* Product' Mathematics for Engineers and Applied Scientists (pp . 207) Heinemann Educational Books.

[98] UNECE (2002) *'TEM STANDARDS'* for United Nations Economic Commission for Europe*"*, (p17-19)

[99] www.nmea.org (2014) '*National Marine Electronics Association - NMEA*.' *National Marine Electronics Association*, (online) www.nmea.org, Accessed Feb 2014.

[100] Kaneswaran, D. et al (2013), '*Replicating reality: The use of a low cost driving simulator for design and evaluation*' in Proceedings of the 24th IET Irish Signals and Systems Conference, Letterkenny, Donegal, Ireland, (pp. 29-35)

[101] NRA Ireland (2014) '*NRA Counter 2006-2012*' [online], Available: https://nraaudit.nra.ie/CurrentTrafficCounterData/index.html [Accessed 16 Jan 2013].